

# For Reference

NOT TO BE TAKEN FROM THIS ROOM

Ex libris  
UNIVERSITATIS  
ALBERTAEENSIS













THE UNIVERSITY OF ALBERTA

RELEASE FORM

NAME OF AUTHOR            M. WYGANOWSKI  
TITLE OF THESIS            HYDRODESULFURIZATION OF BENZOTHIOPHENE  
DEGREE FOR WHICH THESIS WAS PRESENTED    MASTER OF SCIENCE  
YEAR THIS DEGREE GRANTED    FALL, 1982

Permission is hereby granted to THE UNIVERSITY OF ALBERTA LIBRARY to reproduce single copies of this thesis and to lend or sell such copies for private, scholarly or scientific research purposes only.

The author reserves other publication rights, and neither the thesis nor extensive extracts from it may be printed or otherwise reproduced without the author's written permission.

11 11 11



THE UNIVERSITY OF ALBERTA

HYDRODESULFURIZATION OF BENZOTHIOPHENE

by



M. WYGANOWSKI

A THESIS

SUBMITTED TO THE FACULTY OF GRADUATE STUDIES AND RESEARCH  
IN PARTIAL FULFILMENT OF THE REQUIREMENTS FOR THE DEGREE

OF MASTER OF SCIENCE

IN

CHEMICAL ENGINEERING

DEPARTMENT OF CHEMICAL ENGINEERING

EDMONTON, ALBERTA

FALL, 1982





82F-179

THE UNIVERSITY OF ALBERTA  
FACULTY OF GRADUATE STUDIES AND RESEARCH

The undersigned certify that they have read, and recommend to the Faculty of Graduate Studies and Research, for acceptance, a thesis entitled HYDRODESULFURIZATION OF BENZOTHIOPHENE submitted by M. WYGANOWSKI in partial fulfilment of the requirements for the degree of MASTER OF SCIENCE in CHEMICAL ENGINEERING.



## ABSTRACT

The hydrodesulfurization of benzothiophene over a Ni-Mo- $\gamma$ -Al<sub>2</sub>O<sub>3</sub> catalyst was studied in a fixed bed microreactor at 350 to 450°C and atmospheric pressure. Before use, the catalyst was first reduced in situ at 250°C for 4 hours in a stream of hydrogen and then presulfided at 250°C in a 10% mixture of hydrogen sulfide in hydrogen for another 4 hours. The catalyst was kept on stream for up to 40 hours for a given set of reaction conditions, after which point it was discarded.

Ethylbenzene was the major product; dihydrobenzothiophene and styrene were also found in the product stream in much smaller quantities and were identified as intermediates. The overall reaction rate increased from 350 to 400°C, but was virtually identical at 400 and 450°. It was hypothesized that as temperature increases beyond 400°, the major reaction path shifts from initial hydrogenation of benzothiophene to dihydrobenzothiophene to initial desulfurization to styrene, with the decrease in the rate of benzothiophene hydrogenation caused either by adsorption limitations on one of the reactants or by a shift in the equilibrium between benzothiophene and dihydrobenzothiophene.

Catalyst activity was also found to decrease linearly with time on stream, at a rate which ranged from 0.0 to 0.2% per hour. This rate of deactivation was found to be independent of time on stream and to depend only on the reaction





conditions, decreasing with an increase in conversion of benzothiophene and increasing with temperature. It is suggested that the loss of activity was due to a loss of sulfur from the catalyst, and that this was inhibited by the higher hydrogen sulfide partial pressures in the reactor at higher fractional conversions.



## ACKNOWLEDGEMENTS

The author is grateful to his supervisor, I. G. Dalla Lana, for many helpful suggestions during the preparation of this thesis, to Erna Baets for assistance during the experimental phase of this study, and to Jerry Moser and Don Sutherland for advice and assistance in the construction of the apparatus.

Financial assistance from the National Research Council is also appreciated.



## Table of Contents

Chapter	Page
1. INTRODUCTION .....	1
2. LITERATURE REVIEW .....	4
2.1 Hydrodesulfurization of Benzothiophene .....	4
2.2 Chemistry of Sulfided Hydrodesulfurization Catalysts .....	17
2.3 Effect of Catalyst Composition .....	29
2.4 Effect of Catalyst Preparation .....	35
2.5 Effect of Pretreatment Methods .....	37
2.6 On-stream Catalyst Behavior .....	42
3. DESCRIPTION OF EQUIPMENT .....	46
4. EXPERIMENTAL PROCEDURE .....	54
4.1 Catalyst Pretreatment .....	54
4.2 Reactor Operation .....	55
5. EXPERIMENTAL .....	59
6. DATA ANALYSIS .....	62
6.1 Calculation of Reactor Operating Conditions and Feed Rates .....	62
6.2 Calculation of Fractional Conversions of Reactants to Products .....	68
7. RESULTS AND DISCUSSION .....	72
7.1 General .....	72
7.2 Reaction Kinetics .....	90
7.3 Trace Reaction Products .....	103
7.4 Catalyst Deactivation .....	110
8. CONCLUSIONS .....	116
9. RECOMMENDATIONS .....	119





REFERENCES .....	121
APPENDIX A - ROTAMETER CALIBRATION DATA .....	126
APPENDIX B - SYRINGE PUMP CALIBRATION DATA .....	140
APPENDIX C - GAS CHROMATOGRAPH DETECTOR CALIBRATION DATA	143
APPENDIX D - DENSITY-COMPOSITION DATA FOR LIQUID FEED SOLUTIONS .....	149
APPENDIX E - LISTING OF COMPUTER PROGRAMS .....	152
APPENDIX F - CALCULATION OF HEAT LOAD IN REACTOR .....	160
APPENDIX G - CALCULATION OF KINETIC CONSTANTS .....	164



## List of Tables

Table	Page
1. Summary of Chromatographic Analysis Conditions.....	51
2. Summary of Run Conditions.....	60
3. Sample Output from Data Analysis Program.....	63
4. Constants of the Catalyst Deactivation Curve.....	89
5. Fractional Conversion Data.....	91
6. Observed Reaction Rates.....	96
7. Experimental and Literature Values of Activation Energy.....	102
8. Analysis of Reaction Products.....	106
A-1. Rotameter Calibration Data.....	128
B-1. Syringe Pump Calibration Data.....	141
C-1. Gas Chromatograph Detector Calibration Data.....	144
C-2. Experimental Response Factors for Benzothiophene, Ethylbenzene, Styrene.....	150
D-1. Density-composition Data for Benzothiophene-Hexane Solutions.....	153
F-1. Heat Capacities of Reactants and Products.....	162
F-2. Bond Strengths of Reactants and Products.....	163





## List of Figures

Figure	Page
1. Furimsky and Amberg Reaction Scheme.....	9
2. Kwart, Schuit, and Gates Adsorption Model.....	16
3. Equipment Flow Diagram.....	47
4. Sample Chromatogram.....	53
5. Time-dependence of Fractional Conversion to Ethylbenzene.....	73
6. Effect of Space time on Fractional Conversion to Ethylbenzene.....	92
7. Effect of Space time on Fractional Conversion to Styrene.....	93
8. Effect of Space time on Fractional Conversion to Dihydrobenzothiophene.....	94
9. Arrhenius Plot Based on Conversion to Ethylbenzene...	97
10. Chromatogram of Condensed Products.....	104
11. Deactivation Rate as a Function of Fractional Conversion.....	111
A-1. Rotameter Calibration Data.....	136
B-1. Syringe Pump Calibration Data.....	142
C-1. Gas Chromatograph Detector Calibration Data.....	147
D-1. Density-composition Data for Benzothiophene-Hexane Solutions.....	154



## 1. INTRODUCTION

It has long been recognized that the hydrodesulfurization of petroleum fractions has a number of benefits beyond the reduction of sulfur oxide emissions from combustion. Poisoning of precious-metal reforming catalysts is lessened<sup>1</sup>, the ratio of middle distillate to heavy fuel oil obtained from the crude is increased<sup>2</sup>, and the odor and color of the final product are improved.

Until about fifteen years ago, application of hydrodesulfurization to heavy feeds had been deterred by the unique characteristics of these feeds and the associated costly processing requirements. With the increased development in recent years of alternative fuel sources, in particular the high-sulfur and high-nitrogen liquids derived from tar sands, coal, and oil shale, the process of hydrodesulfurization has taken on a new importance.

The design of large scale catalytic reactors usually is improved by an understanding of the reaction mechanisms involved as well as by the availability of kinetic data. Mechanistic data are scarce in the case of hydrodesulfurization reactions, and most of the available data have described the behavior of one of the simpler sulfur compounds, thiophene<sup>3-11</sup>. Detailed kinetic data are even more difficult to obtain, and the available literature has again focused on thiophene.



A significant amount of the sulfur present in crude fossil fuels is present as benzo(b)thiophenes, henceforth referred to as benzothiophenes, however. Martin and Grant<sup>1,2</sup> found that two-ring thiophenes accounted for 22% of the sulfur compounds and 33% of the thiophenic compounds in a sample of Middle East crude, and 14-25% of the sulfur compounds and 23-35% of the thiophenic compounds in a number of samples of American crudes. Clugston et al.<sup>1,3</sup> also found significant quantities of benzothiophenes in samples of bitumen from the Athabasca and Cold Lake districts, and in a sample of heavy oil from the Lloydminster area.

Only a few desulfurization studies<sup>1,4-17</sup> have been performed using benzothiophene as a feed, and these have tended to be more qualitative than quantitative. In addition, there is little agreement among researchers concerning the relative rates of various reaction pathways, or the detailed mechanisms of even the major paths. For this reason, it was decided to investigate the benzothiophene hydrodesulfurization reaction more closely.

Until recently, the standard catalyst for hydrodesulfurization has been sulfided cobalt-molybdenum supported on  $\gamma$ -alumina. Nickel-molybdenum catalysts, however, are coming under much closer scrutiny, partly for economic reasons, and partly because of recent data showing them to be more effective for treating feedstocks high in nitrogen and oxygen compounds than had previously been supposed.



The mode of action of the nickel and the cobalt catalysts is supposed to be very similar<sup>18</sup> and the hydrodesulfurization activities also appear comparable<sup>19-20</sup>. Greater activities for the nickel catalyst have been reported for hydrodenitrogenation<sup>20-21</sup> and for hydrogenation<sup>20</sup>, and although these results have been challenged<sup>19</sup>, this has been another major reason for the reevaluation of nickel-promoted catalysts.

Because no detailed studies of the hydrodesulfurization of benzothiophene had been performed using a nickel catalyst, and because this catalyst may become as industrially important in future as the more heavily-studied cobalt catalysts, it was decided to use a nickel-molybdenum catalyst supported on alumina in the present study.







## 2. LITERATURE REVIEW

### 2.1 Hydrodesulfurization of Benzothiophene

Early work on the hydrodesulfurization of benzothiophene was more concerned with predicting the main reaction products or with proving the effectiveness of a given catalyst than with attempting to discover a reaction network.

In 1960, Thompson and his coworkers<sup>22</sup>, in attempting to devise a method of using the products of hydrodesulfurization as a means for identifying sulfur compounds, found that only ethylcyclohexane was produced when the reaction took place over an alumina-supported palladium catalyst at 155°C. That same year, Hoog et al.<sup>23</sup>, working with a cobalt-molybdenum catalyst, and Yamada<sup>24</sup>, working with a molybdenum trisulfide catalyst, both found only ethylbenzene as a product. Later, Hopkins et al.<sup>25</sup>, desulfurizing benzothiophene in boiling methanol with Raney nickel, again found only ethylbenzene produced.

The first attempt to study the mechanism of benzothiophene hydrodesulfurization in detail was that of Givens and Venuto<sup>16</sup> in 1970. Using a series of alumina-supported catalysts (including two Co-Mo versions) in a continuous-flow reactor at atmospheric pressure and temperatures ranging from 300 to 400°C, these authors found both ethylbenzene and dihydrobenzothiophene as products. Because the latter only appeared at higher space velocities and because it appeared in increasing amounts at lower temperatures with no new



products, it was hypothesized that the reaction was a two-step conversion of benzothiophene through the intermediate dihydrobenzothiophene.

The mechanism postulated was that of a rapidly occurring equilibrium between benzothiophene and dihydrobenzothiophene, with a slow, irreversible desulfurization step draining this equilibrium. This was supported by data from tests of the desulfurization rates of mixtures of benzothiophene and dihydrobenzothiophene in varying proportions, which indicated that an equilibrium between the two was reached quickly, and for this reason the two appeared to form ethylbenzene at comparable rates. It was suggested that if dihydrobenzothiophene were the source of ethylbenzene, desulfurization might be a multistep process involving first a cleavage of one carbon-sulfur bond to give a discrete mercaptan intermediate, followed by a second C-S bond scission to give the hydrocarbon plus hydrogen sulfide. If benzothiophene were the source of ethylbenzene, sulfur would be lost in a one-step process involving the synchronous breaking of two C-S bonds, producing the hydrocarbon without a mercaptan intermediate.

These results were later corroborated by De Beer et al.<sup>26</sup>, who used benzothiophene hydrodesulfurization to test the relative activities of a series of alumina-supported molybdenum and tungsten catalysts promoted by nickel and cobalt. Using a fixed bed reactor operating at atmospheric pressure, these authors also found ethylbenzene and



dihydrobenzothiophene as the only products, and agreed with the hypothesis that dihydrobenzothiophene was an intermediate in the reaction.

The quantitative results of this earlier investigation may be questioned, however, since the products of the reaction were condensed prior to analysis (presumably at room temperature), rather than using an on-line gas sampling technique. Consequently, it is possible that some of the more volatile compounds which could have been produced in this reaction may have been eluted in the gas stream. This would affect the relative amounts of the products analyzed, and could have resulted in a failure to detect other intermediates or side reaction products.

Also, the catalyst was used in a highly reduced state, having been reduced in  $H_2$  at over  $500^\circ C$  prior to use. High reduction temperatures have been reported to seriously degrade the activity of hydrodesulfurization catalysts<sup>27</sup>, and it thus seems possible that many of the catalyst sites may have been destroyed by the time that it was used. If so, little (if any) sulfiding of the catalyst by the  $H_2S$  produced in the reaction may have occurred. (The effects of various methods of catalyst pretreatment are reviewed in more detail in Section 2.5.) This is supported by the fact that the authors found no effect of presulfiding on catalyst activity, and as a result, their catalyst may have borne little resemblance to most current industrial hydrotreating catalysts.





The next study of this reaction was performed in 1974, by Bartsch and Tanielan<sup>15</sup>, who also used a Co-Mo- $\gamma$ -Al<sub>2</sub>O<sub>3</sub> catalyst in a continuous flow reactor at atmospheric pressure, with temperatures in the same range as had been used by Givens and Venuto. In this study, ethylbenzene was again the only product found. Bartsch and Tanielan used their data to derive a pseudo-first order rate expression and an apparent activation energy (4.9 kcal/mol) for the overall reaction.

This investigation unfortunately included most of the deficiencies of the previous one. The reaction products were again condensed at room temperature prior to analysis, and while the prereduction and presulfiding conditions were less severe (400°C), it is still possible that the catalyst may have been adversely affected.

Styrene was discovered in the reaction products along with ethylbenzene by Furimsky and Amberg<sup>14</sup> in 1976. These authors used a series of unsupported molybdenum disulfide catalysts as well as a commercial Co-Mo- $\gamma$ -Al<sub>2</sub>O<sub>3</sub> catalyst and a chromia catalyst in a pulse microreactor at atmospheric pressure and temperatures ranging between 250-400°C. Both benzothiophene and dihydrobenzothiophene were employed as feeds in this study.

Apparent activation energies based on Arrhenius plots were calculated for the desulfurization of benzothiophene and dihydrobenzothiophene (12 kcal/mol and 7 kcal/mol, respectively). In addition, the temperature dependence for





the yield of benzothiophene from dihydrobenzothiophene was used to estimate the activation energy of the dehydrogenation of dihydrobenzothiophene (14.8 kcal/mol). The fact that a higher activation energy was found for dehydrogenation than for desulfurization implied that with increasing temperature, the rate of dehydrogenation would become increasingly important.

Based on these findings, Furimsky and Amberg proposed several reaction routes for the overall desulfurization, as shown in Figure 1.

Reaction route a suggests participation of the  $\beta$ -hydrogen of the thiophene ring in carbon-sulfur bond cleavage, a hypothesis supported by the earlier finding of Givens and Venuto that a marked decrease in the desulfurization rate of benzothiophene was found when this hydrogen was substituted with a methyl group. Route b involves C-S bond cleavage with the participation of hydrogen as the initial step, though 2-mercaptophenylacetylene is too unstable and 2-mercaptostyrene too quickly desulfurized for the authors to have expected to have detected them in their products. Route c represents the saturation of the thiophene ring followed by either migration of one of the  $\beta$ -hydrogens with subsequent C-S bond cleavage or by double C-S bond scission and saturation of the aliphatic carbon.

The presence of styrene in the product stream was verified by Bartsch and Tanielan<sup>28</sup> in 1977, while studying the hydrodesulfurization of benzothiophene over prereduced



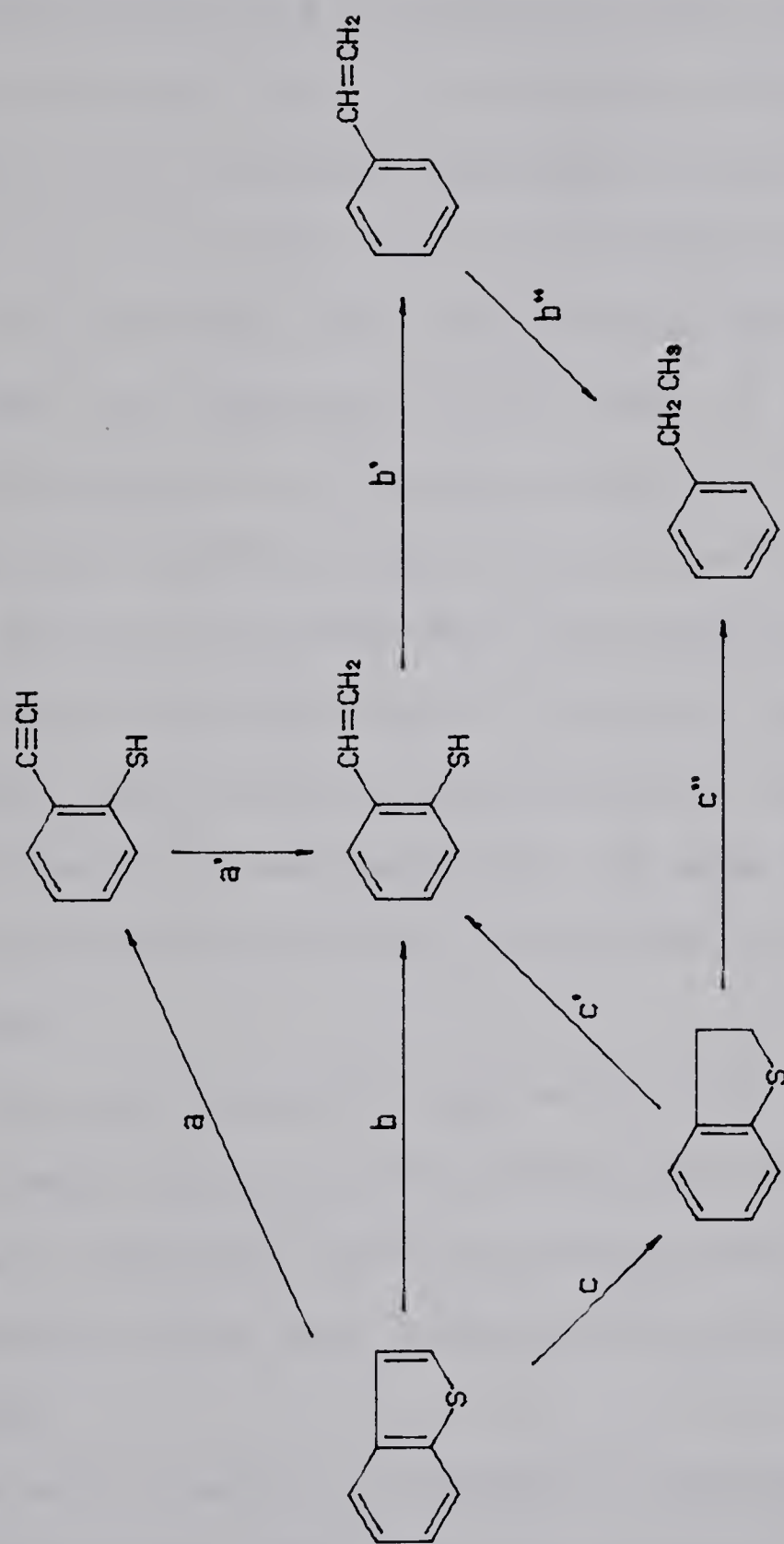


Figure 1 – Furimsky and Amburgey Reaction Scheme



$\text{Fe}_2\text{O}_3$  catalysts at atmospheric pressure and 300-400°C. These authors supported the view that C-S bond cleavage was the primary initial step in the overall desulfurization reaction, and hypothesized two possible main reaction schemes similar to routes b and c of Furimsky and Amberg. Bartsch and Tanielan also allowed cleavage of the S-C<sub>2</sub> bond as an alternative to the S-C<sub>1</sub> bond, with 2-phenylethanethiol and 2-phenylethylenethiol the intermediates produced. A pseudo-first order rate equation was derived for the overall reaction, with apparent activation energies of between 12.5 and 14.0 kcal/mol found for the catalyst reduced at 400°C.

No styrene was found when the catalysts were presulfided, however, and Bartsch and Tanielan suggested that the sulfurized sites aided in hydrogenation. This was supported by data showing a feed consisting of pure styrene to be completely hydrogenated when subjected to their reaction conditions.

It was also found in this study that the amount of styrene produced using prereduced catalysts decreased with time on stream, and these authors concluded that these sulfurized hydrogenation sites were formed during the first few hours on stream.

The early results of Thompson found some support from Rollman<sup>29</sup> in 1977, who also found traces of ethylcyclohexane while hydrotreating mixtures of sulfur and nitrogen compounds in the liquid phase at 2.1-10.3 MPa and 300-450°C over a Co-Mo catalyst. Ethylbenzene was the only other





product found. No mechanism was postulated in this study; the main concern of this investigation was the relative reactivities of the various compounds tested.

The next researcher to investigate benzothiophene hydrodesulfurization was Daly<sup>17</sup> in 1978. This author used a liquid phase stirred-batch minireactor charged with a Co-Mo- $\gamma$ -Al<sub>2</sub>O<sub>3</sub> catalyst, operating at 200-400°C and 8.6 MPa. An apparent activation energy of 16.1 kcal/mole was calculated for the overall reaction.

Traces of 1- and 2-phenylethanethiol were detected in the products along with ethylbenzene and styrene. It was suggested that these thiols resulted from a back-reaction between hydrogen sulfide and an unsaturated hydrocarbon, probably styrene. This was supported by the result that an increased hydrogen sulfide concentration produced an increase in the concentrations of these back-reaction products, and that in the presence of elemental sulfur (known to catalyze the reaction of hydrogen sulfide with olefins<sup>30</sup>), there was also an increase in these products.

Daly proposed a reaction scheme similar to that of Furimsky and Amberg, but incorporated steps in which styrene reacts to form 1- and 2-phenylethanethiol, and dihydrobenzothiophene reacts to form 2-phenylethanethiol, which could subsequently be desulfurized to form ethylbenzene.

The pretreatment in this study was also at a high temperature, and in addition, mass balances were not computed for the products, which may limit the validity of the





quantitative results.

In 1978, Kilanowski et al.<sup>11</sup> used a Co-Mo- $\gamma$ -Al<sub>2</sub>O<sub>3</sub> catalyst in a pulse microreactor to test the relative reactivities of various thiophenic compounds at atmospheric pressure and temperatures of 300-400°C. Styrene and ethylbenzene were the only products found from benzothiophene hydrodesulfurization, and it was concluded that the reaction network could be approximated by a simple sulfur extrusion. The absence of sulfides and mercaptans in the products was taken as evidence of the carbon-sulfur bond scission being a slow reaction step.

In this study, the pretreatment consisted of heating the catalyst to 400°C in hydrogen, then presulfiding at this temperature with a 10% mixture of H<sub>2</sub>S in H<sub>2</sub>. This presulfiding may have had only a short-lived effect on the catalyst, though, since pure hydrogen was passed over the catalyst constantly, with 0.5  $\mu$ l pulses injected only every 35 minutes to 1 hour. Although little data are available on catalysts which have been presulfided and then subjected to severe reducing conditions, it seems likely that a significant amount of sulfur would be lost from the catalyst in such a case.

These authors also speculated on the nature of the adsorption of benzothiophenes on the catalyst surface. It was suggested that single anion vacancies could accommodate the sulfur atom in a "single-point" adsorption, as had been proposed for thiophene, whereas an adjacent pair of



vacancies might allow for a flat adsorption, involving the  $\pi$  electrons of the thiophenic ring.

A second study of benzothiophene hydrodesulfurization by Kilanowski and Gates<sup>32</sup> was published the next year. The same catalyst was used as previously, although this time the reaction took place in a flow microreactor at atmospheric pressure and temperatures of 252, 302, and 332°C. In this study, ethylbenzene was the only reaction product found in greater than trace amounts.

Only one of a number of empirical rate equations tried was found to even roughly fit the data at all three temperatures, and this equation fit the data much more poorly at 332°C than at the two lower temperatures.

It was suggested that the difficulty of finding a rate equation applicable to the full range of temperatures studied was due to a complicated mechanism and changes in the kinetics with temperature. From the data, an apparent activation energy of  $20 \pm 3$  kcal/mol was calculated; the respective heats of adsorption of benzothiophene and  $H_2S$  were calculated as  $-15 \pm 10$  and  $-6 \pm 6$  kcal/mol, with the large uncertainties in these latter figures mainly due to scatter in the data at 252°C.

In 1979, Nag et al.<sup>33</sup> desulfurized benzothiophene in a high pressure (7.2 MPa) batch reactor charged with a commercial Co-Mo- $\gamma$ - $Al_2O_3$  catalyst at 300°C. Pretreatment consisted of presulfiding the catalyst for 2 hours at 400°C in a mixture of 10%  $H_2S$  in  $H_2$ . Ethylbenzene and styrene were the





only products found, in the approximate ratio of 5:1. A pseudo-first order rate constant for the disappearance of benzothiophene of  $2920 \text{ cm}^3/\text{g catalyst-hr}$  was calculated.

Recently, Kwart, Schuit, and Gates<sup>3,4</sup> proposed a model for the adsorption of benzothiophene onto the surface of sulfided catalysts, which they claimed was much superior to both the "one-point" and the "flat" adsorption models which had generally been used to describe the state of thiophenic molecules prior to desulfurization. This new model was then used to make specific predictions about the paths that the desulfurization reaction should take.

These authors claimed that the expected bonding characteristics of thiophenic molecules would lead to adsorption at the  $\text{C}_1\text{-C}_2$  bond, rather than at the sulfur atom: the unshared nonbonded electron pairs on sulfur should be so involved with the resonance of the thiophene nucleus that the sulfur atom should have little residual electron availability for direct coordination by catalyst. It was suggested instead that thiophenic molecules may be chemisorbed such that the  $\text{C}_1\text{-C}_2$  bond is coordinated at an anion vacancy on the catalyst, with the adjacent sulfur center then interacting with a neighboring sulfur atom on the catalyst surface. When the thiophene ring becomes bonded via the  $\text{C}_1\text{-C}_2$  position at the anion vacancy, the result is expected to be a change in the electron distribution of the ring, making the sulfur atom electron-deficient, and consequently promoting its bonding with another sulfur atom of high



electron density on the catalyst surface. These changes should facilitate hydrogen addition to the coordinated  $C_1-C_2$  centers and formation of a dihydrogenated intermediate. This adsorbed species is depicted in Figure 2.

A benzothiophene molecule adsorbed at the  $C_1-C_2$  bond could provide several alternative steps to simple hydrogenation and desorption to form dihydrobenzothiophene. If partial hydrogenation occurs at the  $C_1$  atom, electron delocalization could lead to rupture of the S- $C_1$  bond, which would produce either 2-mercaptostyrene if the sulfur atom were hydrogenated, or styrene, if the sulfur atom became fully bonded to the catalyst surface with subsequent C-S bond scission. Alternatively, the partially bonded protons in the structure of Figure 2 could become involved in covalent bonds to the  $C_1$  and  $C_2$  atoms by a concerted process, with subsequent  $\beta$ -elimination leading to the same products.

These authors agreed with the earlier suggestion of Kilanowski<sup>31</sup> that a one-point site might better account for the high reactivity of hydrogenated compounds lacking the  $\pi$  electrons necessary for this "three-point" model. They considered their model superior to the flat adsorption model in that it did not require the interaction of two separate  $\sigma$  complexes.

In summary, the mechanism by which benzothiophene is desulfurized is still unclear. This reaction has been studied both in the gas phase at atmospheric pressure and in the liquid phase at high pressures. Only Co-Mo- $\gamma$ - $Al_2O_3$  and





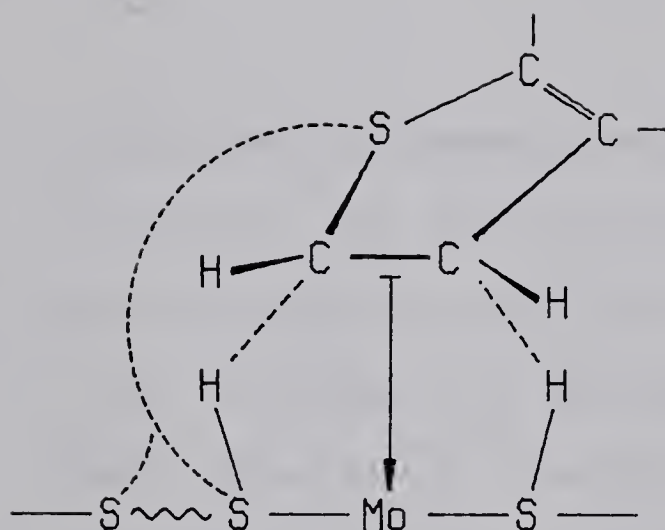


Figure 2 - Kwart, Schuit, and Gates Adsorption Model. The dashed lines indicate a weaker interaction between centers than solid lines; the wavy line indicates a longer or more remote bond between centers.



$\text{Fe}_2\text{O}_3$ - $\gamma$ - $\text{Al}_2\text{O}_3$  have been employed as catalysts, and both have been pretreated by various methods. It is generally agreed that ethylbenzene is the major product, but both styrene and dihydrobenzothiophene have been found in small quantities in the product stream, and it appears that either or both may be intermediates in the overall desulfurization reaction. The kinetics appear to be complicated, and may vary significantly with temperature, type of catalyst used, method of pretreatment, and length of time that the catalyst has been on stream.

## 2.2 Chemistry of Sulfided Hydrodesulfurization Catalysts

Attempts to identify the catalytically active species present in hydrodesulfurization catalysts started with Richardson<sup>3 5</sup> in 1964. By measuring the magnetic susceptibility of various cobalt species in a series of Co-Mo- $\gamma$ - $\text{Al}_2\text{O}_3$  catalysts and correlating this with desulfurization activity, Richardson characterized the catalyst as a mixture of  $\text{Al}_2\text{O}_3$ ,  $\text{CoAl}_2\text{O}_4$  (both inactive),  $\text{Co}_3\text{S}_4$  (very slightly active),  $\text{MoS}_2$  (moderately active itself, but requiring promotion by "active cobalt" for maximum activity), and possibly  $\text{MoO}_2$  (mildly active). This "active cobalt" was considered to be a non-reducible form of the metal, probably in an octahedral coordination, while the inactive cobalt was likely confined to tetrahedral sites.



Richardson also found that catalysts with initial Co:Mo ratios of less than 0.3 had the same final composition when calcined in the range 538-650 °C, but at higher initial Co:Mo ratios, the final composition was dependent on both cobalt content and heat treatment method. The catalyst found to have the greatest activity had a Co:Mo ratio of 0.2, and an active Co:Mo ratio of 0.18.

Two models appeared in the early 1970's to explain the surface chemistry of tungsten and molybdenum catalysts promoted with nickel and cobalt. Both of these models described the effect of the promoters as an increase in the reduction of the catalyst ions, but the mechanisms by which this was achieved were significantly different.

The first of these two models was the intercalation model, proposed by Voorhoeve and Stuiver<sup>36-38</sup> and Farragher and Cossee<sup>39</sup>. It had been found that MoS<sub>2</sub> and WS<sub>2</sub> have a layer structure in which the metal is surrounded by a trigonal prismatic coordination of six sulfur atoms. The stacking of the sulfur layers can be either hexagonal or rhombic; in practice both are found, with frequent defect structures. Although intercalation is impossible for perfect MoS<sub>2</sub> and WS<sub>2</sub> crystals, it was postulated that nickel and cobalt can intercalate appreciably if the crystals are small.

Based on kinetic studies of the hydrogenation of cyclohexene and benzene over a sulfided Ni-W catalyst, Voorhoeve and Stuiver concluded that the active sites were sulfur-



deficient anion vacancies in the metal. This was later supported by Wentrcek and Wise<sup>40</sup>, who found a positive relationship between hydrodesulfurization activity and electronic "holes" in the surface of a single MoS<sub>2</sub> crystal, and by Aoshima and Wise<sup>41</sup>, who found that a small number of S<sup>2-</sup> vacancies in this crystal was beneficial to hydrodesulfurization activity.

From the relationships between an ESR resonance ascribed to W<sup>3+</sup> and H<sub>2</sub>S/H<sub>2</sub> ratio and catalyst nickel content, and from the fact that increasing H<sub>2</sub>S concentration decreased the activity of the catalyst, Voorhoeve concluded that W<sup>3+</sup> was the catalytically active site. This was supported by a correlation between intensity of the ESR signal and catalytic activity for benzene hydrogenation.

The discovery that the alumina carrier had no effect on the types of sites produced, along with the results from optical studies and X-ray line broadening measurements led Voorhoeve and Stuiver to conclude that nickel was located in octahedral holes between layers of WS<sub>2</sub>, which produced an increase in electron concentration in the WS<sub>2</sub> sheets and thus an increase in the number of active tungsten ions on the surface. The lack of correlation between the magnitude of the W<sup>3+</sup> signal and activity in cyclohexene hydrogenation led to the conclusion that this compound was adsorbed on a different type of site, possibly also W<sup>3+</sup> ions but in a different coordination.





Farragher and Cossee extended this model with further optical and X-ray measurements, showing that the nickel ions tended to be located on the edges of the crystals.

Maximum Ni:W ratios based on this extension of the edge-intercalation model were predicted to be in the range of 0.3 to 1; it was suggested that varying crystal size could explain the wide variations in the optimum values of this parameter reported in the literature. In addition, nickel and cobalt were shown to be both physically and thermodynamically ideal for occupation of octahedral holes in the crystal structure.

The two types of sites hypothesized by Voorhoeve and Stuiver were seen as a single  $W^{3+}$  ion connected to an anion vacancy and a combination of two  $W^{3+}$  ions with interconnecting  $S^{2-}$  ions absent.

Although this model was considered to be applicable to the Co-Mo system as well, ESR data for the corresponding compounds had not confirmed this extension, despite attempts by Lo Jacono et al.<sup>42</sup> and others<sup>43</sup>. Lo Jacono mentioned that the absence of an ESR signal was not proof of the absence of  $Mo^{3+}$ , though, due to the possible existence of these ions as diamagnetic pairs.

A second model was developed by Schuit and Gates<sup>43</sup> and Hagenbach, Courty and Delmon<sup>44</sup> to better describe sulfided Co-Mo catalysts. It had been shown that although nickel prefers an octahedral coordination, cobalt has a stronger preference for tetrahedral sites<sup>45</sup>. As a result, these



authors characterized cobalt as incorporated into tetrahedral sites below a layer of ions on the catalyst surface.

In this model,  $\gamma\text{-Al}_2\text{O}_3$  is assumed to consist of particles formed by a one-dimensional stacking of alternating C and D layers, where the D layers have only octahedral Al, and the C layers have an equal number of octahedral and tetrahedral sites.  $\text{MoO}_3$  is present in a monolayer on the alumina surface and is arranged with the opposite symmetry to the top alumina layer. To compensate for the excess positive charge, an anion "capping" layer is assumed to be located on top of the monolayer, consisting of  $\text{S}^{2-}$  ions in sulfided catalysts and  $\text{O}^{2-}$  ions in oxidic and partially reduced catalysts. Incorporation of  $\text{Co}^{2+}$  in the support is assumed to result in the location of these cations in a tetrahedral position somewhere below the monolayer. This is accompanied by expulsion of  $\text{Al}^{3+}$  ions from the support, which then must find tetrahedral positions in the monolayer, which in turn forces the Mo ions to find places in the octahedral interstices. As a result, fewer Mo ions are incorporated and the ratio of capping ions to molybdenum ions is increased. This was supported by pulse-flow data of De Beer et al.<sup>45</sup>, who showed that the addition of Co to a  $\text{Mo-}\gamma\text{-Al}_2\text{O}_3$  catalyst increased the uptake of  $\text{H}_2\text{S}$  and by the diffuse reflectance spectroscopy of Gajardo et al.<sup>46</sup>, confirming the presence of tetrahedral  $\text{Co}^{2+}$  as  $\text{CoAl}_2\text{O}_4$  in oxidic  $\text{Co-Mo-}\gamma\text{-Al}_2\text{O}_3$ . Gajardo et al also found a significant amount of octahedral  $\text{Co}^{3+}$ , however, and suggested a Co-Mo bilayer



might better account for some aspects of this system.

Additional support for the bilayer character of the monolayer model was presented by Delannay et al.<sup>47</sup> whose ion scattering spectrometry experiments confirmed that molybdenum was essentially confined to the surface layer of nonreduced catalysts, and that cobalt was present in a single layer between the  $\gamma$ - $\text{Al}_2\text{O}_3$  support and the molybdenum surface layer.

In the monolayer model, the stability of the monolayer should also be increased, since part of the task of binding it to the surface layer would be taken over by the alumina support. Hagenbach and his coworkers<sup>44</sup> have found that in small quantities, Co does in fact bring about a better crystallinity as well as a decrease in surface area in Co-Mo- $\gamma$ - $\text{Al}_2\text{O}_3$ , although at very low concentrations the incorporation of Co seemed harmful rather than beneficial to catalyst activity.

Another consequence of the monolayer model is the formation in the sulfided catalyst of some  $\text{Mo}^{4+}$  and  $\text{Mo}^{5+}$  ions, depending whether the top  $\text{Al}_2\text{O}_3$  layer is a C or a D layer: replacement of  $\text{O}^{2-}$  ions in the capping layer with the much larger  $\text{S}^{2-}$  ions results in extra anion vacancies when the latter ions are removed with simultaneous reduction of the underlying Mo ions. This aspect of the model received some support from the thiophene hydrodesulfurization data and spectroscopic measurements of Lipsch and Schuit<sup>48-50</sup>. These authors concluded that cobalt was almost entirely present in







a tetrahedral coordination, but they also characterized some of the active sites as including  $\text{Mo}^{4+}$ ,  $\text{Mo}^{5+}$ , and  $\text{Mo}^{6+}$  ions in an octahedral environment. Support for the view that extra anion vacancies are produced by sulfiding and that these are catalytically active was given by the gravimetric data of Massoth<sup>51-52</sup> in 1975 and 1977.

Dufaux, Che, and Naccache<sup>53</sup> found that the intensity of the  $\text{Mo}^{5+}$  signal appeared only at  $\text{MoO}_3$  concentrations above 10%, adding support to the concept of an inert  $\text{MoO}_3$  monolayer. Lo Jacono et al.<sup>42</sup> also found this effect, but also found that a weak  $\text{Mo}^{5+}$  signal disappeared with the addition of a small amount of Co. They concluded that the ESR inertness of the first amounts of  $\text{MoO}_3$  might instead be ascribed to a solution of Mo in the support. In other words, both Co and Mo dissolve in the alumina, and although initially the solubility is restricted, once the two ions are present simultaneously, their solubilities increase.

In contrast to this, Ashley and Mitchell<sup>54-55</sup> found that a considerable amount of  $\text{Co}^{2+}$  was present in an octahedral environment (as would be predicted from the intercalation model), but viewed  $\text{Mo}^{6+}$  as tetrahedrally coordinated. These authors also found a synergic effect in the concurrent adsorption of Co and Mo, and a decrease in the percentage of tetrahedral Co with increasing Mo concentration, interpreted as a competition for tetrahedral sites.

A predominantly tetrahedral coordination of Mo has also been found using diffuse reflectance spectroscopy by Chung



and Massoth<sup>56</sup> and Gajardo et al.<sup>46</sup>. Chung and Massoth suggested that the predominantly tetrahedral or octahedral coordination of Mo depends on calcining temperature as well as on the amounts of both cobalt and molybdenum in the catalyst.

Subsequent spectroscopic data by Mitchell and Trifiro<sup>57</sup> also confirmed the presence of linked  $\text{MoO}_4$  tetrahedra and  $\text{CoO}_6$  octahedra in the fresh catalyst. On sulfiding, it was found that sulfur added to  $\text{MoO}_4$ , and that no more than one or two  $\text{O}^{2-}$  ions per unit cell were replaced by  $\text{S}^{2-}$ , probably those bridging between Mo and Co. No evidence was found for discrete sulfides, such as  $\text{MoS}_2$  and  $\text{Co}_3\text{S}_4$ , and as a result, these authors concluded that the active sites were probably oxysulfides, rather than sulfides. These catalysts were not kept on stream for a great length of time, and consequently, the further removal of  $\text{O}^{2-}$  could be another effect associated with the change of the catalyst state from monolayer to intercalated.

A detailed series of experiments were performed in 1974 by De Beer and his coworkers<sup>58</sup> to test the relevance of the two models to the preparation and operation of active catalysts. Since the intercalation model predicted that the most effective promoter ions should be those that prefer octahedral sites, and the monolayer model predicted that they should prefer a tetrahedral coordination, it was hypothesized that if a certain mobility were assumed, some promoters would become more active with use and some less



active, depending on their initial locations and inherent preferences.

To test this, three methods of preparation were used: a sequential impregnation of the carrier with Mo and Co solutions (to produce an intrinsically ideal monolayer system), a slurring of  $\text{MoS}_2$  with the carrier before the promoter was added (to yield a true intercalation system), and a third method designed to produce a catalyst intermediate between the two.

Thiophene hydrodesulfurization at atmospheric pressure and 400 °C was used as a test reaction. The results indicated that the standard method of catalyst preparation (sequential impregnation) does result in a monolayer catalyst, but that under actual run conditions, the promoter migrates to the surface, and within a matter of hours, the catalyst becomes essentially an intercalated system.

This study also confirmed two predictions of Farragher and Cossee<sup>39</sup>. It was shown that zinc, although highly active initially, was no promoter for the intercalated system and that nickel, less active than cobalt initially, becomes more active after a few hours on stream. This also explained the earlier results of De Beer<sup>45</sup>, who had found zinc and cobalt to be much more effective promoters than nickel. In addition, the prediction that the activities of Co-W and Ni-W catalysts should be nearly equal was also verified.

It was also shown that catalysts prepared to be initially of the monolayer type showed higher activities





after being converted to intercalation systems than did catalysts prepared to be intercalated initially. It was suggested that the stabilization of the monolayer by  $\text{Co}^{2+}$  leads to smaller crystals, which are immediately intercalated by these ions as they rise to the surface.

Schuit and Gates had suggested that that the two models may not be mutually exclusive in either nickel or cobalt catalysts, and that perhaps both systems are present simultaneously with one structure more active for (say) hydrogenation and the other more active for desulfurization.

Behbahany et al.<sup>59</sup> have recently published data supporting this idea; in this study, a maximum in thiophene desulfurization activity corresponded to an intermediate ratio of tetrahedral to octahedral cobalt.

This two-site concept was not without precedent. Desikan and Amberg<sup>5</sup> had concluded from selective poisoning experiments using a  $\text{Co-Mo-}\gamma\text{-Al}_2\text{O}_3$  catalyst that two types of sites were present on the catalyst surface. The first was characterized as being strongly electrophilic, highly sensitive to poisoning by the adsorption of basic nitrogen compounds such as pyridine, and mainly responsible for olefinic hydrogenation (and occasionally dehydrogenation). The other type of site was seen as less electrophilic, more resistant to poisoning, and more important for desulfurization. Mitchell<sup>45</sup> also proposed the necessity for two types of sites, one more active for hydrogenation and isomerization and connected with the presence of  $\text{Co}^{2+}$ , and the other more





directly concerned with desulfurization. Ahuja et al.<sup>60</sup> also concluded that there was a hydrogenation/dehydrogenation function as well as a different acid function operating in sulfided Group VIII-Group VIa catalysts.

In 1973, Smith, Hinckley, and Behbahany<sup>61</sup> combined a selective poisoning technique with the deuteriumolysis of sulfur and nitrogen compounds to offer further evidence of multiple sites on Co-Mo- $\gamma$ -Al<sub>2</sub>O<sub>3</sub>. These authors found evidence for three types of sites: one for low activation energy multiple exchange and hydrogenation located on the  $\gamma$ -Al<sub>2</sub>O<sub>3</sub>, one for desulfurization, and one for  $\alpha$ -exchange, the last two both located on the catalyst itself.

Hargreaves and Ross<sup>62</sup> used the hydrodesulfurization of thiophene at pressures below atmospheric and temperatures in the range 200-400°C to investigate the nature of these two major types of sites in more detail. A variety of Co-Mo- $\gamma$ -Al<sub>2</sub>O<sub>3</sub> formulations were used; it was found that the addition of Co (up to a maximum) increased the rate of desulfurization much more than it increased the rate of hydrogenation. From this, it was concluded that the desulfurization sites were dependent on promotion by Co, while the hydrogenation sites probably were not. Since the selectivity of the reaction did not change while desulfurization activity increased when the degree of sulfiding was increased, it was also concluded that the hydrogenation sites were probably in the sulfided state.



In 1976, Parsons and Ternan<sup>6,3</sup> investigated the desulfurization, denitrogenation, and hydrocracking activities of various formulations of unpromoted Mo- $\gamma$ -Al<sub>2</sub>O<sub>3</sub> catalysts on a gas oil in a high pressure reactor. The fact that the extent of cracking increased significantly with an increase in Mo concentration while desulfurization did not offered additional evidence that these two processes took place on different sites, and that the desulfurization site was more dependent on promotion.

A number of different cations were tested as promoters for this system. No clear correlation was found between ionic radius and activity in any of the three reactions; Parsons and Ternan interpreted this as evidence for the inapplicability of the intercalation model.

The same year, De Beer and his coworkers<sup>2,6</sup> compared the cyclohexane isomerization activities of Mo- $\gamma$ -Al<sub>2</sub>O<sub>3</sub> and W- $\gamma$ -Al<sub>2</sub>O<sub>3</sub> catalysts, both unpromoted and promoted by Ni and Co. The two unpromoted catalysts showed a much higher activity than the promoted catalysts, and the unpromoted catalysts on a more acid support were more active than those on a less acidic base. De Beer suggested that isomerization was essentially a carrier phenomenon, even though unsupported sulfide catalysts had been shown to possess some isomerization activity.

In summary, the complex chemistry of sulfided hydrodesulfurization catalysts has only begun to be understood within the past decade. Both the intercalation and monolayer



models have received some verification from studies of non-reduced, reduced, and sulfided catalysts using various analytical techniques, and both have been extended and refined as a result. Each model has been successful in predicting catalyst behavior under some processing conditions, but the precise conditions under which either (or both) model may be applicable have not yet been defined, and appear to depend on catalyst composition, methods of preparation and pretreatment, and time on stream.

These studies have also revealed that at least two functionally different types of catalyst sites appear to be present on the catalyst surface: one more active for desulfurization and another more active for hydrogenation and dehydrogenation. It also appears that a third type of site responsible for isomerization may be present. To date, there is no conclusive data linking a given structure or configuration on the catalyst with a particular type of catalytic activity.

### 2.3 Effect of Catalyst Composition

Most of the published hydrodesulfurization data have been based on one or more of the Group VIII-Group VIa- $\gamma$ - $\text{Al}_2\text{O}_3$  catalysts. The Group VIII metal is usually cobalt and the Group VIa metal usually molybdenum, but occasionally either nickel or tungsten (or both) have been used in place of these respective elements.





A few studies have attempted to compare two or more of these alternative formulations under various processing conditions. It is generally agreed that Ni and Co are the best promoters for hydrogenolysis reactions, but considerable difference of opinion exists as to which is the better of the two for any of these reactions.

Beuther, Flinn, and McKinley<sup>64</sup> in 1959 were among the first to compare the relative activities of Co-Mo and Ni-Mo catalysts. Using the hydrodesulfurization of a light gas oil at 4.1 MPa and 315-370 °C as a test reaction, cobalt was found to be only slightly more active than nickel, but substantially more nickel than cobalt was required to produce this activity for a given amount of molybdenum.

In 1970, Ahuja, Derrien, and Le Page<sup>65</sup> again tried to compare the activity and selectivity of hydrodesulfurization catalysts. In this investigation, Co-Mo, Ni-Mo, Co-W, and Ni-W catalysts supported on silica and  $\gamma$ -Al<sub>2</sub>O<sub>3</sub> were tested for hydrogenation and desulfurization activity at 350°C and atmospheric pressure. Nickel was found to be the more active promoter for hydrogenation, but no difference was found between the two promoters for desulfurization, or between the catalysts for either hydrogenation or desulfurization. The results of this study have since been challenged on the basis that they may have been based on catalysts of unequal surface area<sup>45</sup>.

De Beer and his coworkers<sup>45</sup> compared a series of Mo- $\gamma$ -Al<sub>2</sub>O<sub>3</sub> catalysts promoted by various amounts of Co, Ni, Zn,



and Mn at 400°C and atmospheric pressure. The hydrodesulfurization of thiophene and the hydrogenation of the butenes produced in this reaction were used to evaluate the performance of the various catalysts. These authors found the rate of hydrogenation to be relatively insensitive to the nature of the promoter ion, and that Co and Zn appeared to have significantly greater desulfurization activity than Mn or Ni, although this latter effect only appeared at higher Group VIII metal to molybdenum ratios. The finding that the maximum activity for each metal occurred at a different metal to molybdenum ratio implied that catalyst activity was not simply a matter of filling tetrahedral vacancies.

After the emergence of the intercalation and monolayer models of catalyst structure, De Beer<sup>5,8</sup> retested the relative activities of various catalysts and promoters. A wide variety of formulations were tested for thiophene hydrodesulfurization activity, including Ni-Mo- $\gamma$ -Al<sub>2</sub>O<sub>3</sub>, Zn-Mo- $\gamma$ -Al<sub>2</sub>O<sub>3</sub>, Co-W- $\gamma$ -Al<sub>2</sub>O<sub>3</sub>, Ni-W- $\gamma$ -Al<sub>2</sub>O<sub>3</sub>, and four Co-Mo- $\gamma$ -Al<sub>2</sub>O<sub>3</sub> variations. All catalysts were used in the reduced state, although two Co-Mo- $\gamma$ -Al<sub>2</sub>O<sub>3</sub> catalysts and one unpromoted Mo- $\gamma$ -Al<sub>2</sub>O<sub>3</sub> catalyst were run in both the reduced and sulfided states. (Presulfiding was found to substantially improve the activity of the promoted catalysts, but to significantly impair the activity of the unpromoted catalyst.)

These authors found nickel to be a much more effective promoter for the molybdenum catalyst than cobalt, while zinc did not show any promoter effect at all; little difference



was found between nickel and cobalt as promoters for the tungsten catalyst. The Co-Mo- $\gamma$ -Al<sub>2</sub>O<sub>3</sub> catalyst was also found to be substantially more active than the Co-W- $\gamma$ -Al<sub>2</sub>O<sub>3</sub> catalyst, although the surface areas and cobalt contents of the two catalysts were not matched as carefully as in the other comparisons of this study. (No corresponding Ni-Mo- $\gamma$ -Al<sub>2</sub>O<sub>3</sub> vs. Ni-W- $\gamma$ -Al<sub>2</sub>O<sub>3</sub> test was made.)

The differences between the results of this study and those of some of the previous studies concerning the relative activities of the various promoters was attributed to a fundamental change in the chemistry of the catalyst surface during the first few hours of operation: previous data may have been based on a catalyst configuration which would be only short-lived under actual processing conditions.

In 1975, Satterfield, Modell, and Mayer<sup>6,5</sup> investigated the concurrent hydrodesulfurization of thiophene and hydrodenitrogenation of pyridine over Co-Mo- $\gamma$ -Al<sub>2</sub>O<sub>3</sub>, Ni-Mo- $\gamma$ -Al<sub>2</sub>O<sub>3</sub>, and Ni-W- $\gamma$ -Al<sub>2</sub>O<sub>3</sub> at atmospheric pressure and 250-425 °C. Because the concentrations of the active ingredients and the surface areas per unit weight of catalyst were somewhat different for the different samples, no direct comparisons could be made, but on a weight basis, the Ni-Mo and Ni-W catalysts were found to be significantly more active than the Co-Mo catalyst for both reactions.

Parsons and Ternan<sup>6,3</sup> recompared the relative activities of various promoters in 1976, with the intention of developing catalysts that would be much less expensive than





current commercial catalysts yet still be reasonably active, for use with feeds with high metals contents (and thus high poisoning rates). A heavy gas oil derived from Athabasca bitumen was treated in a flow reactor at 400°C and 14 MPa, and analyzed for desulfurization, denitrogenation, and hydrocracking activity. Co and Ni were found to be the most active promoters in all cases; the two were virtually identical in desulfurization activity, while Ni appeared slightly more active for denitrogenation and cracking.

That same year, De Beer, Dahlman, and Smeets<sup>26</sup> compared the high pressure desulfurization and hydrogenation activities of W- $\gamma$ -Al<sub>2</sub>O<sub>3</sub> and Mo- $\gamma$ -Al<sub>2</sub>O<sub>3</sub> catalysts promoted by both Ni and Co. Because a number of important parameters were varied in the preparation of the catalyst, only the main effects were reported. The results of thiophene desulfurization were in agreement with De Beer's earlier<sup>58</sup> data. Also, the promoter effects of Co and Ni for desulfurization were much higher for benzothiophene than for thiophene.

In contrast to the data of Hargreaves and Ross<sup>62</sup>, both Co and Ni seemed to be relatively good promoters for benzene hydrogenation. For this reaction, Ni seemed the better promoter and W the better catalyst, as had been found by Ahuja. This result was not in accord with the data of Farragher and Cossee<sup>39</sup>, who found Co to be a much more effective promoter than Ni for benzene hydrogenation on W catalysts.

Ripperger and Saum<sup>20</sup> tested Co-Mo- $\gamma$ -Al<sub>2</sub>O<sub>3</sub> and Ni-Mo- $\gamma$ -Al<sub>2</sub>O<sub>3</sub> catalysts for desulfurization, hydrogenation, and





denitrogenation activity at medium pressure in a trickle-flow reactor with a solution of thiophene and pyridine in isooctane as the feed. It was found that for a given degree of desulfurization, the Ni catalyst possessed a greater activity than the Co catalyst for both hydrogenation and denitrogenation. In addition, the denitrogenation activity of the Ni catalyst (and to a lesser degree, the Co catalyst) could be significantly increased by treatment with phosphoric acid. It was suggested that the denitrogenation occurs on the nickel surface, and that phosphoric acid hinders migration of the nickel ions into the alumina lattice. This effect was also shown for desulfurization, although the increase in activity was much smaller.

In 1978, Furimsky, Ranganathan, and Parsons<sup>19</sup> compared several Ni- and Co-promoted catalysts for hydrodenitrogenation activity by treating two bitumen distillates in a flow reactor at 14 MPa and 320-420°C. No difference between the two promoters was found; the apparent contradiction between this result and those of previous investigators was explained as possibly due to the inapplicability of low-pressure data to high-pressure industrial processes, or to differences in the preparation of the two catalysts in the various studies.

Recently Furimsky<sup>20</sup> retested the hydrogenolysis activities of Co-Mo- $\gamma$ -Al<sub>2</sub>O<sub>3</sub> and Ni-Mo- $\gamma$ -Al<sub>2</sub>O<sub>3</sub> in a similar reactor to the one used previously. Furimsky again found little difference in desulfurization, denitrogenation, or



deoxygenation activity between the two catalysts, and reiterated his earlier explanations for the discrepancies between his results and those of other researchers.

The only evaluation of the effectiveness of various supports found in the literature is that of De Beer et al.<sup>67</sup>. Based on the activity of supported Co-Mo for thiophene desulfurization, it was found that  $\text{SiO}_2$ ,  $\gamma\text{-Al}_2\text{O}_3$ , and  $\eta\text{-Al}_2\text{O}_3$  were all good supports as long as the specific surface areas were high, but that  $\text{Al}_2\text{O}_3$  was preferred to  $\text{SiO}_2$  because it inhibited the formation of  $\text{CoMoO}_4$ .

In summary, the relative activities of various catalyst formulations are still unclear. Cobalt and nickel appear to be the best promoters for hydrodesulfurization, molybdenum the best catalyst, and  $\gamma$ -alumina the best support. The advantage of these materials over others such as iron, tungsten, and silica do not seem to be large however, and cost may become the determining factor for applications where the rate of fouling is great.

## 2.4 Effect of Catalyst Preparation

The most detailed study concerning the optimum methods of preparation of Ni-Mo- $\gamma\text{-Al}_2\text{O}_3$  catalysts available at present is that of Laine, Pratt, and Trimm. Both the concentration of the active metals<sup>68</sup> and the method of preparation<sup>68</sup> were varied in this study.



The best method of preparation was found to be the sequential impregnation of first Ni and then Mo, a result which would support De Beer's<sup>5,8</sup> hypothesis that catalysts initially approximating the monolayer model would produce a better catalyst even after that structure was no longer in existence.

The best starting salt was found to be nickel acetate, despite the fact that it was only partially soluble in the liquid used for impregnation. It was suggested that a favorable anion should interfere with the adsorption of ammonia, and should form an ammonia salt which would easily escape from the catalyst during the calcining period. This was supported by the finding that catalysts prepared from nickel hydroxide, nickel phosphate, and nickel sulfate were the least active. While ammonium acetate and ammonium nitrate would not be removed more easily than the ammonia, ammonium phosphate and ammonium sulfate produced from the unsuccessful starting compounds, decomposition of the nitrate and acetate would be expected to lead to relatively innocuous anions which could then be removed as, for example, carbon oxides during calcination.

The optimum composition of the catalyst was found to be 3% NiO and 35% MoO<sub>3</sub>, although MoO<sub>3</sub> contents of 10-15% were only slightly less active. Below about 2% NiO, the activity of the catalyst decreased considerably; this was explained as being due to the formation of the inert NiMoO<sub>4</sub>.







## 2.5 Effect of Pretreatment Methods

Calcining, prereduction, and presulfiding are all known to produce higher activity and longer life in hydrodesulfurization catalysts<sup>6,9</sup>. In addition, there may be a relationship between coke formation on the catalyst and catalyst sulfur content<sup>4,1</sup>. Despite this, little data are available in the literature concerning the optimum method of pretreatment of these catalysts.

Calcining has been the least studied of the three pretreatment steps, however the available data on the effects of varying calcination temperature are in good agreement.

In 1977, Ripperger and Saum<sup>2,0</sup> tested the effects of calcining temperature on the activities of Co-Mo- $\gamma$ -Al<sub>2</sub>O<sub>3</sub> and Ni-Mo- $\gamma$ -Al<sub>2</sub>O<sub>3</sub> catalysts. The results of this study showed catalyst activity to be significantly impaired at calcining temperatures above 550°C.

This result was supported in 1979 by Laine, Pratt, and Trimm<sup>6,8</sup>, who used the hydrodesulfurization of thiophene over a Ni-Mo- $\gamma$ -Al<sub>2</sub>O<sub>3</sub> catalyst to test the effects of various pretreatment methods on catalyst activity. An optimum calcination temperature was discovered at about 500°C, and a slow rate of heating of the catalyst to the maximum calcination temperature was found to be necessary to avoid a significant loss of activity. Based on X-ray diffraction studies, the authors hypothesized that above 500°C, loss of catalyst activity through the formation of Al<sub>2</sub>(MoO<sub>4</sub>)<sub>3</sub> was the most important factor, rather than sintering. The lower activity



at lower calcination temperatures was explained as due to insufficient reaction between the various inorganic compounds present on the surface of the catalyst. For example, heating the catalyst too quickly could result in vapor phase transport of intermediates between the uncalcined and calcined phases: if decomposition of nickel nitrate were incomplete, it would be expected to boil, resulting in a loss of nickel in the final catalyst. This scenario was verified by X-ray fluorescence analysis. Adsorption of ammonia onto acidic sites was also cited as a possible factor to explain the differences in activity produced by various calcining procedures.

Prereduction has been studied to a much greater degree than calcining, but the results are not quite so conclusive. This may be partly due to the more complex nature of the chemical changes associated with prereduction, and partly because the effectiveness of a given prereduction temperature may depend more on the conditions seen by the catalyst after the prereduction has finished, i.e. the actual reaction conditions and whether or not the catalyst is presulfided prior to use.

Ripperger and Saum<sup>20</sup> found that no appreciable reduction occurred below 250°C for  $\text{MoO}_3\text{-}\gamma\text{-Al}_2\text{O}_3$  or  $\text{Co-Mo-}\gamma\text{-Al}_2\text{O}_3$  catalysts, and that above 500°C excessive oxygen was lost from the catalyst, resulting in a loss of activity. It was suggested that there was an optimum degree of reduction for catalysts used in the sulfided state: excess oxygen should



be removed from the catalyst, but enough should remain to allow formation of oxysulfides rather than the catalytically less active metal sulfides.

Laine, Pratt, and Trimm<sup>18</sup> also found that the lowest prereduction temperature used (300°C) produced the most active sulfided catalyst, and that a high activity was obtained even though no prereduction was carried out. These authors suggested that a reduction of  $\text{MoO}_3$  to  $\text{MoO}_2$  took place at above about 350°C, which was undesirable because the latter was more difficult to sulfide.

In 1977, Massoth and Kibby<sup>52</sup> used a gravimetric technique to test the effects of various catalyst pretreatment methods on the rate of thiophene hydrodesulfurization over  $\text{Mo-}\gamma\text{-Al}_2\text{O}_3$ . These authors also found that prereduced catalysts sulfided to a lesser extent than those which had not been prereduced, but no correlation with catalyst activity was found. It was also found in this study that for a given prereduction temperature, catalysts used in the reduced state showed a higher activity than sulfided catalysts, although little difference was found between the activities of the optimum prereduced catalysts and the optimum (non-prereduced) sulfided catalysts.

Massoth and Kibby hypothesized that sulfur adsorbed onto the catalyst in two ways during the presulfiding step: by the replacement of oxygen atoms with sulfur atoms, producing extra anion vacancies and thus more active sites, and by the irreversible adsorption of inert  $\text{H}_2\text{S}$  onto the





active sites. At low prereduction temperatures, sulfur was added mainly by exchange with oxygen, while at higher temperatures, adsorption of  $H_2S$  was more important.

In 1980, Gissy, Bartsch, and Tanielan<sup>27</sup> used the conversion of benzothiophene over a Co-Mo- $\gamma$ - $Al_2O_3$  catalyst to test the effect of pretreatment temperature on activity. Sulfiding was found to markedly increase the activity of all catalysts studied. A mild degree of prereduction was found to be beneficial; 250°C was found to be inadequate to produce this effect, but 400° was an effective temperature for prereduction prior to presulfiding.

Presulfiding methods have been studied to an even greater degree than those for prereduction. The results are less conclusive still, and are complicated by the fact that the  $H_2S$  produced in the test reaction tends to affect the level of sulfur on the catalyst and thus obscure the effects of the pretreatment.

Ternan and Whalley<sup>70</sup>, using a Ni-Mo- $\gamma$ - $Al_2O_3$  catalyst in a bottom-feed reactor operating on Athabasca bitumen at high pressure, presulfided with mixtures of hydrogen and either feedstock, carbon disulfide, or hydrogen sulfide at various temperatures and pressures to determine the effects of presulfiding conditions on catalyst performance. These authors found that after 8 hours, the sulfur content of the catalyst approached an asymptotic value, regardless of the presulfiding conditions. Although there were initial differences in catalyst activity, no differences were found after the 8





hour break-in period in any of the properties of the liquid hydrocarbon product. The fraction of coke in the catalyst was also found to be independent of presulfiding conditions.

In 1976, De Beer et al.<sup>21</sup> tested the effects of various presulfiding conditions on the sulfur contents of various catalysts, including Co-Mo- $\gamma$ -Al<sub>2</sub>O<sub>3</sub>. At a presulfiding temperature of 400°C, catalyst sulfur content increased with time, levelling off after about 2 hours. Higher presulfiding temperatures produced higher sulfur contents in the range 250-500°C, and in general, higher sulfur contents correlated with higher hydrodesulfurization activities, based on conversion of thiophene.

Composition of the presulfiding mixture was also tested; an increase in H<sub>2</sub>S:H<sub>2</sub> ratio from 0.04 to 1.0 produced only a 10% increase in sulfur content.

It was also found that as much as 30% of the sulfur present after presulfiding could be removed within 2 hours by subsequent reduction. This surprisingly had no effect on hydrodesulfurization activity, and it was concluded that a significant amount of "mobile sulfur" was present which had no involvement in the desulfurization activity of the catalyst.

The next year, Ripperger and Saum<sup>20</sup>, working with both Co-Mo- $\gamma$ -Al<sub>2</sub>O<sub>3</sub> and Ni-Mo- $\gamma$ -Al<sub>2</sub>O<sub>3</sub> catalysts also used mixtures of either carbon disulfide or hydrogen sulfide as presulfiding agents. In this study, it was found that presulfiding should take place at about 250°C for optimum performance. It



was suggested that complete reduction of the oxides before conversion to oxysulfides was the main reason for the loss of activity when prereduction and presulfiding took place at higher temperatures.

Gissy, Bartsch, and Tanielan<sup>27</sup> in 1980 also found 250°C to be the optimum temperature for presulfiding, and that a high catalyst sulfur content at steady state corresponded to a high catalyst activity. These authors also saw presulfiding as an important step in protecting the catalyst against coking.

Laine, Pratt, and Trimm<sup>18</sup> also tested presulfiding methods in their thiophene hydrodesulfurization studies. While standard presulfiding techniques involve a mixture of 10-15% H<sub>2</sub>S in H<sub>2</sub>, Laine et al. found the most effective presulfiding mixture to be pure H<sub>2</sub>S, and the most effective temperature (when using pure H<sub>2</sub>S) to be 400°C.

In conclusion, the method of catalyst pretreatment appears to have a significant effect on catalyst activity. Calcination should take place at about 500°C, followed by prereduction in hydrogen at about 300°C and presulfiding, for which the data on the optimum method is inconclusive.

## 2.6 On-stream Catalyst Behavior

Catalyst behavior over long periods of time has been one of the least studied aspects of the hydrodesulfurization process. It has been found that the activities of prereduced



catalysts increase from near zero and asymptotically approach much higher values during the first few hours on stream, while presulfided catalysts start off much more active, and level off at a much lower activity after the first few hours on stream<sup>18,27,71</sup>.

De Beer<sup>71</sup> suggests that the increase in activity of prereduced catalysts appears to be due to sulfiding by  $H_2S$  produced in the reaction, while the decrease in activity of sulfided catalysts is due to the establishment of a new oxidation/reduction equilibrium on the catalyst. Although a significant loss of sulfur from the fresh catalyst and a correlation between sulfur content and activity were observed, De Beer hesitated to attribute the initial loss in activity to a loss of sulfur. It was suggested that the high activities found in catalysts which had not been presulfided would have required unreasonably high rates of on-stream sulfidation.

After a catalyst has been on stream for 4 or 5 hours, most researchers have assumed the activity to be constant, and there is little data available in the literature describing catalyst behavior beyond this point.

Rollman<sup>29</sup>, working at high pressure, recorded the activities of his catalysts for dibenzothiophene hydrodesulfurization over a period of several days, but did not detect any change in activity during this time.

Aitken et al.<sup>72</sup>, working with a Co-Mo- $\gamma$ - $Al_2O_3$  catalyst in a trickle-bed reactor did find a linear drop in activity





over a period of hundreds of hours, with the rate increasing exponentially with a decrease in hydrogen partial pressure; this was attributed to coking via dehydrogenation reactions on the catalyst surface.

The only study to date devoted to monitoring the changes in hydrosulfurization catalysts over long periods of time is that of Broderick, Schuit, and Gates<sup>73</sup>. In this study, the hydrosulfurization of dibenzothiophene over a Co-Mo- $\gamma$ -Al<sub>2</sub>O<sub>3</sub> catalyst was studied in a liquid phase flow reactor at 10 MPa and 300°C, with space velocity and amount of H<sub>2</sub>S added to the feed the independent variables. Typically, catalyst activity increased by about 10% over the first 10-20 hours of operation, after which point no change was observed up to 150 hours of operation.

From the results of step changes in the reaction conditions, the authors concluded that at low H<sub>2</sub>S concentrations in the reactor, a decrease in H<sub>2</sub>S concentration resulted in an irreversible loss of catalytic sites, while at higher H<sub>2</sub>S concentrations, changes in this parameter affected the reaction only by the competitive (reversible) adsorptions of dibenzothiophene and H<sub>2</sub>S.

In 1980, Kilanowski and Gates<sup>32</sup> reported a loss in conversion of benzothiophene with time in their flow reactor operating at atmospheric pressure and low conversions. These authors agreed with the hypothesis of Broderick et al.<sup>73</sup>, that the loss in activity was attributable to structural changes in the catalyst associated with sulfur depletion. To



counter this loss in activity, approximately 2%  $\text{H}_2\text{S}$  was added to their feed; this proved successful in stabilizing the catalyst.

Also in 1980, Gissy, Bartsch, and Tanielan<sup>74</sup> reported a similar loss in activity, again desulfurizing benzothiophene over  $\text{Co-Mo-}\gamma\text{-Al}_2\text{O}_3$  in a flow reactor at atmospheric pressure. It was also found that the presence of  $\text{H}_2\text{S}$  eliminated this deactivation, but Gissy et al. concluded that the loss in activity was due to coke formation from the cracking of n-dodecane, the solvent used for benzothiophene. (No solvent had been used in the Kilanowski and Gates study.) It was suggested that the presence of  $\text{H}_2\text{S}$  improves the hydrogenation activity of the catalyst, and in this way interfered with the coking process. Substitution of n-hexane for n-dodecane was found to eliminate the deactivation; on the other hand, substitution of n-dodecene markedly increased the rate of loss of activity.



### 3. DESCRIPTION OF EQUIPMENT

The basic design of the experimental apparatus was that of a fixed bed reactor with on-line gas sampling, similar to that used by Satterfield<sup>6,5</sup>. A flow diagram of the equipment is shown in Figure 3.

The liquid feed to the reactor was a 30% (wt.) solution of benzothiophene (Aldrich Chemical, specified 95% pure, although a chromatographic analysis showed the purity to be approximately 99.8%) in n-hexane (Fisher Chemicals, 99% pure). Gases fed to the reactor were hydrogen (99.9995%), nitrogen (99.998%), and hydrogen sulfide (99.6%), and the carrier gas for the gas chromatograph was helium (99.9999%), all supplied by Union Carbide.

Trace oxygen in the hydrogen and nitrogen streams was converted to water by a Matheson OR-10 catalytic converter. The water was subsequently removed by passing the gas stream through a glass tube 22 mm in diameter packed with 10 cm of 1/16" pellets of Molecular Sieve Type 4A. A 2.5 cm layer of Drierite (indicating calcium sulfate) was located above and below the bed to indicate when the molecular sieve needed replacing. The Drierite and molecular sieve were held in place with plugs of glass wool. Trace water in the helium was removed by passing the gas through a steel tube 1/2" in diameter containing a 35 cm bed of molecular sieve.

Gas flow rates were monitored with Matheson Type 600 rotameters and controlled by needle valves. The hydrogen and





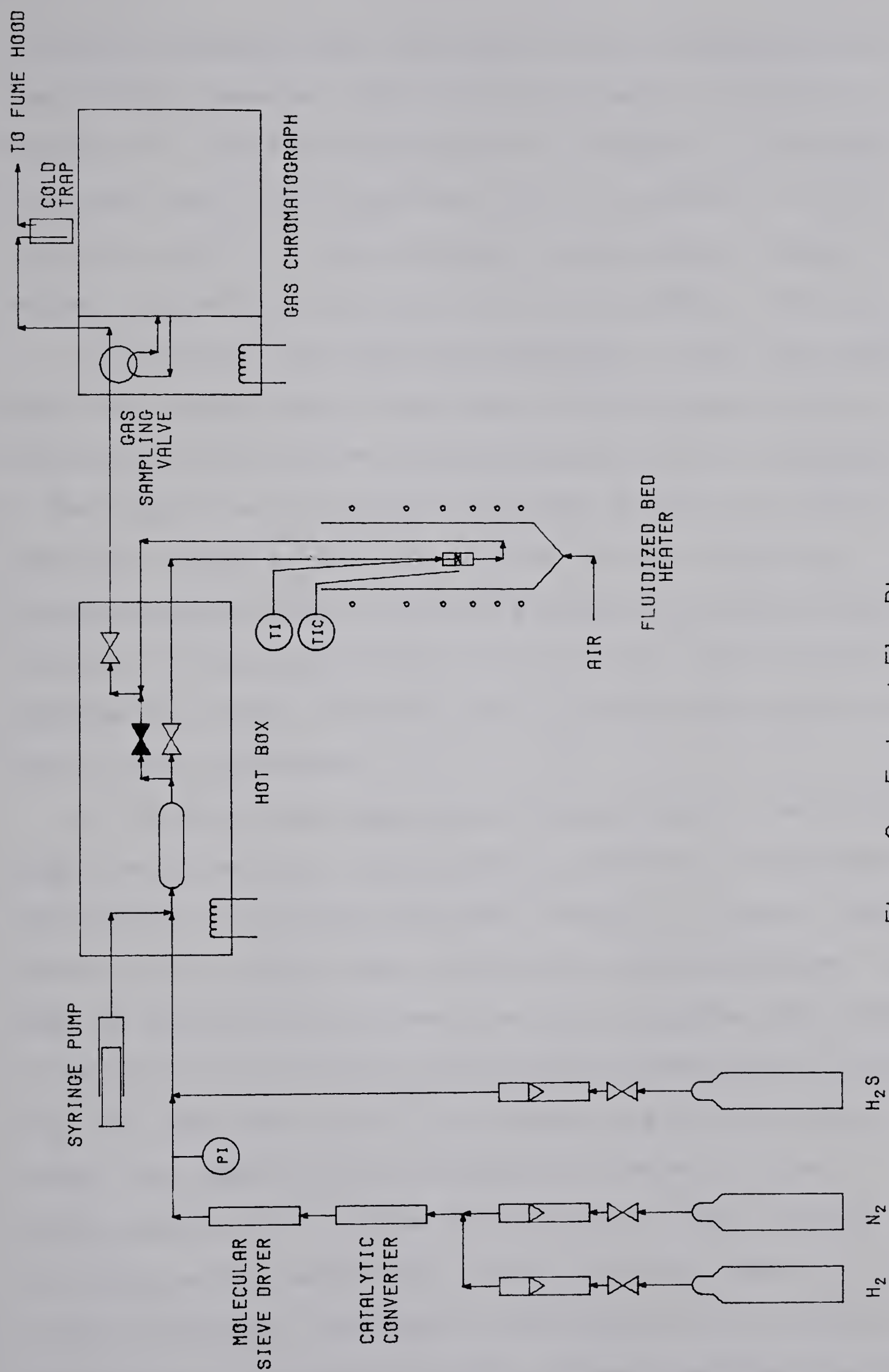


Figure 3 -- Equipment Flow Diagram



nitrogen rotameters were calibrated using a stopwatch and a soap bubble flowmeter (the calibration data are given in Appendix 1), while the manufacturer's supplied calibration curve was used for the hydrogen sulfide rotameter, with a correction made for the difference in molecular weights between the calibration fluid (air) and hydrogen sulfide.

Liquid feed rate was controlled with a Sage Instruments Model 355 syringe pump fitted with a 50 ml glass syringe; calibration data for the syringe pump are given in Appendix 2. The liquid was vaporized in the gas stream in an insulated box heated to 300°C by a strap heater. A mercury-filled barometer used to measure atmospheric pressure and a manometer filled with Meriam fluid (density 1.75) located upstream of the hot box were used to measure the gauge pressure of the gas stream.

A 100 ml cylinder was located downstream of the syringe pump to eliminate any concentration gradients in the feed to the reactor which might have been caused by irregular vaporization of the liquid feed. Preliminary tests had shown that when the liquid feed rate was too high, droplets were formed on the end of the syringe tubing which flashed quickly when they fell onto the wall of the flowing gas stream tubing, rather than vaporizing continuously at the end of the syringe tubing. This caused oscillations in the pressure in the tubing with a magnitude of about 0.25 kPa, measured using the manometer. Because no oscillations were observed during the actual experimentation, it was concluded that any



concentration gradients in the gas stream entering this 100 ml cylinder were very small and would have been eliminated in this tank, although the mean residence time was only 8 s at the highest flow rate used.

The reactor consisted of a 0.1000 g ( $\pm 0.0004$  g) bed of catalyst (depth approximately 5 mm) contained in 1/2" (nom.) stainless steel tubing. The bed was supported by a 100 mesh stainless steel screen, which was in turn supported by a bed of 1.0 mm glass beads. The bottom of the tubing was plugged with a small piece of glass wool, to keep the beads in place while the reactor was operating. The catalyst bed was covered by a 5 mm layer of -40+60 mesh glass beads, to produce a more constant velocity profile of the reactant gas stream when it came into contact with the catalyst. This was covered by a second 5 mm layer of 1.0 mm glass beads to hold the smaller beads in place. Both the glass beads and the stainless steel screen were verified to be catalytically inert prior to experimentation.

The catalyst used was a commercial catalyst, Nalco NM 502, containing 3% Ni and 14% Mo (wt.) supported on  $\gamma$ -alumina, ground in the laboratory and sieved to -40+50 mesh. The surface area'' of the catalyst was 270 m<sup>2</sup>/g, and the pore volume was 0.55 cm<sup>3</sup>/g. The pellet density was 680-780 kg/m<sup>3</sup>.

The reactor was held at a constant temperature in a fluidized bed of 90 mesh Alundum, which was heated externally with nichrome wire. The fluidized bed was





approximately 10 cm in diameter and 30 cm deep when fluidized; the catalyst bed was located approximately 10 cm below the surface of the fluidized bed. The top of the fluidized bed was contained by approximately 6 cm of 1/4" glass Raschig rings, supported on a coarse wire screen. The temperature of the fluidized bed was controlled by a Techne TC4A temperature controller to within 2°C and monitored by a Type J (iron-constantan) thermocouple located close to the reactor tubing at about the same height as the catalyst bed. Temperature in the reactor was measured using a Type J thermocouple inserted into the catalyst bed. (The temperature of the catalyst bed did not differ significantly from that of the fluidized bed at any time.) Pressure in the reactor was held at 101 kPa ( $\pm 3$  kPa) using a globe valve located in the hot box downstream of the reactor. The pressure in the reactor was assumed not to differ significantly from that of the gas stream as measured by the manometer upstream of the syringe feeder.

The products were sampled with a Valco model V-4-HT gas sampling valve (internal volume 3  $\mu$ l) located in an insulated steel box mounted on the side of the gas chromatograph and heated to approximately 250°C by a strap heater. Analysis was performed using a dual column F & M 720 gas chromatograph; the conditions under which this analysis was performed are summarized in Table 1. The sampling valve, injection port, and detector temperatures shown are approximate, and varied by about  $\pm 5^\circ$  over the course of this study. The



## Table 1 - Summary of Chromatographic Analysis Conditions

Column: Length: 10'

Diameter: 1/8"

Packing: Dexsil 300 on 80/100 Chromosorb W/AW

Carrier gas: Helium

Flow Rate: 40 cm<sup>3</sup>/min

Detector Type: Thermal Conductivity

Current: 150 ma

Temperatures: Gas Sampling Valve: 260°C

Injection Port: 200°C

Detector: 260°C

Temperature Programming: Rate: 10°/min

Initial Temperature: 40°C

Final Temperature: 190°C

Total Analysis Time: 15 min



flow of carrier gas was checked regularly with a soap bubble flowmeter. Output from the gas chromatograph was integrated and recorded using an HP 3380A integrator.

To illustrate the degree of separation of the major components of the product stream, a typical chromatogram is shown in Figure 4. (Note that the peak heights have been plotted on a logarithmic scale, and as a result the relative peak areas may be deceptive.)

Liquid products were collected in a glass condenser held at room temperature (approximately 22°C) to obtain a concentrated sample of the heavier products for qualitative analysis. Non-condensibles were vented to a fume hood. No mass balances were computed for either the liquid products or the gas stream leaving the condenser.

All equipment in direct contact with the reactants or products was constructed of Type 316 stainless steel unless noted otherwise. All equipment was connected with 1/4" tubing, except the line from the syringe pump to the flowing gas stream and the lines connecting the gas sampling valve to the columns, all of which were 1/16". All lines between the reactor, hot box, sampling valve, and condenser were electrically traced with "Heats-by-the-Yard" and insulated. The temperatures of these lines were monitored with Type J thermocouples inserted under the tracing. The voltages across each strap heater and section of tracing were controlled manually using Variac variable voltage transformers.





RT	TYPE	AREA	AREA %
1.07		37373	40.86
1.80	M	37192	40.66
5.75		2201	2.406
6.64		283	.3094
12.00		14229	15.56
13.17		195	.213 2

HP 3380A  
DLY OFF  
MV/M .03

STOP 15  
ATTN LOG

REJECT OFF

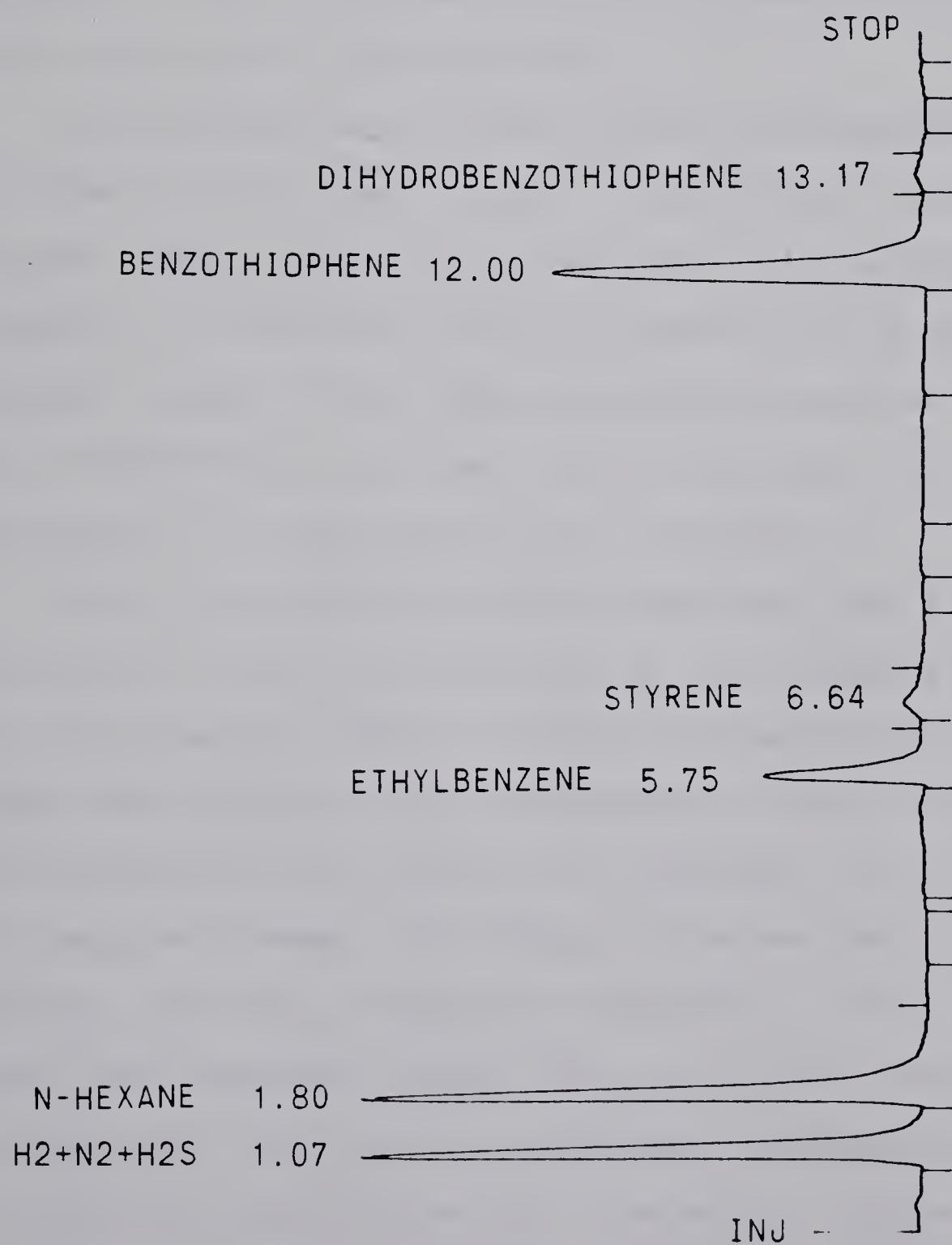


Figure 4 - Sample Chromatogram



## 4. EXPERIMENTAL PROCEDURE

### 4.1 Catalyst Pretreatment

No tests were done in the present study to assess the effects of various pretreatment methods. Instead, it was decided to use the basic method of Ripperger and Saum<sup>20</sup>: 5 hours calcining in air at 500°C, followed by 4 hours prere-duction at 250°, followed by 4 hours presulfiding at 250° with a mixture of 10% H<sub>2</sub>S in H<sub>2</sub>.

The catalyst was ground, sieved and graded as to particle size, and calcined in air at 500°C for 5 hours. Following the suggestions of Laine et al.<sup>68</sup>, the catalyst was heated to the maximum calcining temperature as slowly as possible, about 2°/min. This heatup time was not included in the 5 hours calcining time. After calcining, the catalyst was stored in a desiccator until required.

When a new catalyst bed was required, the fluidized bed was cooled to 250°C and the system was flushed with nitrogen. The reactor tube was cleaned and packed with the glass beads and catalyst, then transferred to the fluidized bed and connected to the rest of the equipment. The nitrogen flow was terminated, the hydrogen flow was set at 50 cm<sup>3</sup>/min, and the pressure was adjusted to 101 kPa. After 4 hours, the hydrogen sulfide flow was set at 5 cm<sup>3</sup>/min, while the hydrogen flow was left unchanged. After another 4 hours, the hydrogen sulfide flow was terminated, and the reactor



operating conditions were set at the desired values.

#### 4.2 Reactor Operation

When the pretreatment had ended, the fluidized bed temperature controller was reset to the desired reaction temperature, the syringe pump was started, the hydrogen flow rate was reset, and the pressure was adjusted. This was considered the start of reactor operation.

After the reactor temperature had risen to the desired value, (the temperature of the fluidized bed could be raised by about  $10^{\circ}/\text{min}$ ) and a stabilization period of about 15 minutes had passed, gas samples from the product stream were taken at varying intervals and analyzed for the next 25 to 30 hours, after which the run was terminated and the catalyst discarded.

The syringe usually had to be refilled at least once during a run. When this became necessary, the gas flow was terminated and the syringe was disconnected from the rest of the apparatus and refilled. This usually took about 5 minutes, during which time the connection between the syringe and the gas stream was kept sealed. A period of at least 15 minutes after the syringe was reconnected and the gas flow restarted was allowed for reactor conditions to restabilize before sampling was resumed.

When either the syringe was refilled (i.e. a new liquid feed batch) or a new catalyst bed was installed, the





subsequent gas samples were considered to constitute a new series. Approximately halfway through each series, the following data on the operating conditions were taken: atmospheric pressure, reactor gauge pressure, hydrogen and nitrogen rotameter readings, syringe feeder setting, and fluidized bed temperature set point.

When a new catalyst bed had been installed and the reactor was operating, the reactor temperature was monitored for a period of about 15 minutes using the thermocouple located in the catalyst bed itself. Since no significant differences were ever found between these readings and those from the fluidized bed temperature controller, no record was kept of these data. At this time, the temperatures of the hot box, gas chromatograph detector, sampling valve and injection ports were also checked.

Solutions of benzothiophene in n-hexane were made up as required. Typically, a 100 g bottle of benzothiophene was first heated in a steam bath to liquify the contents. (The melting point of benzothiophene is  $32^{\circ}\text{C}^{75}$ .) This was added to a 500 ml flask containing 200 ml of n-hexane plus any solution left over from the previous batch. Another 100 ml of n-hexane was used to dissolve any residual benzothiophene remaining in the original bottle; this was also added to the 500 ml flask. The flask was then sealed with a ground glass stopper, shaken to mix the contents thoroughly and dissolve any benzothiophene which might have crystallized on the sides or in the neck, and left to cool to room temperature





in a fume hood. These solutions were intended to have an approximate benzothiophene/n-hexane weight ratio of 0.4. This value was chosen so that the solution would be concentrated enough to minimize refilling of the syringe during reactor operation, but still be dilute enough that the reaction products would not solidify in the condenser.

The high volatility of n-hexane resulted in slight differences in concentration of the contents of the syringe between one series of gas samples and the next series after it had been refilled, due to such factors as evaporation in the storage bottle subsequent to the previous filling of the syringe, evaporation during the transfer of solution from bottle to syringe, and differences in the original composition of the solution as it was made up. Cooling the solution was impractical, since benzothiophene would start to crystallize out of solution at temperatures only slightly below room temperature. It was impossible to sample the contents of a given syringe directly in many cases (such as when the syringe was refilled in the middle of a run), so instead it was decided to calculate the composition of the feed solution from a molar balance based on an analysis of the product stream. The details of this calculation are given in the next chapter.

When the reactor was not in operation, all equipment was kept hot (above 250°) and a small flow of nitrogen was kept running through all lines.



The products of typical runs were condensed at room temperature and compared to a sample of "condensed feed", produced by injecting the liquid feed into the flowing gas stream and recondensing it after it had bypassed the reactor. These products were qualitatively analyzed by a combination of gas chromatography and mass spectrometry.



## 5. EXPERIMENTAL

A summary of the run conditions is given in Table 2. Where the series numbers are not consecutive, this indicates that the accumulated data for a single run ("Data Point") is a composite of data from two separate catalyst beds.

All experiments were conducted with hydrogen present in great excess. The hydrogen and benzothiophene partial pressures in the feed to the reactor were held fairly constant at about 97 and 1.7 kPa, respectively. The temperatures used were 350, 400, and 450°C, and 7, 5, and 4 data points were obtained at each of these respective temperatures. At each temperature, runs were performed with the space time ranging from  $1 \times 10^4$  to  $7 \times 10^4$  g catalyst-s/mol benzothiophene.

To verify the absence of internal mass transfer limitations, one run (Data Point 6) was performed using a significantly smaller catalyst pellet size than was used in the other runs (-60+70 mesh, as opposed to -40+50). It was assumed that if the absence of internal diffusion effects could be shown, it would also eliminate the possibility of external mass transfer limitations on the reaction.

Although the thermocouple inserted in the catalyst bed gave some evidence against any significant thermal gradients in the bulk phase, it could not rule out completely the possibility of internal or external heat transfer limitations on the reaction rate. This reaction is highly exothermic, and if the entire heat load from the reaction were absorbed





Table 2 - Summary of Run Conditions

Data Point	T (°C)	W/F $\times 10^{-4}$	p(BT) kPa	p(H <sub>2</sub> ) kPa	Series
1	400	5.912	1.74	102.60	62,63
2	400	4.750	1.28	97.32	73,74
3	400	1.244	1.77	97.24	75,76,96
4	400	3.031	1.65	96.97	90,91
5	400	2.947	1.87	91.10	92,93
6	400	4.011	1.73	96.10	94,95
7	400	1.947	1.60	101.35	68,69,70,97
8	450	5.991	1.65	96.15	80
9	450	2.057	1.34	96.73	83,84,85
10	450	1.227	1.79	97.55	86,87,88,89
11	450	4.057	1.63	96.29	79,98
12	450	3.082	1.53	96.71	81,82,99
13	350	5.500	1.68	95.08	113,114
14	350	3.001	1.54	97.94	102,103,104
15	350	3.636	1.90	96.41	115,116
16	350	6.031	1.44	97.63	108



by the gas stream, it is estimated that the rise in temperature would be approximately 50°C (cf. Appendix F).

To test this, one run (Data Point 5) was made with about 9% of the hydrogen in the feed replaced with nitrogen. If the mass heat capacities of the two gases were similar, this would increase the specific heat of the mixture by about 25%. However, calculations made subsequent to the actual experimentation showed that these mass heat capacities differed greatly, and that the effect of substituting hydrogen with nitrogen on heat capacity was negligible.

Another data point (Point 4) was run using a more dilute liquid feed solution than in the other runs (0.34 rather than 0.43 wt. ratio benzothiophene to n-hexane); this was estimated to have increased the specific heat of the mixture by about 6%. Two more data points (Points 13 and 14) used a more concentrated solution (0.51) than normal; this was estimated to have decreased the specific heat of the mixture by about 9%.



## 6. DATA ANALYSIS

All calculations described in the following sections were done using the computer programs listed in Appendix 5, unless noted otherwise. A sample output from the main data analysis program is shown in Table 3. This series was chosen because it represents both an entire data point (Point 5) and a single complete liquid feed batch. The chromatogram shown in Figure 4 represents Run 18 in this series.

### 6.1 Calculation of Reactor Operating Conditions and Feed Rates

Reactor temperature for any data point was considered identical to the set point of the fluidized bed temperature controller. Total pressure in the reactor was calculated as the sum of atmospheric pressure and the gauge pressure measured by the manometer upstream of the syringe pump. (It was assumed that the pressure losses caused by the 1/4" tubing and the glass beads above the catalyst bed and the bed itself were negligible.)

Volumetric flow rates of hydrogen and nitrogen were computed by fitting third- and fourth-order polynomials respectively to the calibration data using the method of least squares (cf. Appendix 1). Molar flow rates were calculated assuming ideal gas behavior.

Calculation of the flow rates of n-hexane and benzothiophene was more complex. Calibration data for the





Table 3 - Sample Output from Data Analysis Program

SERIES 92  
800123

TOTAL PRESSURE IN REACTOR: 104.59 KPA  
TEMPERATURE IN REACTOR: 673.2 DEG. K  
CATALYST: NALCO NM 502, 0.1002 G., -40+50 MESH  
CATALYST BED NUMBER: 23  
LIQUID FEED BATCH NUMBER: 36  
FEED RATES TO REACTOR:

H2: 0.1672E-03 GMOL/SEC  
BT: 0.3420E-05 GMOL/SEC  
HEX: 0.6826E-05 GMOL/SEC  
N2: 0.1340E-04 GMOL/SEC

PARTIAL PRESSURES OF FEED TO REACTOR:

H2: 91.63 KPA  
BT: 1.87 KPA  
HEX: 3.74 KPA  
N2: 7.34 KPA

W/F= 0.2930E+05 G-SEC/GMOL(BT)

RAW DATA (AREA %):

RUN	N2+H2 +H2S	N-HEXANE	ETHYL- BENZENE	STYRENE	BENZO- THIOPHENE	DIHYDROBENZO THIOPHENE
1	39.7765	43.3200	2.8470	0.0193	14.0100	0.0
2	40.0670	42.4100	2.5060	0.0	14.8300	0.0
3	40.6509	42.0400	2.6660	0.0	14.6500	0.0
4	43.7300	38.0400	2.7270	0.0	15.3000	0.1859
5	42.7600	40.1900	2.5360	0.0	14.4600	0.0
6	43.1632	39.3900	2.6610	0.0534	14.5200	0.0
7	41.5336	41.7900	2.5520	0.0	14.0100	0.0
8	41.6775	40.9200	2.4150	0.0	14.8800	0.0361
9	42.3756	39.8500	2.4650	0.0	15.1500	0.1322
10	39.8329	43.9200	2.3020	0.0	13.9100	0.0344
11	40.3800	42.7600	2.4060	0.1629	14.1500	0.0
12	44.0360	38.5700	2.6010	0.0	14.7600	0.0
13	40.2400	42.4600	2.5820	0.0305	14.6900	0.0
14	37.9236	44.6100	2.3330	0.0655	15.0600	0.0
15	38.3500	44.6800	2.8410	0.0860	14.0500	0.0
16	40.5959	40.9100	2.5580	0.0	15.6700	0.0
17	38.7200	43.8700	2.3510	0.0	14.9000	0.0647
18	40.8600	40.6600	2.4060	0.3094	15.5600	0.2132
19	37.8500	44.3700	2.3240	0.1304	15.2600	0.0
20	41.2700	40.6100	2.5790	0.0	15.2300	0.1217
21	37.9300	44.5800	2.2850	0.0	14.8400	0.0672
22	42.7300	39.4100	2.3960	0.0	15.2900	0.1004
23	43.0700	39.6100	2.3040	0.0572	14.9200	0.0
24	42.4700	39.2200	2.4740	0.0	15.8400	0.0
25	38.9100	43.0900	2.3280	0.0	15.3900	0.0
26	42.9600	38.5500	2.6930	0.0	15.6900	0.0
27	38.9500	42.8900	2.6850	0.0	15.3800	0.0641
28	40.9800	41.0600	2.4860	0.0	15.4300	0.0476
29	41.2400	41.0000	2.1170	0.0	15.5300	0.0
30	45.1200	37.3800	2.1170	0.0	15.1700	0.0
31	39.3600	42.3400	2.7230	0.0	15.4700	0.0
32	39.3652	43.1600	2.1700	0.0	15.1200	0.0
33	41.3000	41.9200	2.2900	0.0	14.4000	0.0610
34	40.8700	41.8100	2.1260	0.0	15.1200	0.0452
35	40.8100	42.0900	2.1830	0.1189	14.5900	0.0522
36	40.9500	41.6700	2.1960	0.1023	14.9700	0.0900



Table 3 (cont.)

37	42.4600	40.4000	2.2460	0.0	14.8700	0.0
38	39.8200	42.4800	2.1010	0.0314	15.3800	0.0
39	44.0400	37.7200	2.1480	0.0	16.0800	0.0

## LIQUID FEED COMPOSITION BASED ON MASS BALANCE (WT. RATIO):

RUN	BT/HEX
1	0.415425
2	0.433518
3	0.437722
4	0.508265
5	0.448947
6	0.465315
7	0.421179
8	0.448654
9	0.471679
10	0.392046
11	0.415453
12	0.477912
13	0.432769
14	0.414391
15	0.405397
16	0.472103
17	0.417778
18	0.482340
19	0.422835
20	0.468145
21	0.407936
22	0.477575
23	0.461886
24	0.494204
25	0.434830
26	0.505943
27	0.448601
28	0.463342
29	0.454029
30	0.488106
31	0.456208
32	0.423094
33	0.423040
34	0.436525
35	0.426088
36	0.440563
37	0.448008
38	0.435034
39	0.509521

## FRACTIONAL CONVERSION OF BENZOTHIOPHENE:

RUN	TIME	TO EB:	TO STY:	TO DHBT:	EB+STY:
1	1.667	0.198996	0.001340	0.0	0.200336
2	2.000	0.171453	0.0	0.0	0.171453
3	2.333	0.182237	0.0	0.0	0.182237
4	2.917	0.177416	0.0	0.009731	0.177416
5	3.583	0.176797	0.0	0.0	0.176797
6	3.917	0.182621	0.003640	0.0	0.186261
7	4.500	0.182381	0.0	0.0	0.182381
8	4.833	0.165466	0.0	0.001990	0.165466
9	5.250	0.164961	0.0	0.007118	0.164961
10	5.583	0.168168	0.0	0.002022	0.168168
11	5.917	0.170363	0.011458	0.0	0.181821
12	6.333	0.177493	0.0	0.0	0.177493



Table 3 (cont.)

13	10.333	0.176749	0.002074	0.0	0.178823
14	10.583	0.158749	0.004427	0.0	0.163176
15	10.917	0.197295	0.005933	0.0	0.203228
16	11.167	0.166599	0.0	0.0	0.166599
17	11.500	0.161353	0.0	0.003573	0.161353
18	11.833	0.154317	0.019713	0.011003	0.174030
19	12.167	0.155817	0.008685	0.0	0.164502
20	12.583	0.170638	0.0	0.006479	0.170638
21	12.917	0.158049	0.0	0.003740	0.158049
22	13.250	0.160131	0.0	0.005399	0.160131
23	13.667	0.158409	0.003907	0.0	0.162316
24	14.167	0.160555	0.0	0.0	0.160555
25	14.500	0.156288	0.0	0.0	0.156288
26	14.750	0.173680	0.0	0.0	0.173680
27	15.083	0.175536	0.0	0.003372	0.175536
28	15.417	0.164369	0.0	0.002532	0.164369
29	16.833	0.143051	0.0	0.0	0.143051
30	17.167	0.145950	0.0	0.0	0.145950
31	17.500	0.177326	0.0	0.0	0.177326
32	17.833	0.149479	0.0	0.0	0.149479
33	18.167	0.162432	0.0	0.003481	0.162432
34	18.417	0.146525	0.0	0.002507	0.146525
35	18.750	0.153113	0.008284	0.002946	0.161398
36	19.083	0.150466	0.006963	0.004962	0.157429
37	19.500	0.156092	0.0	0.0	0.156092
38	19.750	0.143007	0.002123	0.0	0.145130
39	20.083	0.140585	0.0	0.0	0.140585
MEAN:		0.164997	0.002014	0.001817	0.167011
+/-		0.004562	0.001336	0.000928	0.004635

LIQUID FEED BATCH: 36

COMPOSITE MASS BALANCE BASED ON 39 DATA POINTS  
AVG. FEED RATIO BT/HEX: 0.4484 +/- 0.0098





syringe pump yielded a linear relationship between volumetric flow rate and flow setting (cf. Appendix 5). It had been verified that the volumes of solid benzothiophene and liquid n-hexane were additive in forming solutions in the range of concentrations of interest (cf. Appendix 4), and so, given the relative concentrations of benzothiophene and n-hexane in the solution, the molar flow rate could be readily calculated.

The concentration of the liquid feed solution was estimated from an analysis of the product stream. Since one mole of each of the reaction products, ethylbenzene, styrene, and dihydrobenzothiophene, represents one mole of benzothiophene in the original feed, and since these three products comprised an estimated 99.5% of the total reaction products, the mole ratio (and thus weight ratio) of "equivalent benzothiophene" to n-hexane could be calculated for each gas sample. These weight ratios were averaged to give a value for each liquid feed batch. The values of liquid feed concentration obtained from this method were precise to within about 3% based on 95% confidence limits; this precision varied from about 1% to 5% depending mainly on the number of mass balances averaged to obtain this concentration.

The space time of benzothiophene for each series of gas samples was calculated as the quotient of the catalyst bed mass and the molar feed rate of benzothiophene computed from the mean batch composition for that series. The space time for each data point was calculated as a weighted mean of the





space times of each series of samples used to generate that point:

$$\tau_p = \Sigma(ns \times \tau_s) / \Sigma(ns) \quad (1)$$

where:

$\tau_s$  = space time for a given series

$\tau_p$  = space time for a given data point

$ns$  = total number of gas samples in a given series

The partial pressure of each feed component was calculated for each series as the product of the mole fraction of that component in the feed and the total pressure.

Because space time for a given data point was calculated from the molar feed rate of benzothiophene to the reactor, which was in turn based on an analysis of the product stream, a relationship is introduced between the measurement errors of the independent variable, space time, and the dependent variable, rate of conversion of benzothiophene. Consequently, any subsequent statistical analyses which were based on this assumption (such as nonlinear regression) are technically invalid. The relationship between the errors of these two variables appeared to be fairly weak, however, and for this reason it was assumed that no serious errors should result from this slight relaxation of statistical rigor.



## 6.2 Calculation of Fractional Conversions of Reactants to Products

For each gas sample, the fractional conversions of benzothiophene to ethylbenzene, styrene, and dihydrobenzothiophene were calculated as the quotients of the molar concentrations of each product in the sample and the total of the molar concentrations of these four components in the sample.

It was discovered early in the course of this study that the fractional conversion of benzothiophene to ethylbenzene decreased noticeably with time. Typically, the catalyst activity would decay quickly for the first 0 to 3 hours, after which time the rate of loss of activity would decrease, reaching a constant value after about 5 to 10 hours and continuing for as long as it was monitored (40 hours in the longest case).

Kilanowski and Gates<sup>3,2</sup> had independently found this same phenomenon, and had eliminated it by adding small quantities of  $H_2S$  to their feed. Rather than introduce any additional variables into this study, (i.e. the competitive adsorption between  $H_2S$  and benzothiophene), it was decided to eliminate the effects of a decay in catalyst activity by applying a transformation to the data. To obtain a consistent value for catalyst activity, a hypothetical "zero-time activity" was defined, representing that activity which the catalyst would have had if it were in equilibrium with its surroundings at the moment it went on stream, before the



long-term linear decay had had any effect. To obtain an estimate of this, a function of the following form was fitted<sup>76</sup> to the data:

$$F = C_1 + C_2 * t + C_3 * \exp(C_4 * t) \quad (2)$$

where:

F= Fractional conversion to ethylbenzene

t= Time

$C_1, C_2, C_3, C_4$  = Parameters to be fitted by the method of least squares

The following constraints were placed on the parameters:

$$0.0 < C_1 < 1.0 \quad (2a)$$

$$-1.0 < C_2 < 0.0 \quad (2b)$$

$$0.0 < C_3 < 1.0 \quad (2c)$$

$$-1.0 < C_4 < -0.3 \quad (2d)$$

The linear portion of this function was extrapolated back to the ordinate, and this initial value of fractional conversion (i.e.  $C_1$ ) was the value subsequently used. Two further advantages of this treatment of the data were that it enabled all of the data from a given catalyst bed to be used, and it avoided the necessity of making any arbitrary decisions concerning the length of time required for a catalyst bed to reach steady state.





While the constraints on the parameters may seem considerable, their removal had virtually no effect on the resultant values of  $C_1$  in any of the cases examined. Further, there was in most cases some physical justification for their use.

The reasons for the upper and lower limits on  $C_1$  are self-evident: fractional conversion must by definition fall between zero and unity.

The upper limit on  $C_2$  precluded a steady state increase in activity; while this boundary was encountered in one instance, there was no statistical justification for its elimination. The lower limit on  $C_2$  was arbitrary; in any case it was never encountered.

Forcing  $C_3$  to be positive precluded the possibility of catalyst activity increasing initially and later decreasing. Although this physical situation was never encountered, the mathematical constraint frequently was. If the decay in catalyst activity was linear by the time that sampling began (as it occasionally was) and if the residual error of the first sample was negative, then the curve fitting program would attempt to force a negative  $C_3$  (and a positive  $C_4$ ) in order to better accommodate this point. The lower boundary on  $C_3$  was designed to counteract this. The upper boundary on  $C_3$  theoretically should be  $(1-C_1)$  and not 1, since  $(C_1+C_3)$  represents the extrapolation of the experimental data to time zero, and it is this value which must be kept below unity. Neither value for the upper limit of  $C_3$  was



approached in this study, however.

The lower limit on  $C_4$  was again chosen to counteract the problem of the residual of the first gas sample affecting the shape of the exponential portion of the fitted curve. A value of 1.0 seemed to keep the problem reasonably well under control while still leaving enough flexibility to allow a good fit for the cases in which there actually was a large initial rate of decay. The upper limit on  $C_4$  was chosen to force the fitted curve to become linear after a maximum of about 15 to 20 hours.

In Table 3, it can be seen that there is a very large amount of scatter in the measurements of the concentrations of styrene and dihydrobenzothiophene, and that the amounts of these compounds in the gas sample are very close to the minimum that could be detected by the gas chromatograph. Because of this, no conclusions could be drawn concerning a relationship between the fractional conversions to these compounds and the time that the catalyst had been on stream, and it was decided instead to calculate the fractional conversion for a given data point as the mean of the values for each individual gas sample. It should be noted that the errors in the fractional conversions to these two compounds is probably very large - both the fact that catalyst deactivation was not taken into account and the fact that these data were taken so close to the limits of detection of the apparatus would tend to yield values of conversion lower than the actual ones.



## 7. RESULTS AND DISCUSSION

### 7.1 General

The three main products from this reaction (if  $H_2S$  is not considered) were ethylbenzene, styrene, and dihydrobenzothiophene. Ethylbenzene was the dominant product, and comprised over 95% of the organic carbon in the products in all but two of the cases studied. Thus, many features of the overall reaction can be approximated by a study of this one component.

The time-dependence of the fractional conversion of benzothiophene to ethylbenzene for each run is shown in Figures 5a through 5p. Where the use of a second catalyst bed was necessary to supplement the data for a particular set of reaction conditions, the data from this second bed have been shown as '+'s rather than 'x's. The constants of the exponential curves which were fitted to these data are summarized in Table 4. In all cases, the curves appeared to fit the data extremely well.

The shapes of these curves were similar for all runs: either the rate of loss of activity was rapid at first, decreasing asymptotically to a constant, or else the rate of deactivation was essentially constant from the time that sampling was started. This is in agreement with the results of most desulfurization studies reported in the literature.

The only exception to this behavior was for data point 12. The low conversions obtained during the first 5 hours of



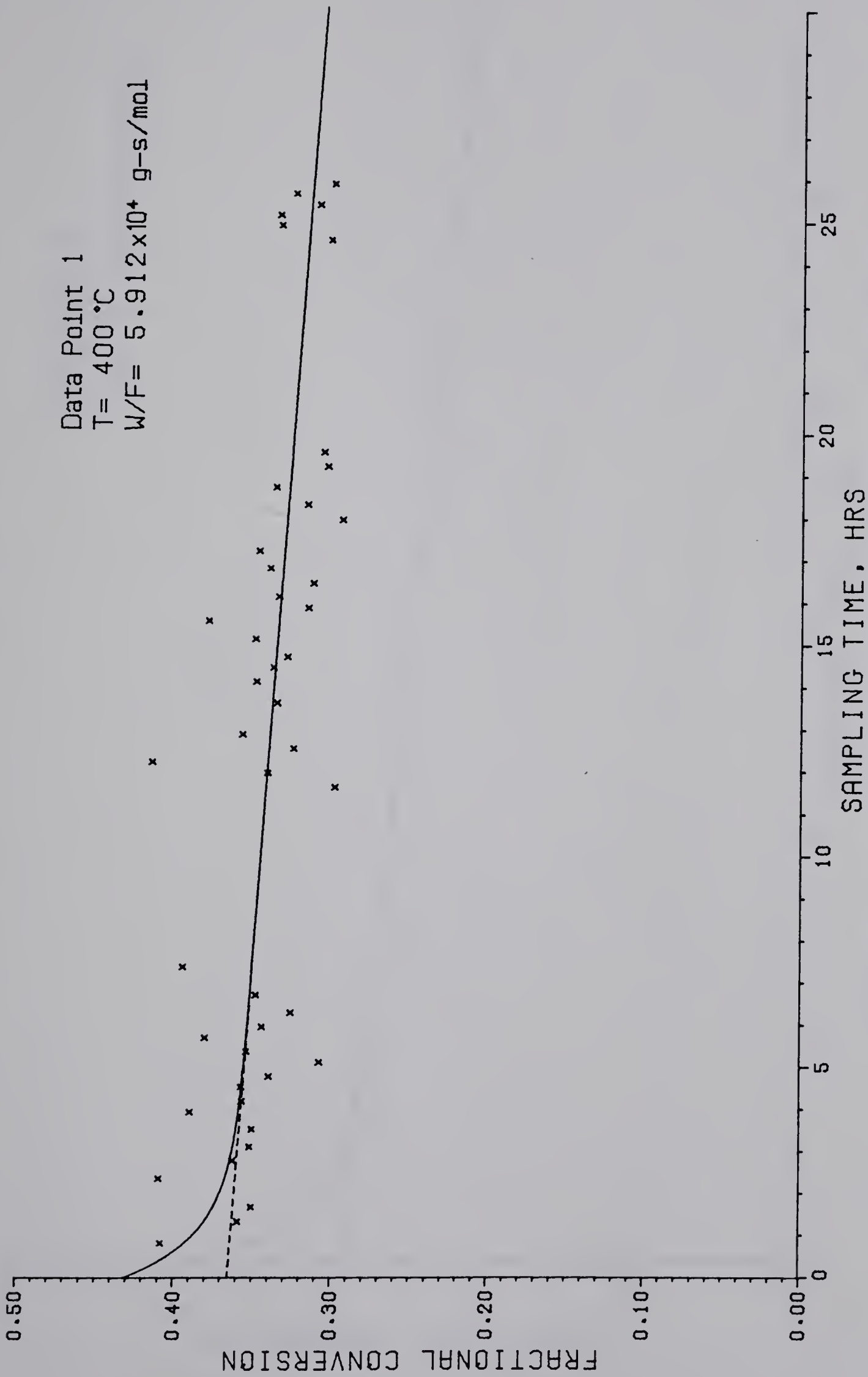


Figure 5a - Time-dependence of Fractional Conversion to Ethylbenzene





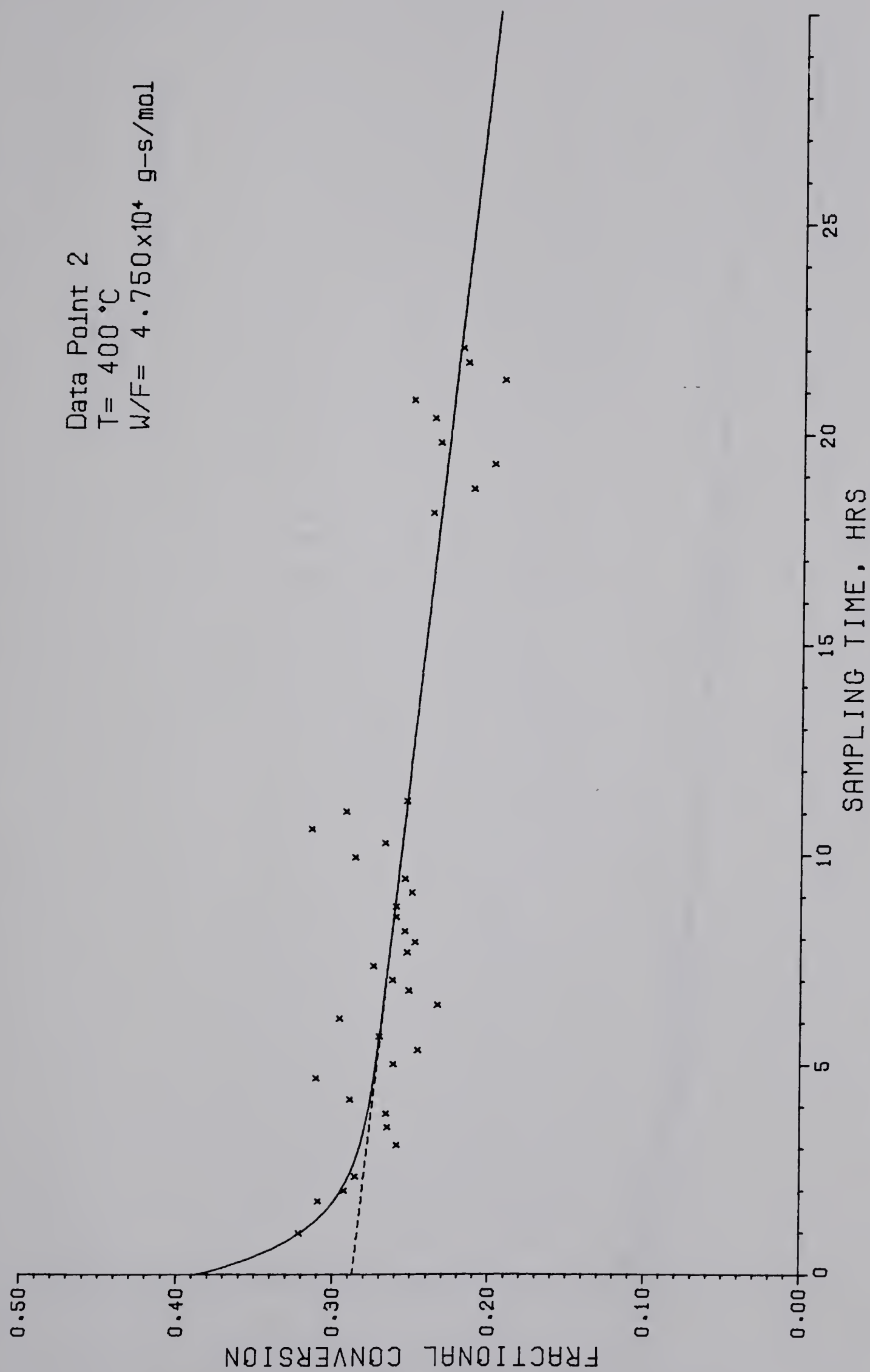


Figure 5b - Time-dependence of Fractional Conversion to Ethylbenzene



Data Point 3  
T= 400 °C  
W/F=  $1.244 \times 10^4$  g-s/mol

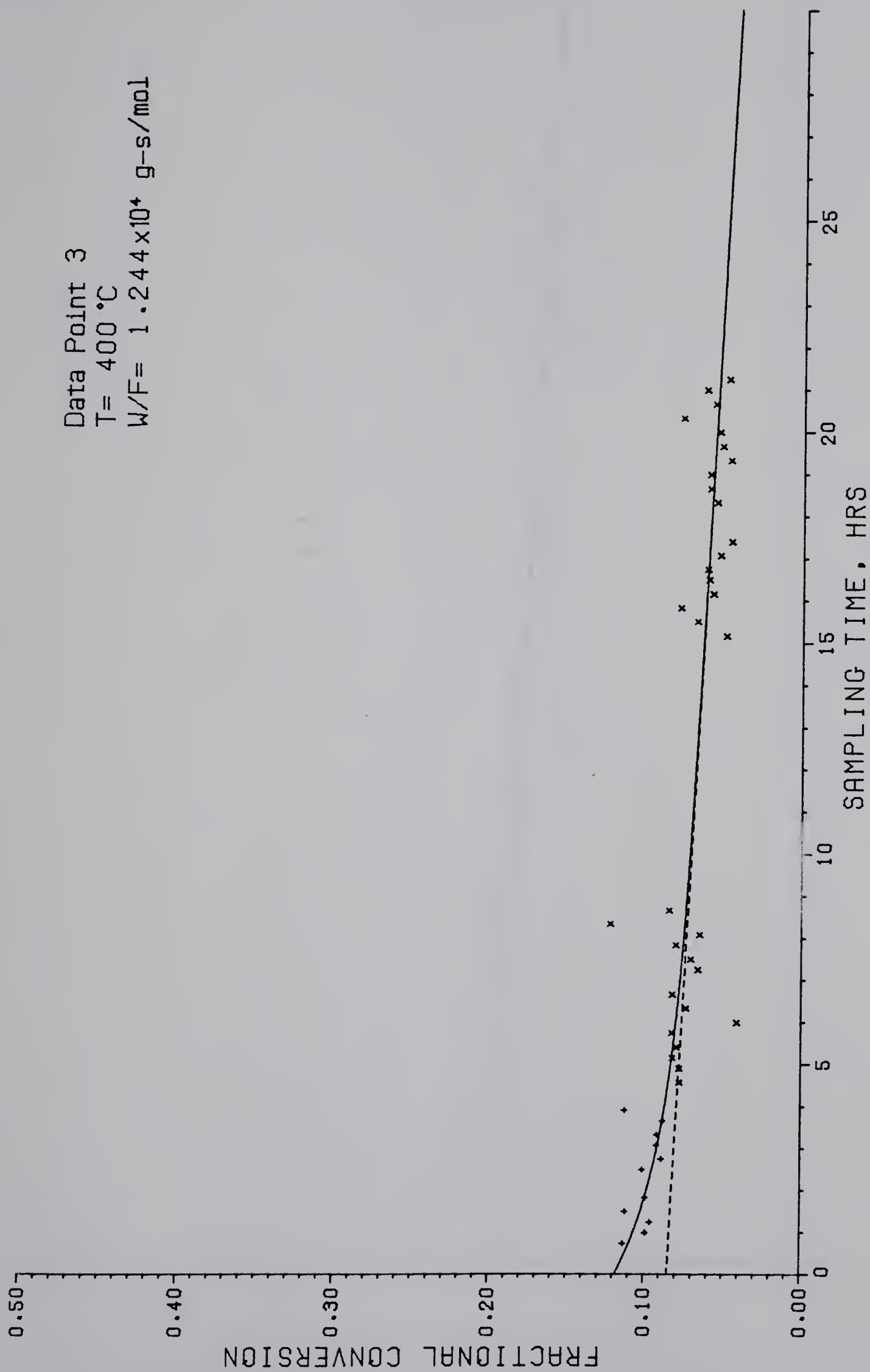


Figure 5c - Time-dependence of Fractional Conversion to Ethylbenzene



Data Point 4  
T= 400 °C  
W/F=  $3.031 \times 10^4$  g-s/mol

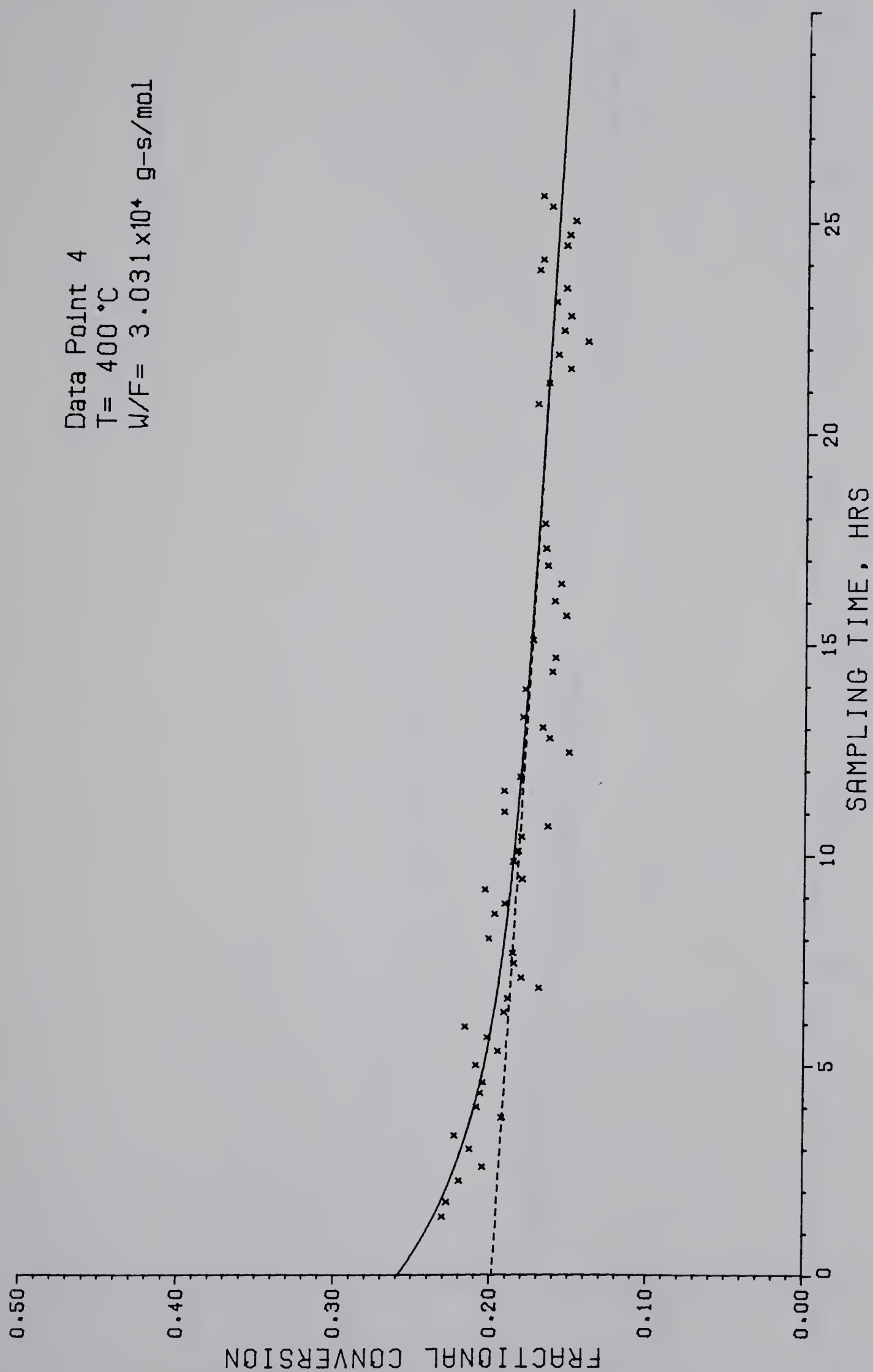


Figure 5d - Time-dependence of Fractional Conversion to Ethylbenzene





Data Point 5  
T= 400 °C  
W/F=  $2.947 \times 10^4$  g-s/mol

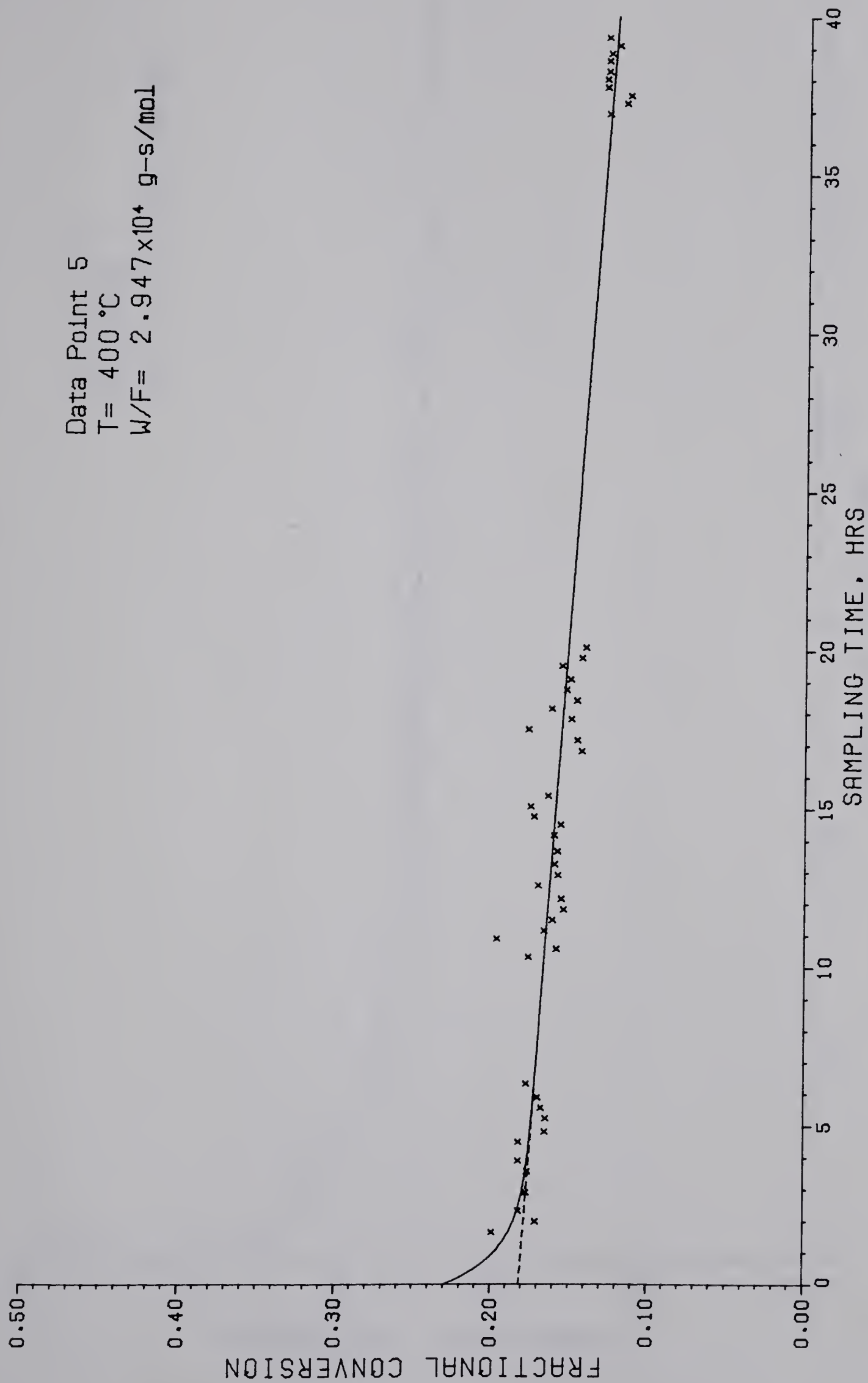


Figure 5e - Time-dependence of Fractional Conversion to Ethylbenzene



Data Point 6  
 T= 400 °C  
 W/F=  $4.011 \times 10^4$  g-s/mol

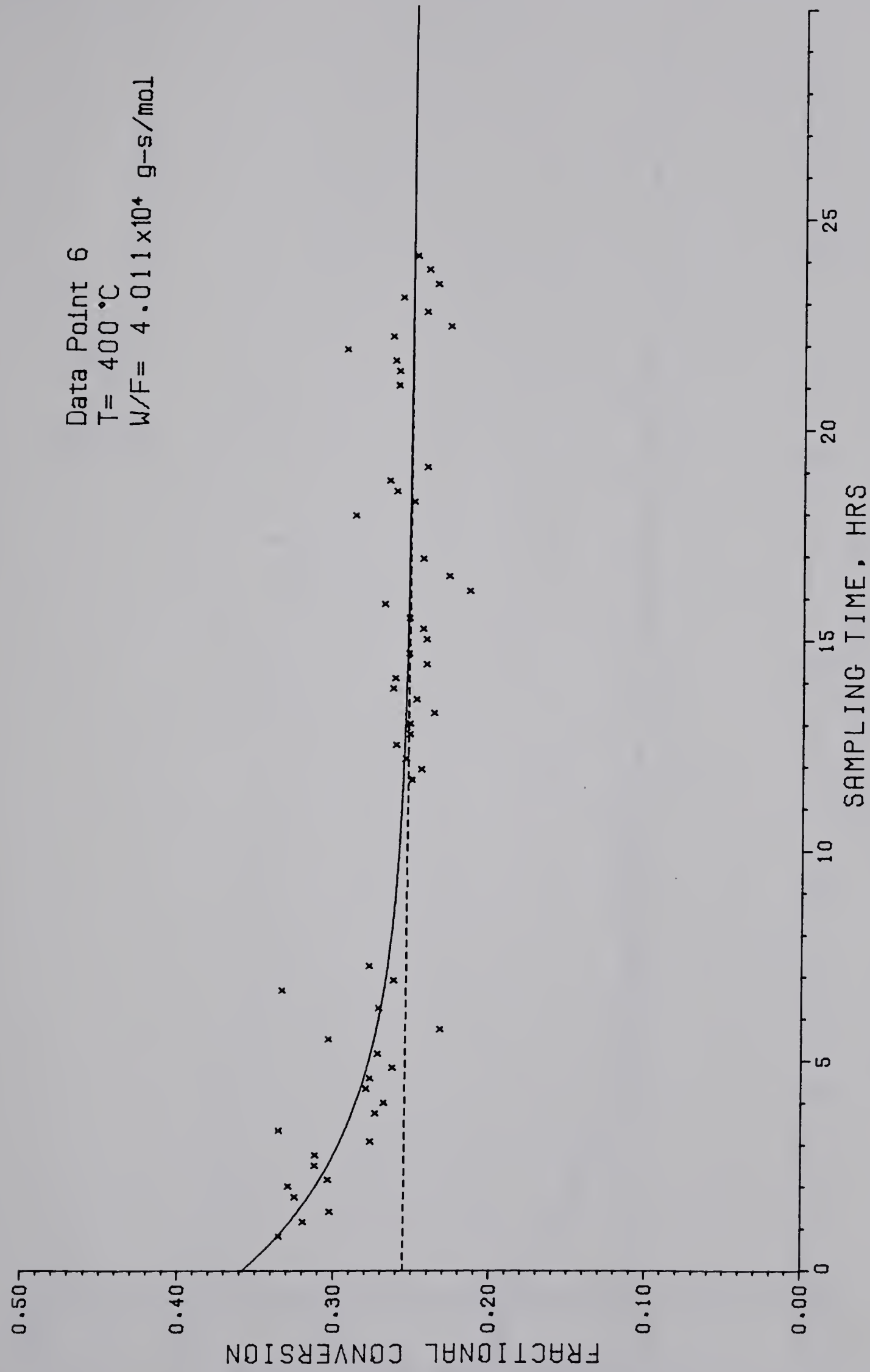


Figure 5f - Time-dependence of Fractional Conversion to Ethylbenzene



Data Point 7  
T= 400 °C  
W/F=  $1.947 \times 10^4$  g-s/mol

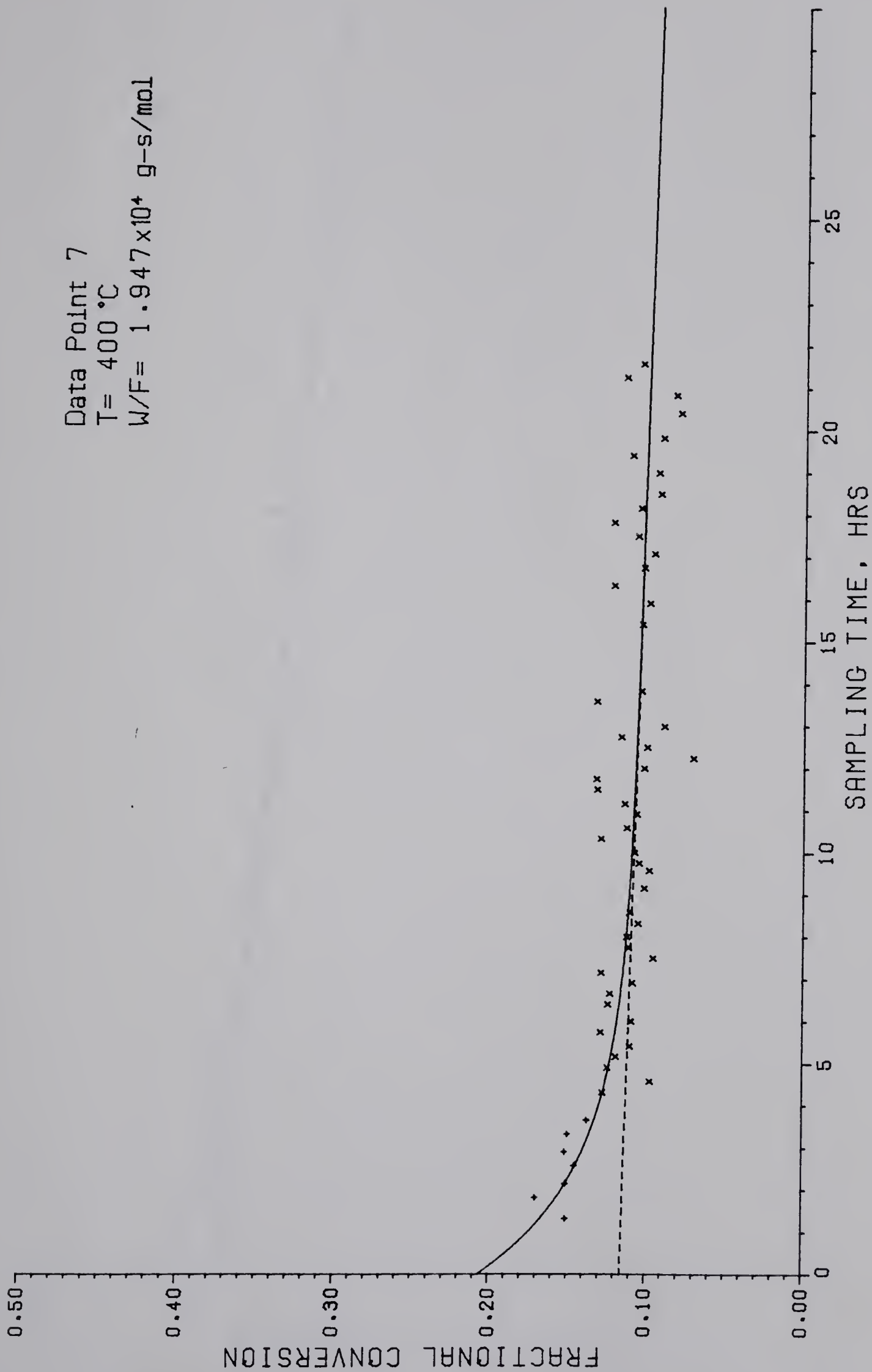


Figure 5g - Time-dependence of Fractional Conversion to Ethylbenzene



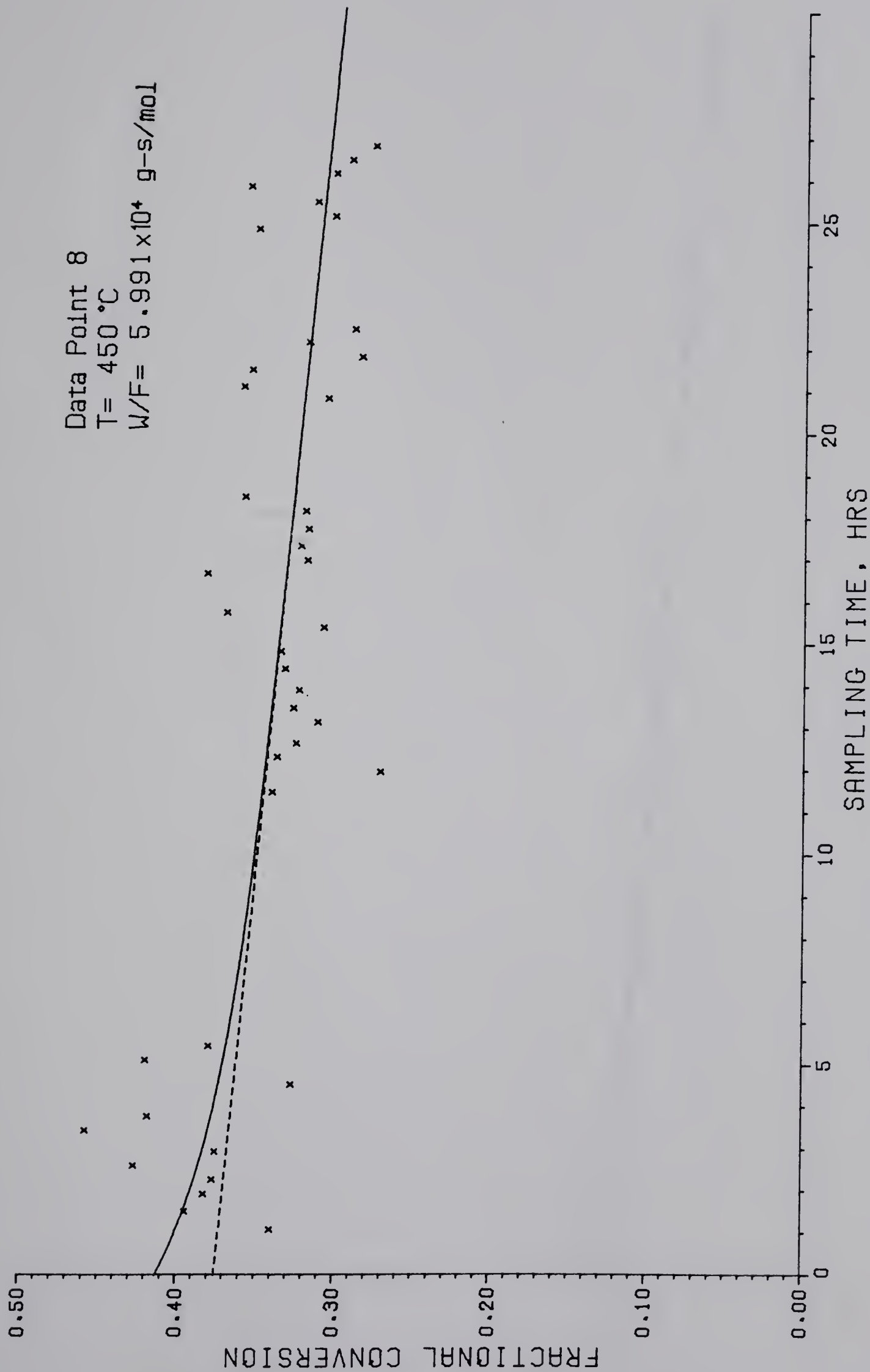


Figure 5h -- Time-dependence of Fractional Conversion to Ethylbenzene





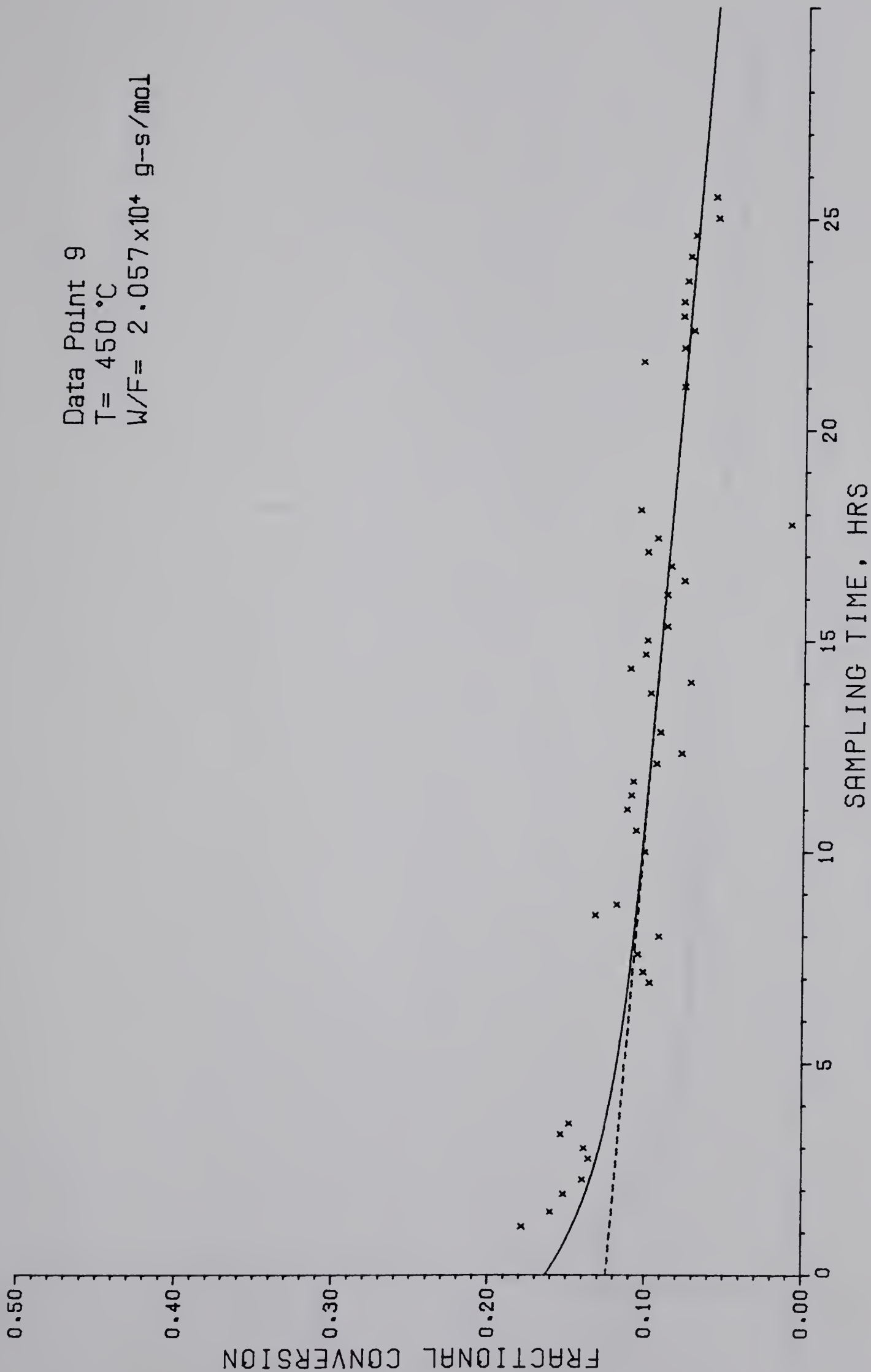


Figure 51 - Time-dependence of Fractional Conversion to Ethylbenzene



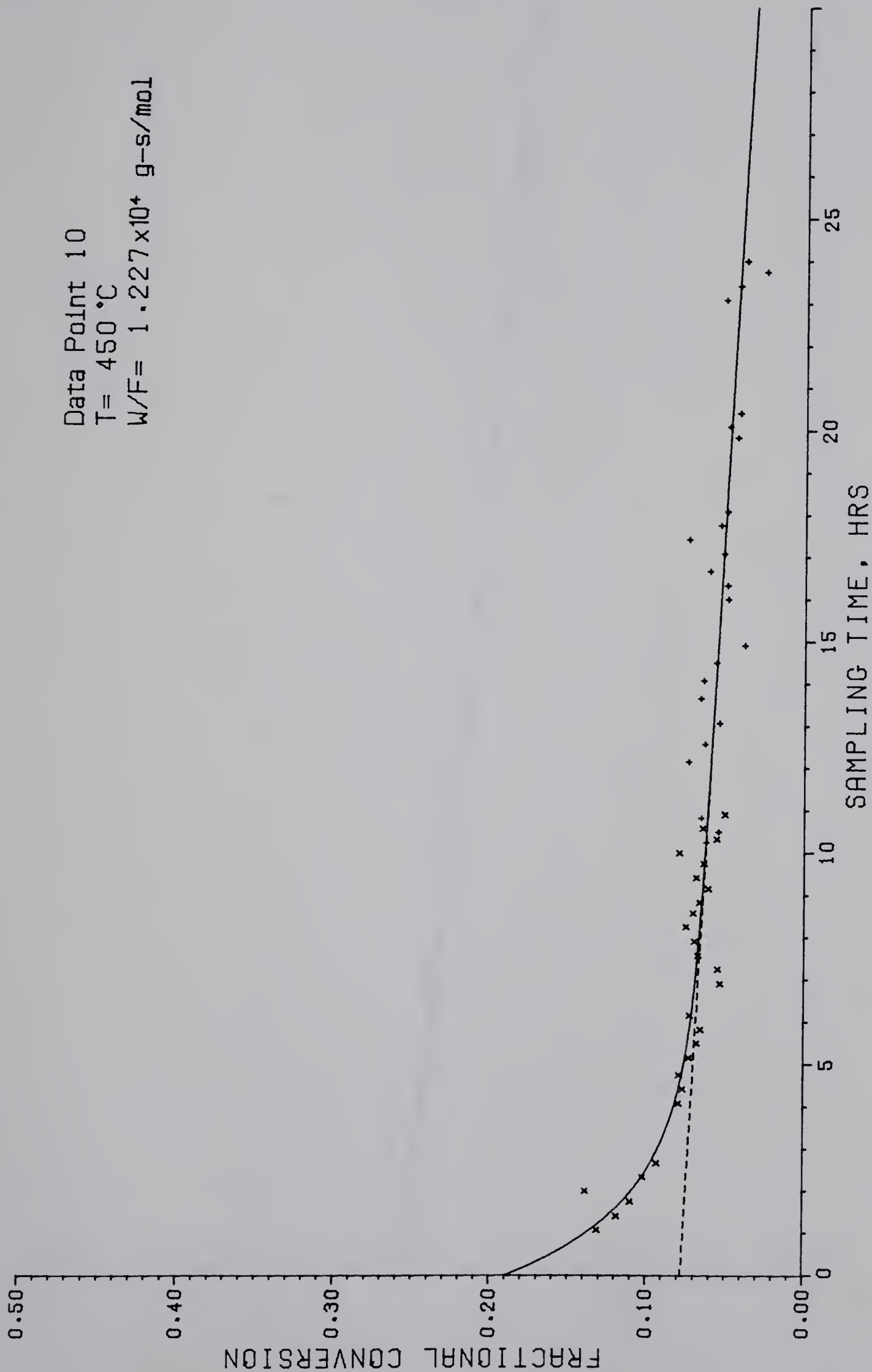


Figure 5j - Time-dependence of Fractional Conversion to Ethylbenzene



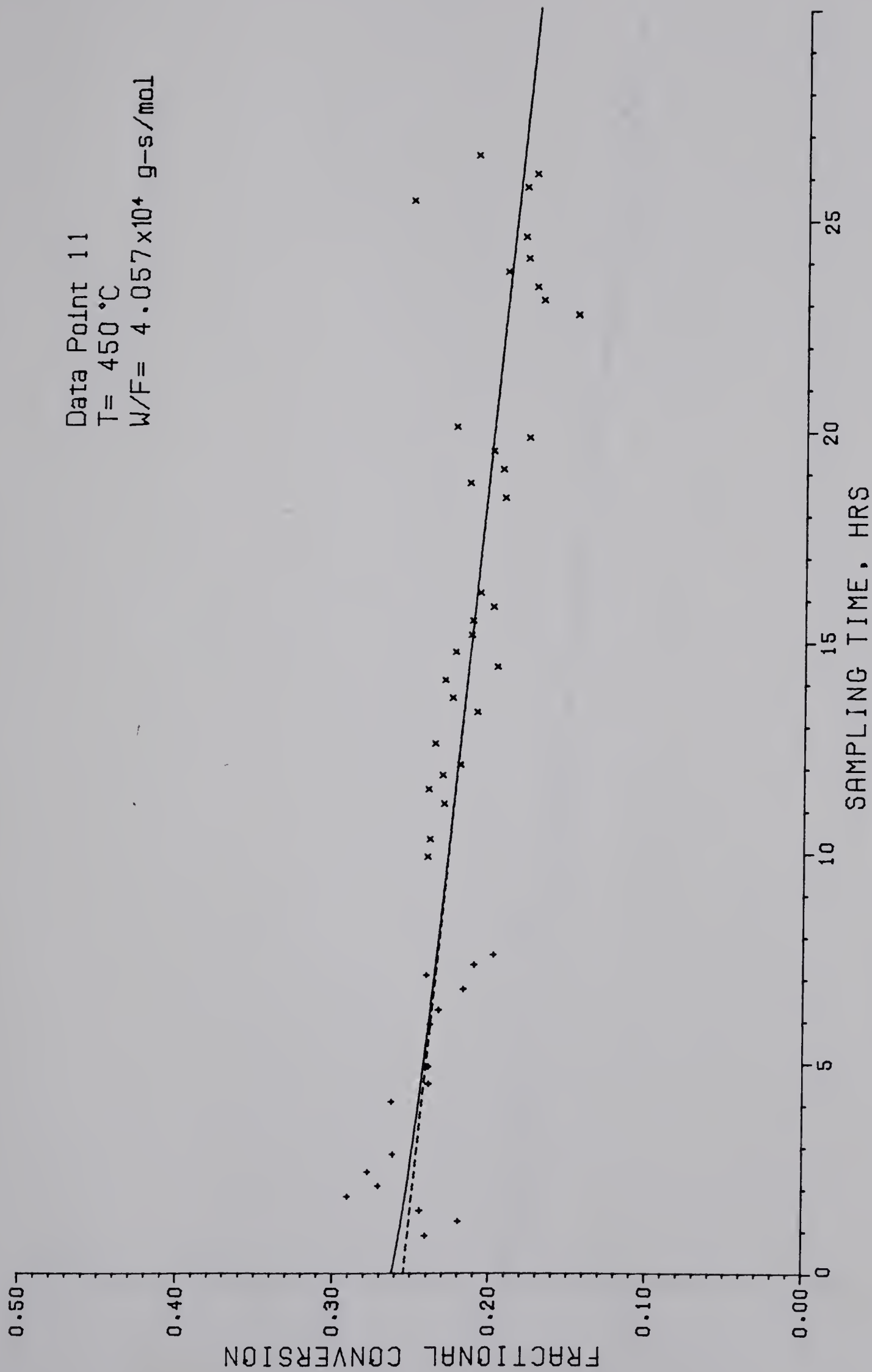


Figure 5k - Time-dependence of Fractional Conversion to Ethylbenzene





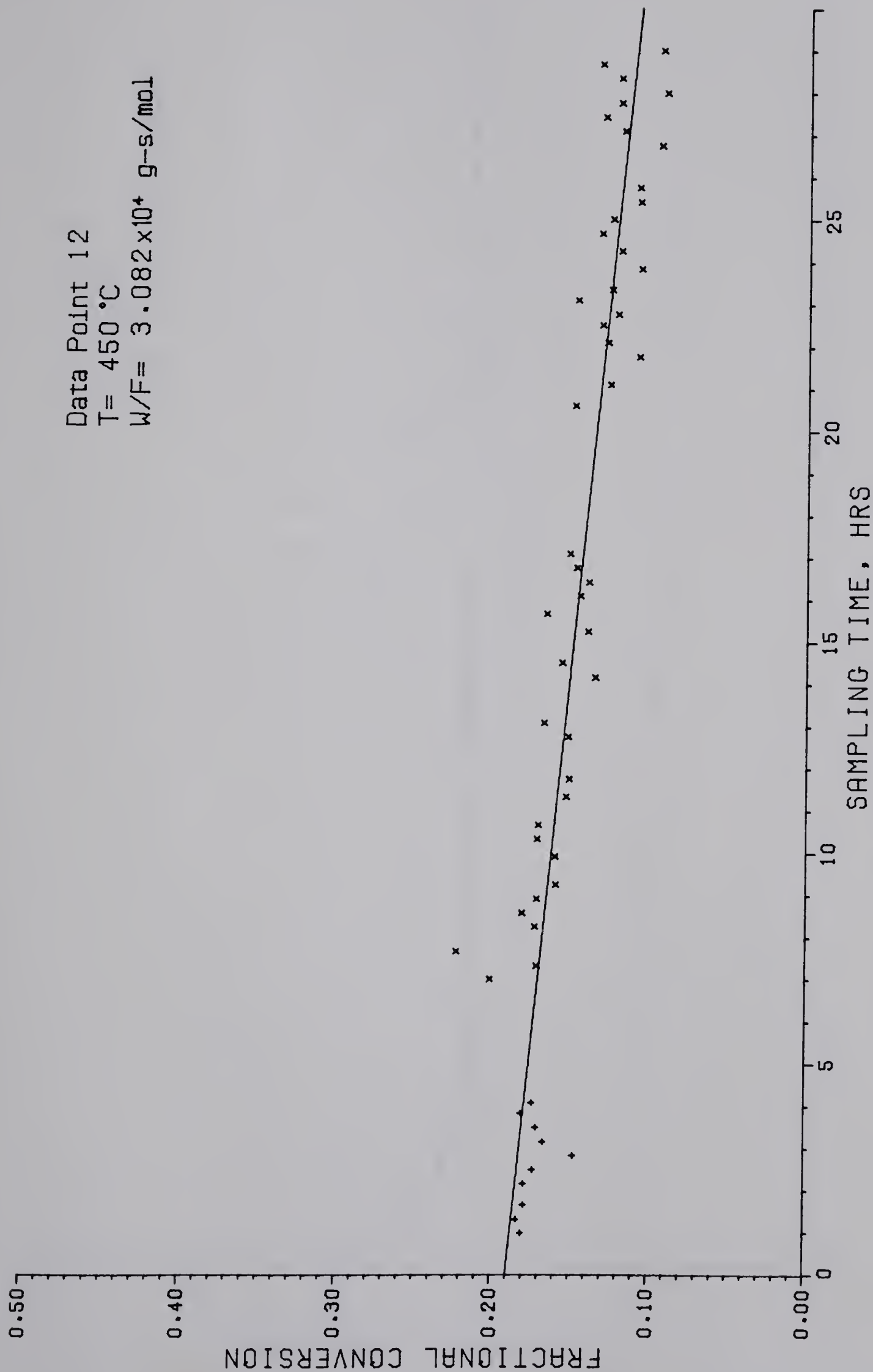


Figure 51 - Time-dependence of Fractional Conversion to Ethylbenzene



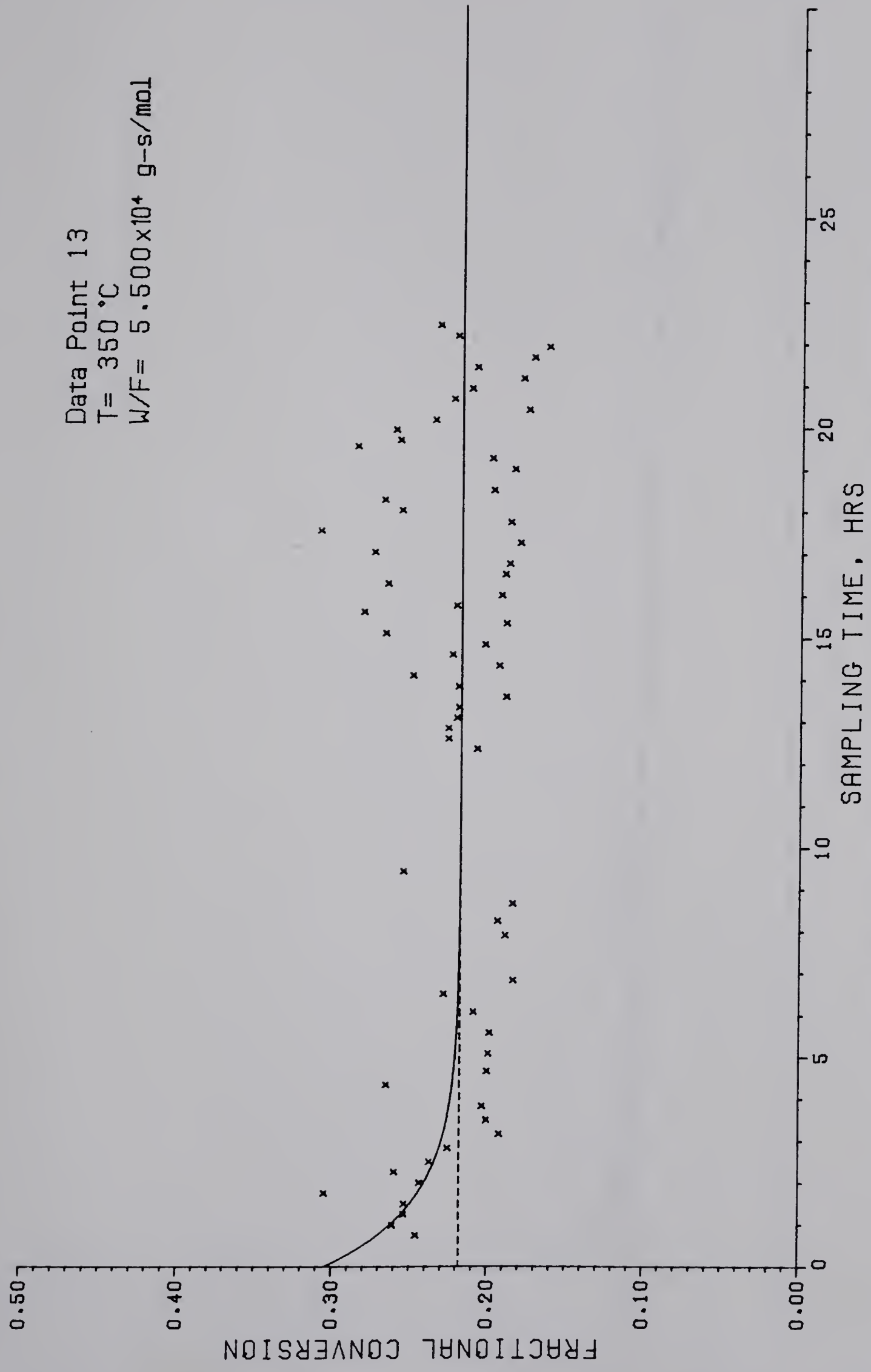


Figure 5m - Time-dependence of Fractional Conversion to Ethylbenzene



Data Point 14  
T= 350 °C  
W/F=  $3.001 \times 10^4$  g-s/mol

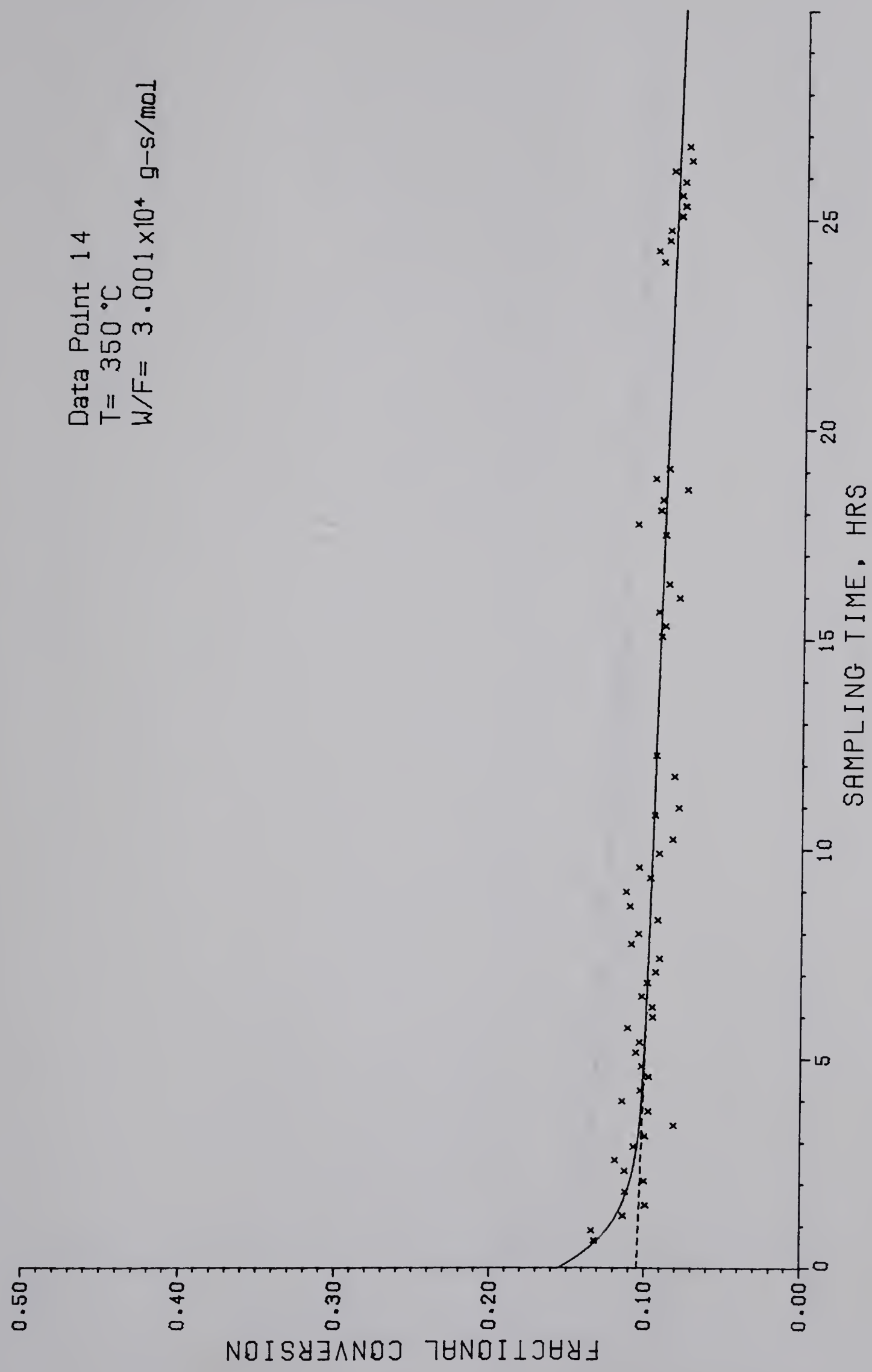


Figure 5n - Time-dependence of Fractional Conversion to Ethylbenzene



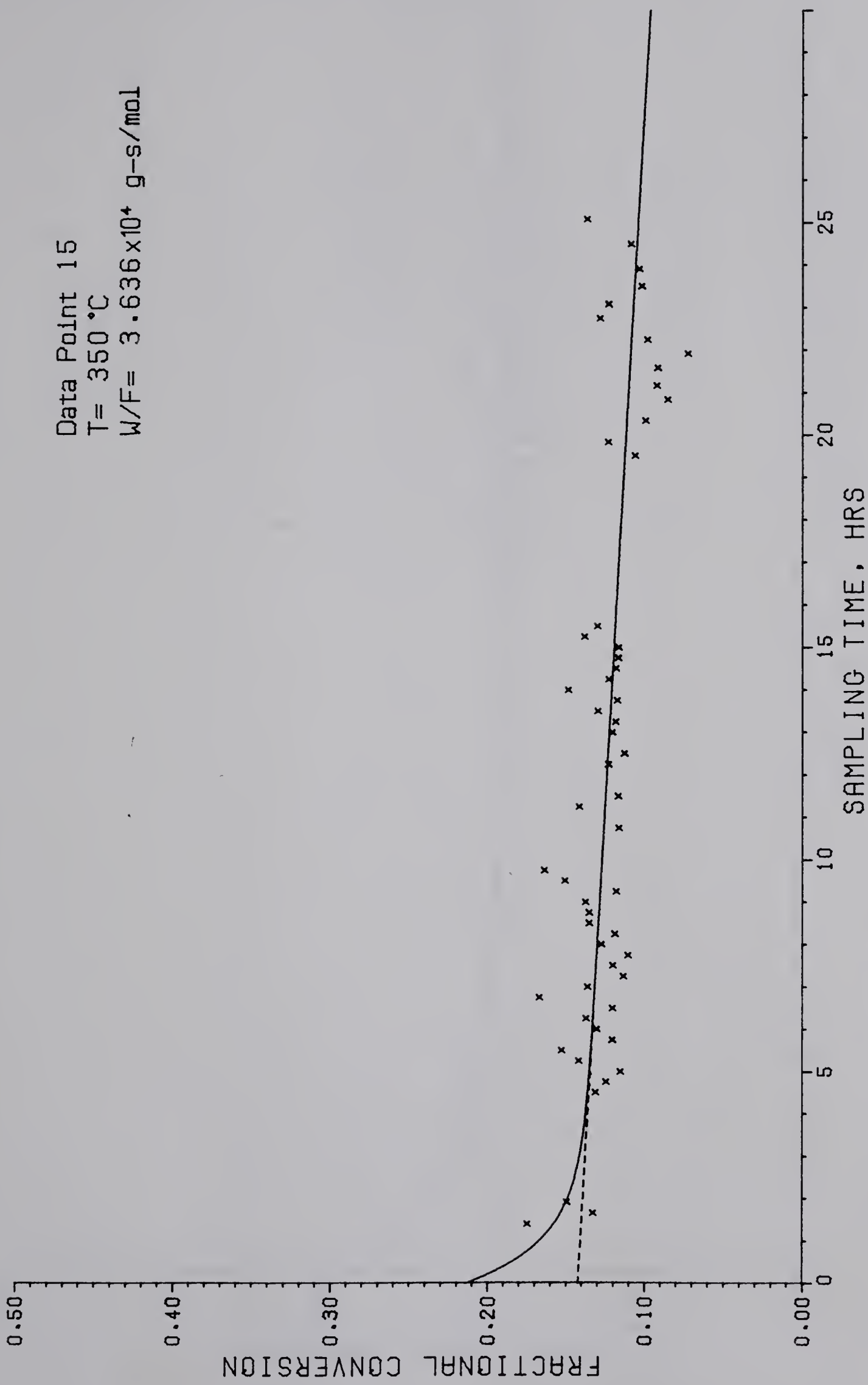


Figure 50 - Time-dependence of Fractional Conversion to Ethylbenzene





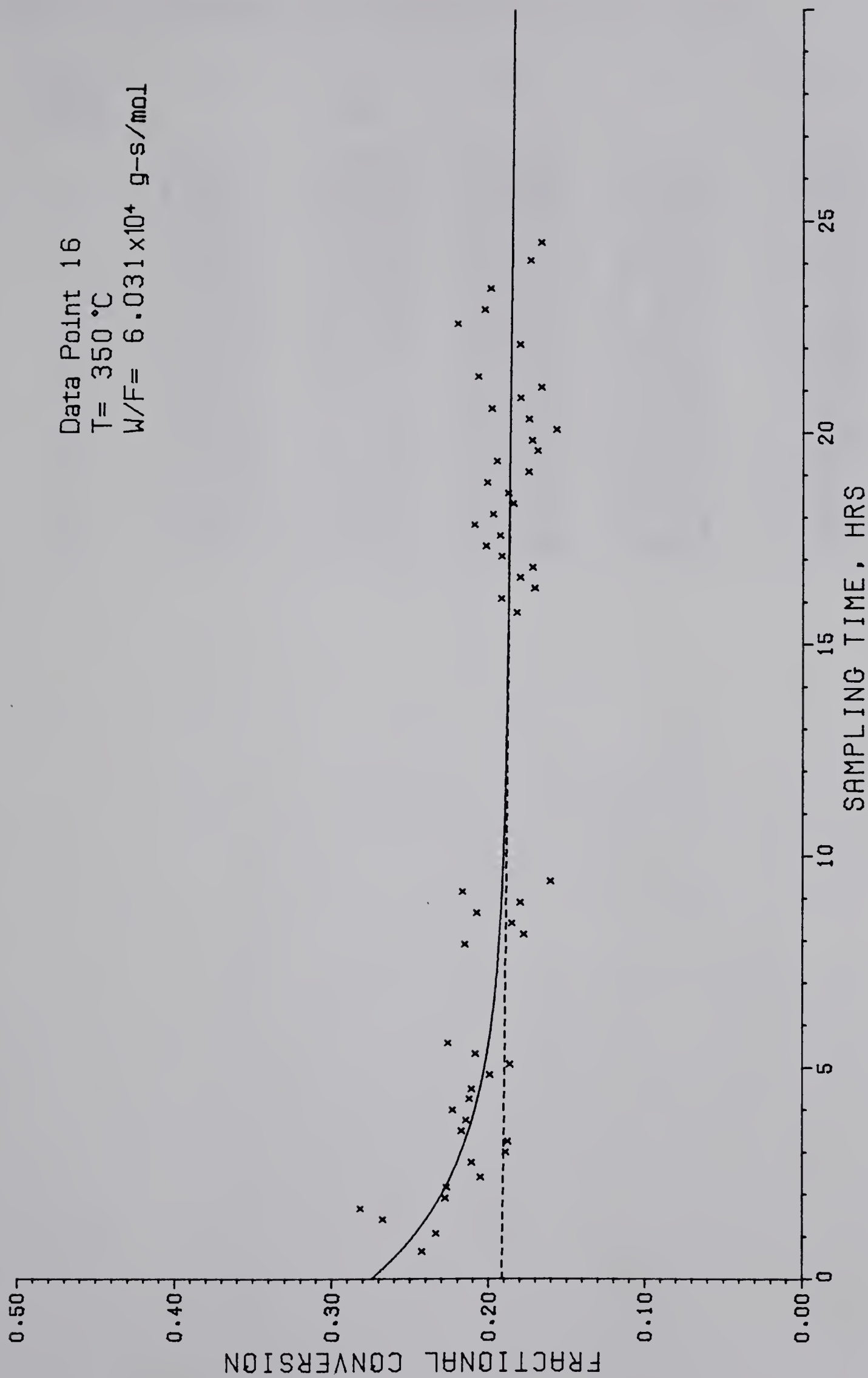


Figure 5p - Time-dependence of Fractional Conversion to Ethylbenzene



Table 4 - Constants of Catalyst Deactivation Curve

Data Point	$C_1$	$C_2 \times 10^3$	$C_3$	$C_4$	$C_2/C_1$
1	0.3651	1.9996	0.0667	0.0667	0.5476
2	0.2873	3.0126	0.0996	0.0996	1.0486
3	0.0850	1.4343	0.0330	0.0330	1.6874
4	0.1983	1.5598	0.0610	0.0610	0.7866
5	0.1815	1.4702	0.0487	0.0487	0.8100
6	0.2556	1.8228	0.1033	0.1033	0.7131
7	0.1155	0.7339	0.0911	0.0911	0.6354
8	0.3753	2.6228	0.0377	0.0377	0.6989
9	0.1244	2.2231	0.0392	0.0392	1.7822
10	0.0777	1.4813	0.1125	0.1125	1.9052
11	0.2546	2.7376	0.0075	0.0075	1.0752
12	0.1898	2.7186	0.0000	0.0000	1.4323
13	0.2182	0.0000	0.0876	0.0876	0.0000
14	0.1045	0.8593	0.0512	0.0512	0.8223
15	0.1421	1.5221	0.0719	0.0719	1.0922
16	0.1912	0.2048	0.0836	0.0836	0.1071



operation for this point were due to a different catalyst bed having been used in this period, for which the operating conditions may have differed slightly. Rather than discard these data, it was decided that a composite of the data from the two beds would give a better estimate of the initial activity of the catalyst than would either bed alone, and for this reason, this bed was treated identically to the other beds used to obtain the rest of the data.

The conversion for Point 5 was found to be slightly low; this may be explained by the fact that the hydrogen partial pressure was a few percent lower than those in the other runs.

## 7.2 Reaction Kinetics

The fractional conversions of benzothiophene to ethylbenzene, styrene, and dihydrobenzothiophene are presented in Table 5 and plotted as a function of space time in Figures 6 - 8, respectively.

From Figure 6, it can be seen that over the range of reaction conditions used, the reaction rate, obtained from the slope of the curve, is independent of the conversion of benzothiophene up to fractional conversions as high as 0.4. This may be interpreted as evidence for intrinsic zero-order kinetics, however if the space time is increased much beyond the range used here, the conversions do begin to fall below the linear relationships shown in this figure. This





Table 5 - Fractional Conversion Data

Data Point	T (°C)	W/F $\times 10^{-4}$	To EB	To STY	To DHBT
1	400	5.912	0.3670	0.0018	0.0005
2	400	4.750	0.2870	0.0011	0.0002
3	400	1.244	0.0984	0.0035	0.0007
4	400	3.031	0.1949	0.0021	0.0019
5	400	7.947	0.1832	0.0024	0.0017
6	400	4.011	0.2590	0.0021	0.0012
7	400	1.947	0.1219	0.0027	0.0005
8	450	5.991	0.4007	0.0080	0.0002
9	450	2.057	0.1268	0.0100	0.0004
10	450	1.227	0.1815	0.0073	0.0006
11	450	4.057	0.2701	0.0143	0.0014
12	450	3.082	0.1985	0.0152	0.0011
13	350	5.500	0.2195	0.0013	0.0043
14	350	3.001	0.1047	0.0001	0.0012
15	350	3.636	0.1420	0.0009	0.0063
16	350	6.031	0.1950	0.0009	0.0027



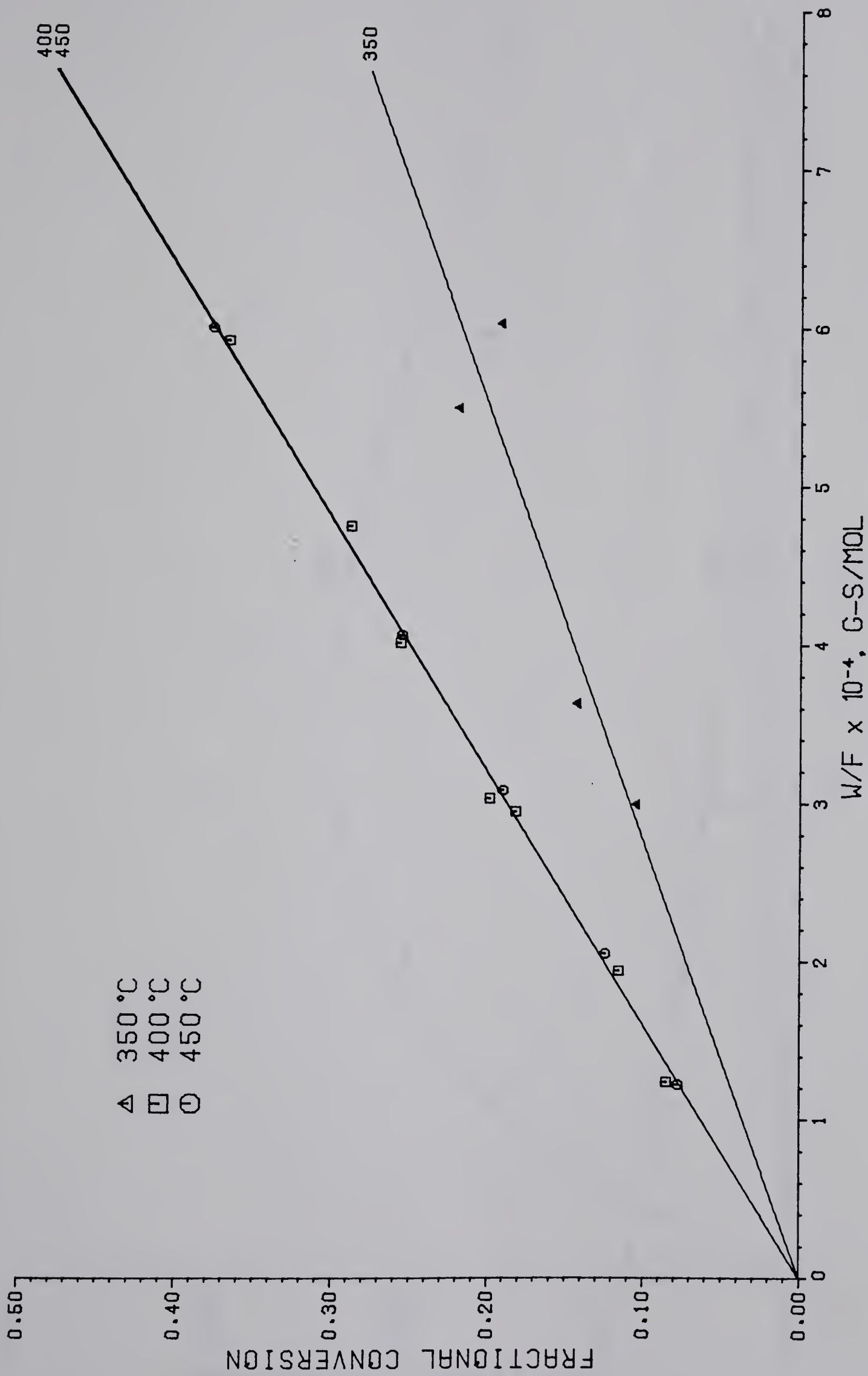


Figure 6 - Effect of Space Time on Fractional Conversion to Ethylbenzene



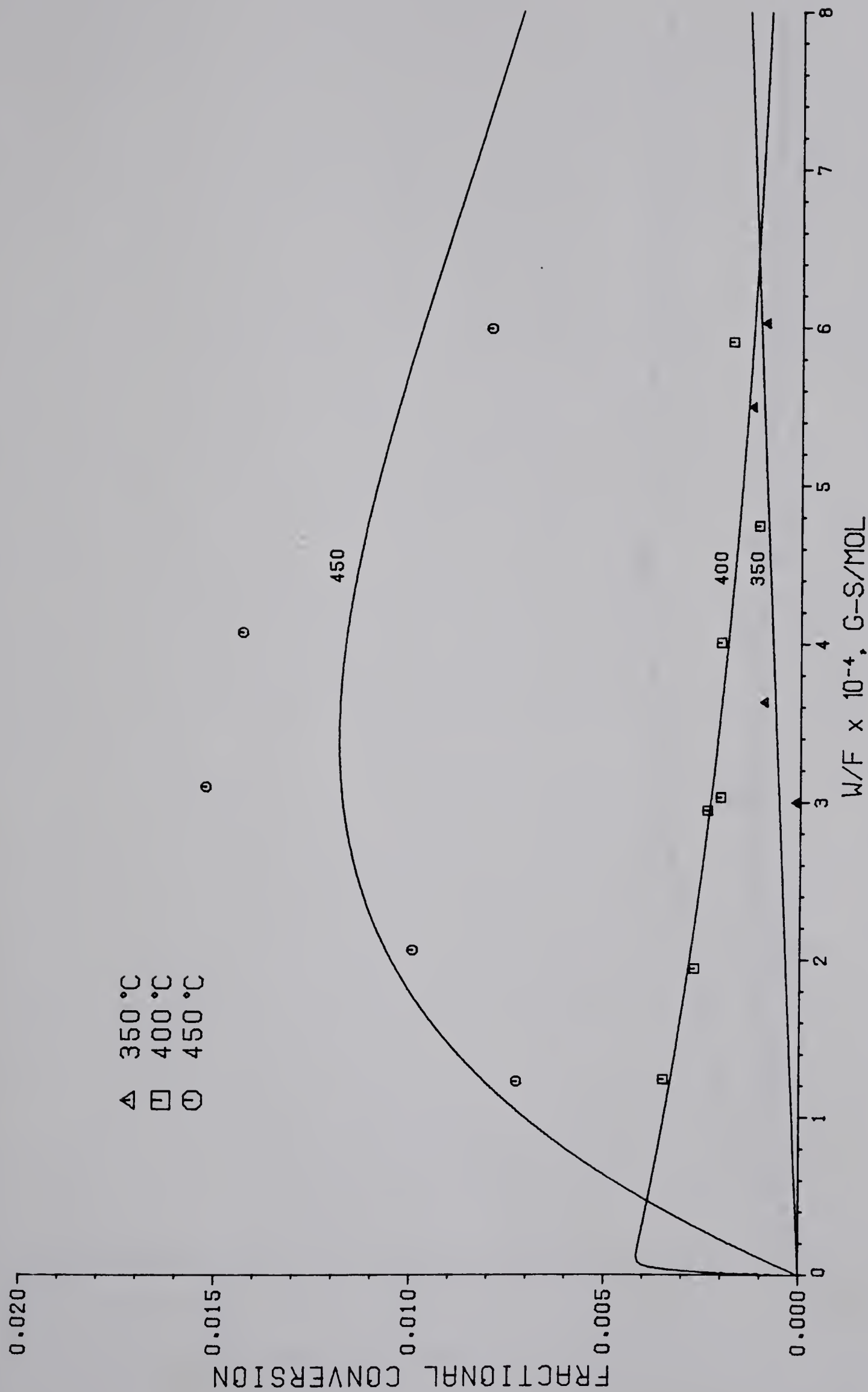


Figure 7 - Effect of Space Time on Fractional Conversion to Styrene



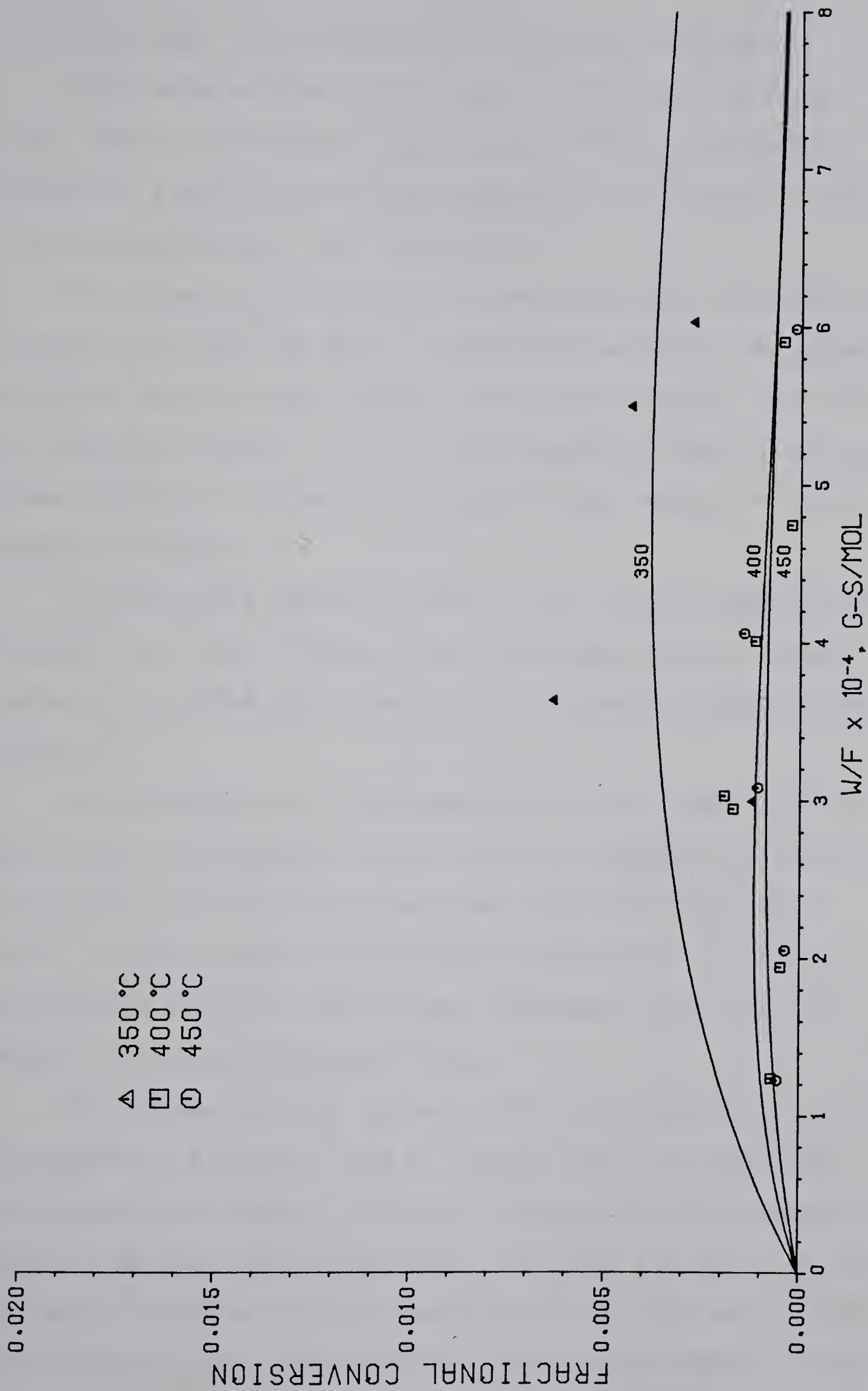


Figure 8 - Effect of Space Time on Fractional Conversion to Dihydrobenzothiothiophene





indicates that the intrinsic rate is not zero-order.

Much more scatter can be seen in the data taken at 350°C than at the other temperatures. This was probably caused by a much slower equilibration of the catalyst with its surroundings at this temperature.

The absence of effects from heat and mass transfer limitations can also be seen in Figure 6: neither a decrease in catalyst particle size (Point 6) nor an increase (Point 4) or decrease (Points 13, 14) in the specific heat of the gas phase appeared to produce any significant effect on fractional conversion.

The observed reaction rates at the three temperatures studied are shown in Table 6 and the logarithms of these rates are plotted as a function of reciprocal temperature in Figure 9.

The dependence of the reaction rate on temperature is striking: although the overall rate increased significantly from 350 to 400°C, no increase was observed from 400 to 450°C, implying the existence of a maximum or a point of inflection in this relationship. Possible causes of this behavior will be discussed below.

The conversions to styrene and dihydrobenzothiophene are shown in Figures 7 and 8, respectively. In each case, the conversion appears to rise to a maximum with increasing space time and then to decrease, although the data for dihydrobenzothiophene are too scattered to be conclusive. This would support the conclusion of Furimsky and Amberg<sup>14</sup> that



Table 6 - Observed Reaction Rates

Temperature °C	Rate mol/g cat-s
350	0.03611
400	0.06243
450	0.06225



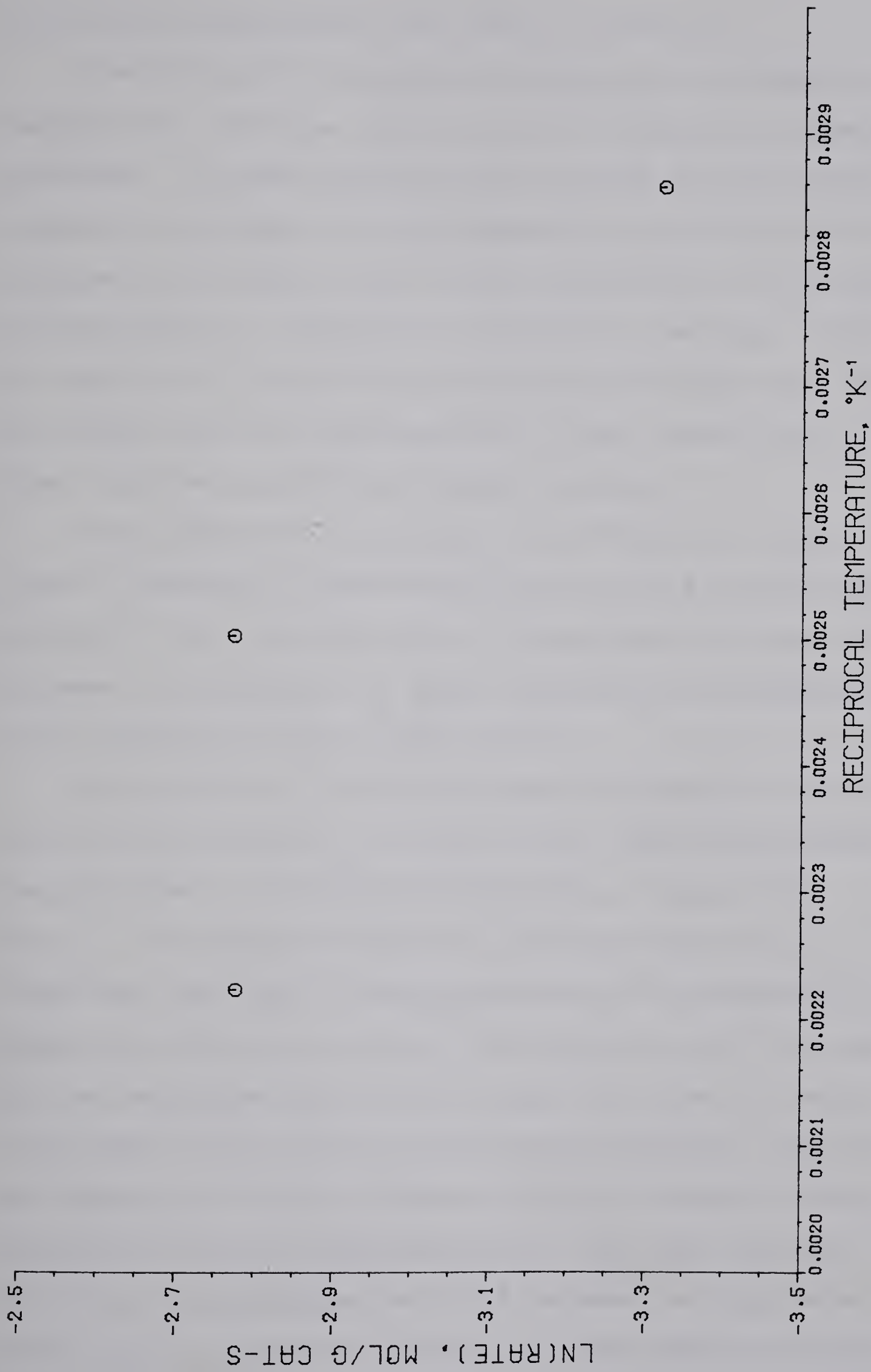


Figure 9 - Arrhenius Plot Based on Conversion to Ethylbenzene





both are intermediates in the overall reaction.

The conversion to styrene increases with increasing temperature, while the conversion to dihydrobenzothiophene decreases. If these intermediates are seen as representing respective hydrogenolysis-hydrogenation and hydrogenation-hydrogenolysis paths, and if direct conversion from dihydrobenzothiophene to styrene is considered to be small, then it is implied that the activation energies for hydrogenolysis are higher than for hydrogenation in both cases. This is what would be expected from kinetic theory.

This mechanism is in itself insufficient to explain the lack of increase in the overall reaction rate between 400 and 450°C, even if conversion of dihydrobenzothiophene to styrene is considered. At least two alternative hypotheses could reasonably explain this result.

One possibility is that the lack of change in reaction rate is a consequence of a shift in the equilibrium between benzothiophene and dihydrobenzothiophene. Givens and Venuto<sup>16</sup>, Furimsky and Amberg<sup>14</sup> and Kilanowski et al.<sup>31</sup> all found that the rate of dehydrogenation of dihydrobenzothiophene was significant even at the relatively high hydrogen partial pressures used in this study (3-4 orders of magnitude higher than those of dihydrobenzothiophene). Furimsky and Amberg also found a higher activation energy for dehydrogenation than for desulfurization, and from this predicted that dehydrogenation would increase in importance with respect to desulfurization as a rate-limiting step as



the temperature increased.

If this reverse reaction is in fact rate-limiting, it is important to estimate its relevance for the operation of commercial hydrotreating reactors. Since these reactors operate at hydrogen partial pressures approximately two orders of magnitude higher than in the present study, it is expected that the temperature at which the rate of dehydrogenation becomes critical should be higher than found here. If the forward reaction is first order in hydrogen (as has been found for the overall desulfurization reaction by Rollman<sup>29</sup> and Bartsch and Tanielan<sup>15</sup>), and the heat of reaction is assumed to be 30 kcal/mole (typical for hydrogenations), then an increase in hydrogen partial pressure by a factor of 100 would raise this "critical temperature" by about 175°C. This is in agreement with the prediction of Furimsky<sup>66</sup> that the dehydrogenation reaction should not be an important factor at high pressures. This estimate of "critical temperature" may be misleading, however, in that it does not allow for any effects of H<sub>2</sub>S, which has been found to severely retard some hydrogenations<sup>9</sup>. Consequently, the actual temperature at which this dehydrogenation rate should become important in an industrial hydrotreater with high H<sub>2</sub>S partial pressures may be much lower (or even in the opposite direction) than the predicted value.

A second possible cause of the unusual character of the temperature dependence of the overall rate is that the rate of adsorption of one of the reactants may have been a rate-



controlling step. If, for example, the reaction took place on two different catalyst sites, one more active for initial hydrogenolysis of benzothiophene to styrene and one more active for initial hydrogenation to dihydrobenzothiophene, and if the exothermic adsorption of either benzothiophene or hydrogen onto the latter site were stronger than onto the former, then (at some point), an increase in temperature could also result in no change in the overall rate as well as in an increase in styrene and a decrease in dihydrobenzothiophene in the reaction products. Consequently, a reaction model incorporating adsorption limitations on the reaction path through dihydrobenzothiophene could also predict kinetic data consistent with the results of this study.

Most studies relevant to the evaluation of this hypothesis have been conducted at too low a temperature to permit any definite conclusions to be drawn with respect to the present data. Lipsch and Schuit<sup>49</sup> found a maximum in the adsorption of hydrogen onto supported cobalt-molybdenum catalysts at about 550°C, and Owens and Amberg<sup>77</sup> found that the activation energy for chemisorption of hydrogen onto chromia had the right order of magnitude to have been able to affect the rate of thiophene desulfurization at 250°C. Owens and Amberg also found that the adsorption of thiophene did not appear to be a rate controlling step in this reaction at temperatures up to about 370°C, but allowed that this may not be true at higher temperatures.





Desikan and Amberg<sup>78</sup>, working with methyl-substituted thiophenes at temperatures up to 350°C, concluded that adsorption of either thiophene or hydrogen onto Co-Mo- $\gamma$ -Al<sub>2</sub>O<sub>3</sub> could not be the only rate-determining step, and Kawaguchi et al.<sup>11</sup>, studying thiophene desulfurization in the same temperature range, concluded that adsorption of hydrogen onto Ni-Mo- $\gamma$ -Al<sub>2</sub>O<sub>3</sub> was not significant in determining the overall reaction rate. Frye and Mosby<sup>79</sup>, working at high pressures and 330°C, also suggested that hydrogen chemisorption was probably not significant.

If the reaction path is highly temperature-dependent, then one may ask on what basis have previous researchers calculated apparent activation energies and pseudo-first order rate constants for this reaction. From the experimental data for 350 and 400°C, two points alone, a value of 9.1 kcal/mol was estimated as a minimum value for the apparent activation energy of the reaction path through dihydrobenzothiophene. From this, a pseudo-zero order preexponential factor of 57.33 mol/g cat-s was calculated. This value of activation energy is shown in Table 7, along with the previously reported literature values. The details of this calculation are given in Appendix G.

The experimentally obtained minimum value for the activation energy falls within the range of values reported by other researchers, however the error in this value is significant, and it is likely that the true apparent activation energy for this path may be somewhat higher. The use of only





Table 7 - Experimental and Literature Values of  
Activation Energy

Reference	Catalyst	Ea kcal/mol	Temp. Range °C
Bartsch and Tanielan <sup>1 5</sup>	Co-Mo- $\gamma$ -Al <sub>2</sub> O <sub>3</sub>	4.9	300-400
Bartsch and Tanielan <sup>2 8</sup>	Fe <sub>2</sub> O <sub>3</sub> - $\gamma$ -Al <sub>2</sub> O <sub>3</sub>	7.9-14.0	300-400
Furimsky and Amberg <sup>1 4</sup>	Co-Mo- $\gamma$ -Al <sub>2</sub> O <sub>3</sub>	12.0	250-400
Daly <sup>1 7</sup>	Co-Mo- $\gamma$ -Al <sub>2</sub> O <sub>3</sub>	16.1	200-400
Kilanowski and Gates <sup>3 2</sup>	Co-Mo- $\gamma$ -Al <sub>2</sub> O <sub>3</sub>	20±3	252-332
Present Study	Ni-Mo- $\gamma$ -Al <sub>2</sub> O <sub>3</sub>	>9.1	350-400



two points in the estimation of this activation energy certainly introduces some error into the calculations, and the fact that the minimum temperature used in this calculation was somewhat higher than those used in previous studies meant that the present value is probably less reliable as an estimate of the true activation energy of the low temperature reaction path than are the other reported values. Since the apparent activation energy accounts for the kinetics of the adsorption and desorption of the reactants and products as well as for the kinetics of the actual reaction, it is possible that the use of a nickel-promoted catalyst in the present study rather than a cobalt catalyst may also have been responsible for some of the discrepancy between the observed minimum value of apparent activation energy and previously reported values of this parameter.

### 7.3 Trace Reaction Products

A chromatogram of the condensate from a typical set of reaction conditions is shown in Figure 10 along with the molecular weights associated with each peak by mass spectrometry. These results are only qualitative (and at best incomplete), since most of the lighter products would have been lost from the condenser in the flowing gas stream, but it is estimated (using benzothiophene as a basis) that none of these trace products was present in excess of 0.1% of the total products, and that most were present at a level of



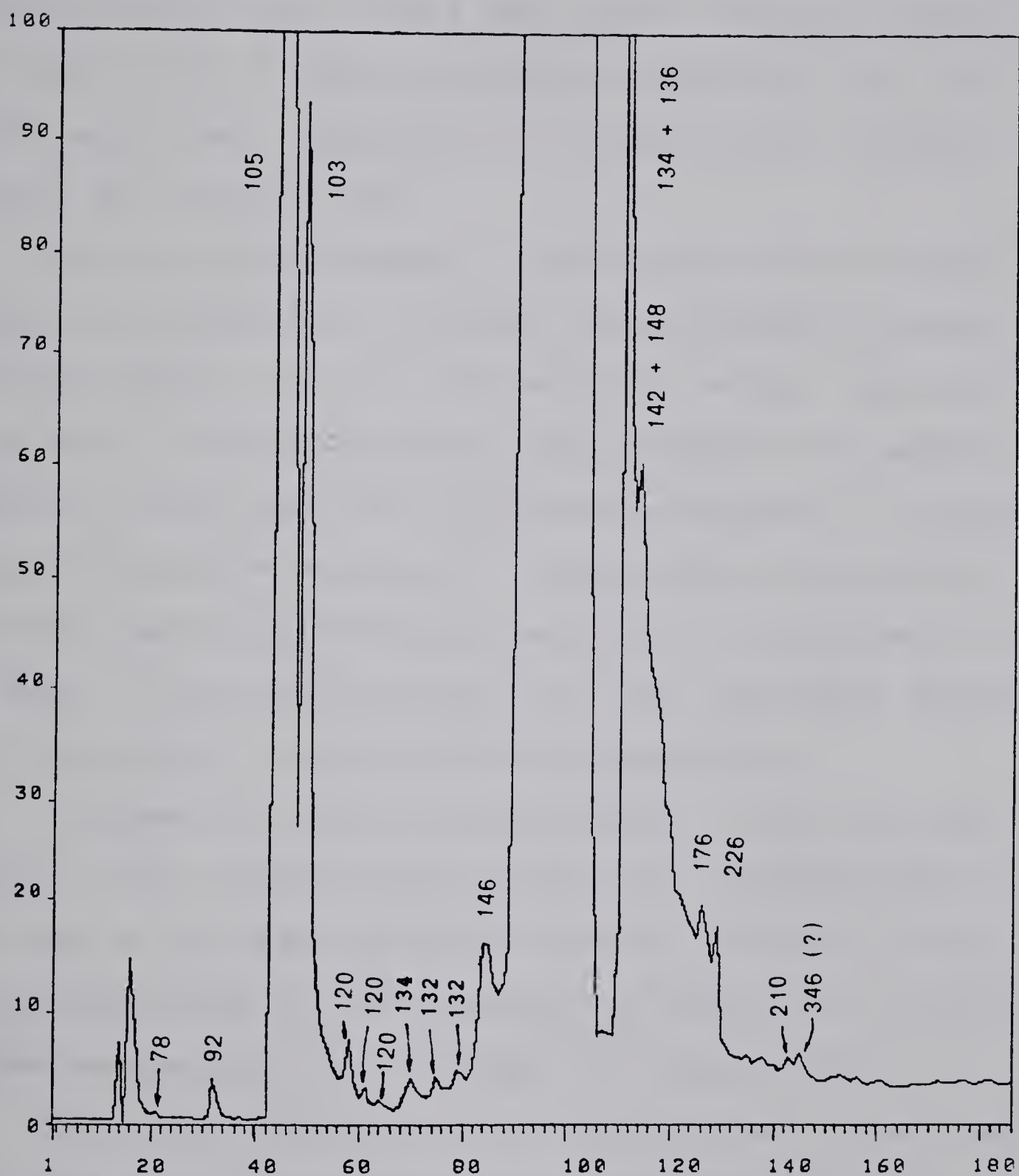


Figure 10 - Chromatogram of Condensed Products





0.01% or lower. Another factor affecting these results is the relatively large amounts of the four main components of the product stream with respect to the trace products: it is almost certain that a small peak with a retention time close to that of one of the main products would have been lost in this larger peak, especially if it had the same molecular weight as the large peak.

The only peaks present in an analysis of the liquid feed were ethylbenzene, styrene, benzothiophene, dihydrobenzothiophene, the peak with molecular weight 146 eluted just prior to benzothiophene, and the peaks with masses 176 and 226 eluted just after dihydrobenzothiophene. It appeared that the relative areas of all these peaks in the product analysis were significantly greater than in the feed, and as a result it was concluded that all were legitimate products of the reaction, rather than just impurities.

A summary of the molecular weights of all the components of the product stream, along with possible identities of some of the trace products is given in Table 8. These identities could not be checked by an analysis of retention times because the pure compounds were unavailable.

From this table, it can be inferred that a small degree of cracking of the reactants and/or products occurs, along with some recombination of the hydrocarbon fragments. The presence of some species implies that their isomers should also be present; in some cases peaks corresponding to possible structural isomers were found, in some cases they



Table 8 - Composition of Product Stream

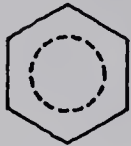
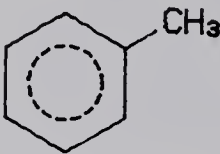
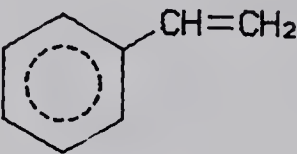
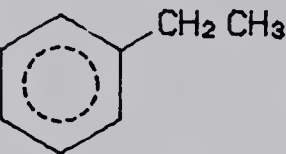
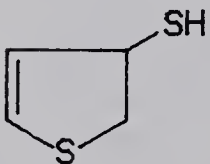
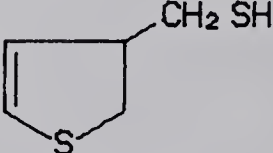
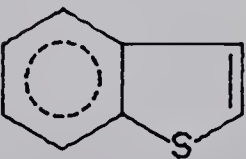
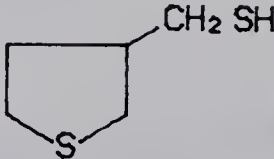
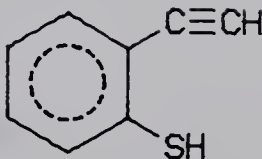
Molecular Weight	Number of Peaks	Possible Identity
78	1	
92	1	
104	1	
106	1	
120	3	 + isomers
132	2	 + isomers
134	2	  



Table 8 (cont.)

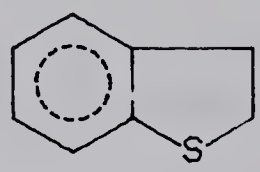
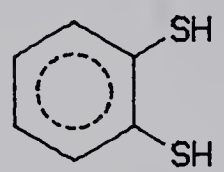
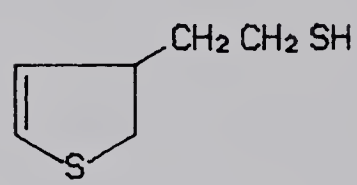
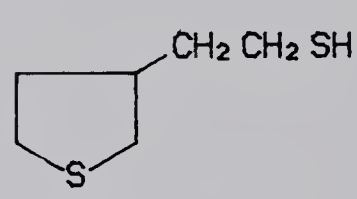
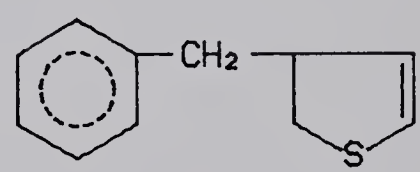
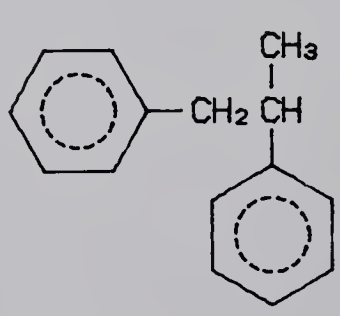
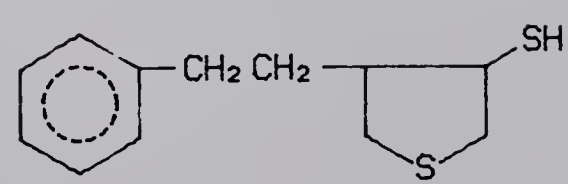
Molecular Weight	Number of Peaks	Possible Identity
136	1	
142	1	
146	1	
148	1	
176	1	
210	1	
226	1	

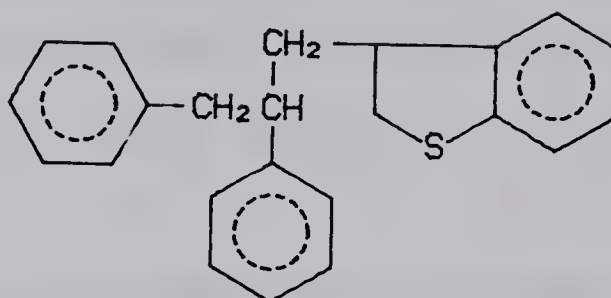


Table 8 (cont.)

Molecular Weight	Number of Peaks	Possible Identity
------------------	-----------------	-------------------

346

1







were not, possibly due to inadequate separation or sensitivity of the apparatus.

A peak at molecular weight 210 was identified as distyrene and a second peak at M.W. 346 could represent the product of a reaction between distyrene and benzothiophene. This indicates that even at 400°C some degree of styrene polymerization was occurring.

Furimsky and Amberg had predicted that 2-mercapto-phenylacetylene (M.W. 134) and 2-mercaptostyrene (M.W. 136) might be found in the reaction products in trace quantities. In the present analysis, only one unidentified peak corresponding to either of these masses was found, at M.W. 134.

Daly<sup>17</sup> found separate peaks which were attributed to 1- and 2-phenylethanethiol. The reaction conditions used in the present study (low pressure and low conversion) would not be expected to favor a back-reaction between styrene and H<sub>2</sub>S, Daly's major path for the formation of these products, but it could allow for 2-phenylethanethiol to be formed from dihydrobenzothiophene through 2-phenylethenethiol. No evidence was found for the presence of either of these compounds in the reaction products, although it is quite possible that a peak representing the intermediate may have been lost in the much larger dihydrobenzothiophene peak.



#### 7.4 Catalyst Deactivation

Only one researcher (Kilanowski et al.<sup>32</sup>) has reported a loss in catalyst activity comparable to that found in the present study. Kilanowski concluded that the decrease in activity was due to a loss of sulfur from the catalyst surface.

To test whether this explanation is consistent with the results of the present study, or whether another explanation such as coking on the catalyst might be required, the rate of deactivation was normalized for each data point to account for differences in fractional conversion between the runs. This normalized rate of decay (expressed as the fraction of initial activity lost per hour) was calculated as the rate of decrease of fractional conversion divided by the initial fractional conversion (i.e.  $C_2/C_1$ ). (Although a mean value of fractional conversion might have been chosen rather than the initial value, this would not have affected the normalized rate significantly.)

The normalized deactivation rate is shown in Table 4, and is plotted against fractional conversion to ethylbenzene in Figure 11. (Since fractional conversion to ethylbenzene was found to be directly proportional to space time, the shapes of these curves will be similar regardless of which of these variables is used as the abscissa.) The curves in this figure are exponentials which were fitted using a least squares algorithm with no constraints on either of the parameters, and were included only to show the general



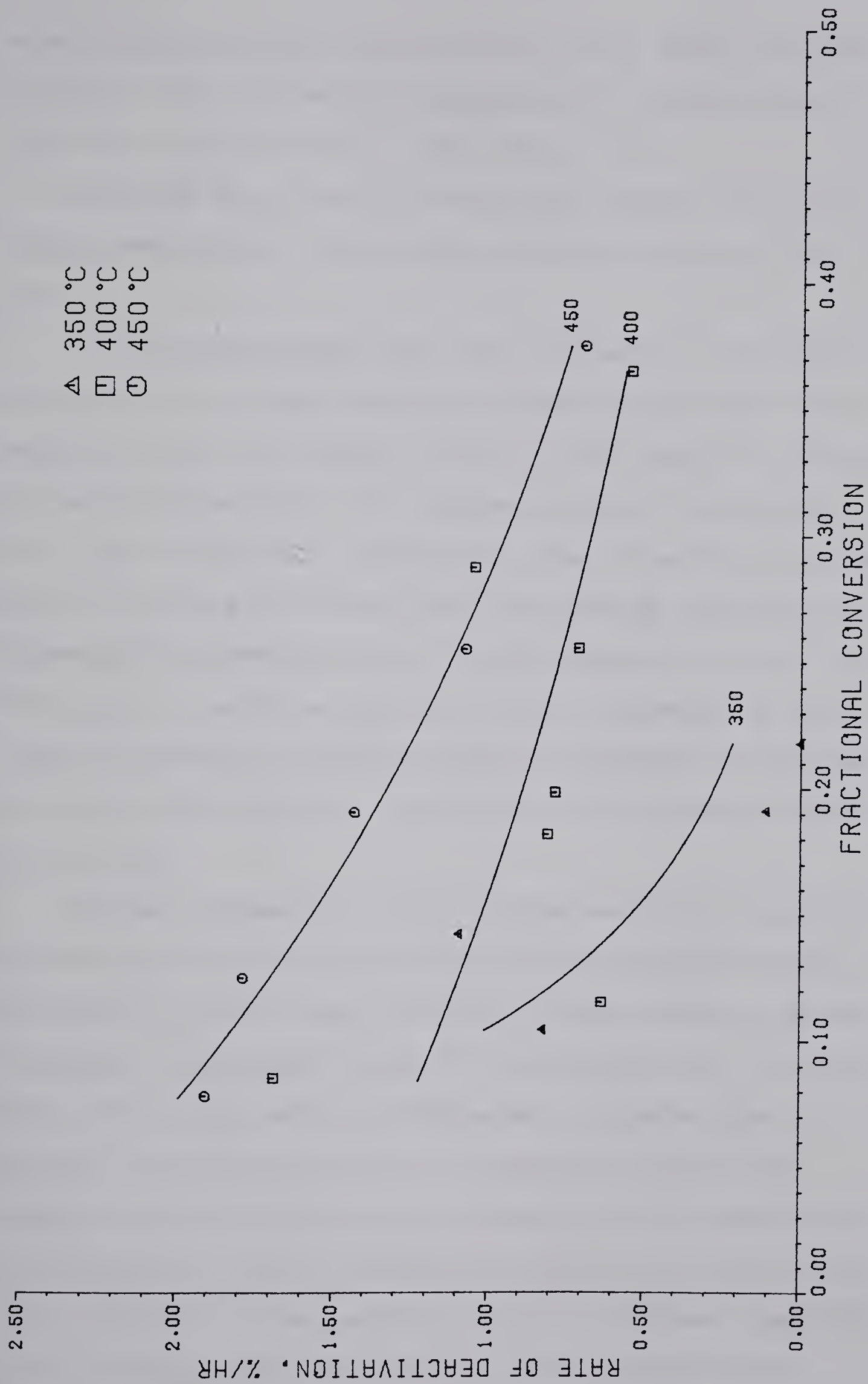


Figure 11 - Effect of Fractional Conversion to Ethylbenzene on Rate of Catalyst Deactivation





relationships between the variables rather than to suggest any particular mathematical dependence or to provide any basis for extrapolation of these data.

Although the errors in these deactivation rates are large, some general conclusions can still be drawn from the data.

If the deactivation rate were related to a chemical change on the catalyst surface, a deactivation rate with a negative order with respect to one of the reaction products may be more plausible. One hypothesis which would predict this type of behaviour is that the loss in activity is the result of a loss of sulfur from the catalyst surface, as suggested by Broderick et al.<sup>73</sup> and Kilanowski et al.<sup>32</sup> In this case, it would be expected that an increase in fractional conversion of benzothiophene (and hence an increase in  $H_2S$  partial pressure) would lead to a decrease in deactivation rate.

Another explanation for this observed long term deactivation might be coking reactions on the catalyst surface. If the overall rate of coke formation is zero order in benzothiophene (as has been found for desulfurization), then this deactivation rate will be independent of space time. If, in addition, the rate of coking is a positive order with respect to any (or all) of the products of the desulfurization reaction, then an increase in space time would result in an increase in the partial pressures of these components in the reactor, and thus the deactivation rate should



increase with increasing space time. It is only when the rate of coking has a negative order with respect to one of the reaction products (perhaps due to blocking of one of the catalyst sites by a harmless component) that a negative reaction order may be possible.

The nature of the trace products of the desulfurization reaction would seem to indicate that coke formation could result from reactions between styrene, benzothiophene, hydrogen sulfide, and thiophenic fragments formed by cracking of the benzene ring in benzothiophene. If this is in fact occurring, then the rate of coking should have a positive order with respect to these compounds. A negative order with respect to dihydrobenzothiophene is also unlikely, since it appears to be in equilibrium with benzothiophene, and consequently an increase in dihydrobenzothiophene partial pressure would also be associated with an increase in that of benzothiophene. Since an increase in ethylbenzene pressure can only be the result of increased amounts of styrene and/or dihydrobenzothiophene, it is also unlikely to be an inhibitor of coking.

Hydrogen sulfide was found by Gissy et al.<sup>74</sup> to inhibit coking of n-dodecane on Co-Mo- $\gamma$ -Al<sub>2</sub>O<sub>3</sub> in a similar reactor to that used in the present study. It was suggested by Gissy that H<sub>2</sub>S protected the catalyst by improving its hydrogenation function, and thus limiting the concentration of olefinic coke precursors in the reactor. If this hypothesis is applicable to the present case, then the rate of



deactivation should decrease with increasing space time - the same result as would be predicted by the "loss of catalyst sulfur" hypothesis.

The data in Figure 11 support both the hypothesis that deactivation is the result of a loss of sulfur from the catalyst and the hypothesis that  $\text{H}_2\text{S}$  inhibits coking by improving the hydrogenation function of the catalyst: even very small  $\text{H}_2\text{S}$  partial pressures (on the order of 0.5 kPa) are associated with a significant decrease in the rate of loss of activity.

Other data in the present study would also seem to favor the former explanation, however. Not only were heavy aliphatic hydrocarbons such as n-dodecane absent from the present study, but an analysis of the reaction products would seem to indicate a greater effect of increasing temperature on potential for coking than was observed. It appears that the change in deactivation rate from 350 to 450°C is fairly small for a fixed conversion of benzothiophene, increasing by a factor of between two and ten, but that the ratio of the amounts of styrene (presumably a main coke precursor) produced by the reaction at these two temperatures may be much greater, perhaps between 20:1 and 50:1, based on the relative amounts of styrene and dihydrobenzothiophene in the product stream. In addition, the data for all three temperatures show both a low rate of deactivation and a relatively high degree of unsaturation in the products stream at intermediate to high values of space





time. Unfortunately, these data are not sufficiently accurate to completely eliminate the possibility of coking. Regardless of which of these two explanations is correct (if either), if the protection of the catalyst is in fact due to  $\text{H}_2\text{S}$ , this type of deactivation would not be expected to be a significant factor in high-pressure processes, and could explain why this effect has not been found in similar studies conducted at high pressure.

Other hypotheses could also be consistent with the catalyst deactivation data of the present study. For example, the presence of hydrogen sulfide may protect the catalyst surface in a different way (perhaps by hindering migration of metal ions below the catalyst surface), or that this protection may be mainly due to the presence of a different product, or that deactivation may be the result of several concurrent processes. If desulfurization occurs on two different sites, it is also possible that one may be affected and not the other, or that one type of site may be slowly transformed into the other. These possibilities were not investigated further, due to the large amount of scatter in the data and the consequent difficulty of obtaining meaningful results from subsequent tests.





## 8. CONCLUSIONS

1. A fixed-bed microreactor with on-line gas sampling provides an effective method for studying hydrodesulfurization reactions, and has the advantages over an analysis of condensed products that the analysis is quantitative and that small changes in catalyst activity with time on stream can be detected more easily.
2. The pretreatment method of Ripperger and Saum<sup>20</sup> is effective in producing a catalyst with consistent activity.
3. Benzothiophene is desulfurized via two main reaction paths. At lower temperatures, benzothiophene is first hydrogenated to dihydrobenzothiophene, which is then desulfurized to ethylbenzene. At higher temperatures, benzothiophene is first desulfurized to styrene, which is then hydrogenated to produce ethylbenzene. It is suggested that this could have been due either to a shift in the equilibrium between benzothiophene and dihydrobenzothiophene or to adsorption limitations on one of the reactants. Because of this, a rate expression which does not allow for a change in the main reaction path with a change in temperature may be applicable only over a very limited range of temperatures.



4. A minimum value of 9.1 kcal/mol was calculated for the apparent activation energy of the reaction path through dihydrobenzothiophene. This is within the range of other reported literature values, however it is suggested that the true value may be somewhat higher. Possible reasons for this discrepancy include the error caused by the fact that the rates at only two temperatures were used to calculate this quantity, the wider temperature range used by other researchers which may be more representative of the reaction path, and the differences between the nickel-molybdenum catalyst used in this study and the cobalt-molybdenum and iron catalysts used by other researchers.
5. Other reactions taking place to a lesser degree in the reactor include cracking of the benzene ring, dealkylation of ethylbenzene, and reaction of the resultant hydrocarbon fragments with each other, hydrogen sulfide, and the other reactants and products. It is estimated that these reactions involve only about 0.5% of the total reaction products. In addition to this, evidence was found for a slight degree of styrene polymerization in the reactor.
6. Catalyst activity was found to decay linearly at a rate on the order of 0.1%/hr. Although this necessitated defining a hypothetical "zero-time" activity for the



catalyst, this was not considered to have affected the other results in any way. Because this deactivation rate varied inversely with space time (and with hydrogen sulfide partial pressure), it was concluded that coking was not the cause of this deactivation. It is suggested instead that a loss of sulfur from the catalyst may be a more reasonable explanation, suggesting that the loss in activity could be significantly reduced by a slight increase in the hydrogen sulfide partial pressure in the reactor.

7. Because the equilibria between benzothiophene and dihydrobenzothiophene and between  $H_2S$  in the gas phase and sulfur on the catalyst surface are strongly dependent on pressure, data from atmospheric studies should not be extrapolated to the high-pressure trickle-bed reactors used in industry.





## 9. RECOMMENDATIONS

1. Analysis of the intermediates styrene and dihydrobenzothiophene would be improved using a gas sampling valve with a larger internal volume than was used in the present study, preferably at least  $10\ \mu\text{l}$ , and/or a more sensitive gas chromatograph.
2. The limitations introduced by inconsistent liquid feed concentrations could be lessened if the apparatus were redesigned to allow refilling of the syringe without exposing the solution to the atmosphere. One possible modification to the apparatus may be to include a three-way valve in the line between the syringe and the hot box, the third arm of which is connected to a large reservoir of feed solution kept under pressure, and from which the syringe could be refilled once it was empty. This modification would have the additional advantage that a more dilute feed solution could be used. As a result, the heat capacity of the gas stream in the reactor would be increased, and this would lessen any possible effects of heat transfer limitations on the reaction rate.
3. The reaction mechanism for the hydrodesulfurization of benzothiophene should be studied in more detail. If dihydrobenzothiophene and styrene are included in the



feed, this would assist in obtaining more data on the rates of the individual reactions making up the overall network.

4. The cause of the long term catalyst deactivation should also be investigated further. The addition of small amounts of hydrogen sulfide to the gas stream should show whether or not this compound is involved in the deactivation, although spectroscopic measurements of the catalyst itself would probably be necessary to draw any conclusions concerning the actual mechanism of the deactivation.



## REFERENCES

1. Schuman, S. C., Shalit, H., Catal. Rev., 4(2), 245, (1970)
2. Beuther, H., Schmid, B. K., 6th World Petrol. Congress., Section III, Paper 20, June, 1963
3. Chakraborty, P., Kar, A. K., Ind. Eng. Chem. Process Des. Dev., 17, 252, (1978)
4. Chang, H.-R., Weller, S. W., Ind. Eng. Chem. Process Des. Dev., 17, 310, (1978)
5. Desikan, P., Amberg, C. H., Can. J. Chem., 42, 843, (1964)
6. Kolboe, S., Amberg, C. H., Can. J. Chem., 44, 2623, (1966)
7. Lee, H. C., Butt, J. B., J. Catal., 49, 220, (1977)
8. Morooka, S., Hamrin, C. E., Jr., Chem. Eng. Sci., 32, 125, (1977)
9. Owens, P. J., Amberg, C. H., Adv. Chem. Ser., 33, 182, (1961)
10. Satterfield, C. N., Roberts, G. W., Am. Inst. Chem. Eng. J., 14, 159, (1968)
11. Kawaguchi, Y., Dalla Lana, I. G., Otto, F. D., Can. J. Chem. Eng., 56, 65, (1978)
12. Martin, R. L., Grant, J. A., Anal. Chem., 37(6), 645, (1965)
13. Clugston, D. M., George, A. E., Montgomery, D. S., Smiley, G. T., Sawatzky, H., Dept. of Energy, Mines and Resources Research Report R-279, (1972)
14. Furimsky, E., Amberg, C. H., Can. J. Chem., 54, 1507, (1976)
15. Bartsch, R., Tanielan, C., J. Catal., 35, 353, (1974)
16. Givens, E. N., Venuto, P. B., Amer. Chem. Soc. Div. Petrol. Chem. Prepr., 15(4), A183, (1970)
17. Daly, F. P., J. Catal, 51, 221, (1978)
18. Laine, J., Pratt, U. C., Trimm, D. L., Ind. Eng. Chem.





Product Res. Dev., 18, 329, (1979)

19. Furimsky, E., Ranganathan, R., Parsons, B. I., Fuel, 57, 427, (1978)
20. Ripperger, W., Saum, W., J. Less-Common Metals, 54, 353, (1977)
21. Thomas, C. L., "Catalytic Processes and Proven Catalysts", Academic Press, New York, 1970, p. 158
22. Thompson, C. J., Coleman, H. J., Ward, C. C., Rall, H. T., Anal. Chem., 32, 425, (1960)
23. Hoog, H., Reman, G. H., Smithuysen, W. C. B., Proc. 3rd World Petrol. Cong., Sect. IV, 282, (1951)
24. Yamada, M., Chem. Abstr., 60, 11978g, (1964)
25. Hopkins, R. L., Coleman, H. J., Thompson, C. J., Rall, H. T., Anal. Chem., 41, 2041, (1969)
26. De Beer, V. H. J., Dahlmans, J. G. J., Smeets, J. G. M., J. Catal., 42, 467, (1976)
27. Gissy, H., Bartsch, R., Tanielan, C., J. Catal., 65, 150, (1980)
28. Bartsch, R., Tanielan, C., J. Catal., 50, 35, (1977)
29. Rollman, L. D., J. Catal., 46, 243, (1977)
30. Jones, S. O., Reid, E. E., J. Am. Chem. Soc., 60, 2452, (1938)
31. Kilanowski, D. R., Teeuwen, H., De Beer, V. H. J., Gates, B. C., Schuit, G. C. A., Kwart, H., J. Catal., 55, 129, (1978)
32. Kilanowski, D. R., Gates, B. C., J. Catal., 62, 70, (1980)
33. Nag, N. K., Sapre, A. V., Broderick, D. H., Gates, B. C., J. Catal., 57, 509, (1979)
34. Kwart, H., Schuit, G. C. A., Gates, B. C., J. Catal., 61, 128, (1980)
35. Richardson, J. T., Ind. Eng. Chem. Fund., 3, 154, (1964)
36. Voorhoeve, R. J. H., Stuiver, J. C. M., J. Catal., 23, 228, (1971)
37. Voorhoeve, R. J. H., J. Catal., 23, 236, (1971)





38. Voorhoeve, R. J. H., Stuiver, J. C. M., J. Catal., 23, 243, (1971)
39. Farragher, A. L., Cossee, P., Proc. 5th Int. Cong. Catal., 1301, Palm Beach, (1973)
40. Wentrcek, P. R., Wise, H., J. Catal., 51, 80, (1978)
41. Aoshima, A., Wise, H., J. Catal., 34, 145, (1974)
42. Lo Jacono, M., Verbeek, J. L., Schuit, G. C. A., J. Catal.,
43. Schuit, G. C. A., Gates, B. C., Am. Inst. Chem. Eng. J., 19, 417, (1973)
44. Hagenbach, G., Courty, P., Delmon, B., J. Catal., 31, 264, (1973)
45. De Beer, V. H. J., Van Sint Fiet, T. H. M., Engelen, J. F., Van Haandel, A. C., Wolfs, M. W. J., Amberg, C. H., Schuit, G. C. A., J. Catal., 27, 357, (1972)
46. Gajardo, P., Grange, P., Delmon, B., J. Catal., 63, 201, (1980)
47. Delannay, F., Haeussler, E. N., Delmon, B., J. Catal., 66, 469, (1980)
48. Lipsch, J. M. J. G., Schuit, G. C. A., J. Catal., 15, 163, (1969)
49. Lipsch, J. M. J. G., Schuit, G. C. A., J. Catal., 15, 174, (1969)
50. Lipsch, J. M. J. G., Schuit, G. C. A., J. Catal., 15, 179, (1969)
51. Massoth, F. E., J Catal., 36, 164, (1975)
52. Massoth, F. E., Kibby, C., L., J. Catal., 47, 300, (1977)
53. Dufaux, M., Che, M., Naccache, C., J. Chim. Phys., 67, 527, (1970)
54. Ashley, J. H., Mitchell, P. C. H., J. Chem. Soc. (A), 2821, (1968)
55. Ashley, J. H., Mitchell, P. C. H., J. Chem. Soc. (A), 2730, (1969)
56. Chung, K. S., Massoth, F. E., J. Catal., 64, 320, (1980)



57. Mitchell, P. C. H., Trifiro, F., J. Catal., 33, 350, (1974)
58. De Beer, V. H. J., Van Sint Fiet, T. H. M., Van Der Steen, G. H. A. M., Zwaga, A. C., Schuit, G. C. A., J. Catal., 35, 297, (1974)
59. Behbahany, F., Sheikhrezai, Z., Djalali, M., Salajegheh, S., J. Catal, 63, 285, (1980)
60. Ahuja, S.P., Derrien, M. L., Le Page, J. F., Ind. Eng. Chem. Prod. Res. Dev., 9, 272, (1970)
61. Smith, G. V., Hinckley, C. C., Behbahany, F., J. Catal., 30, 218, (1973)
62. Hargreaves, A. E., Ross, J. R. H., Proc. 6th Int. Cong. Catal., 937, London, (1976)
63. Parsons, B. I., Ternan, M., Proc. 6th Int. Cong. Catal., 965, London, (1976)
64. Beuther, H., Flinn, R. A., McKinley, J. B., Ind. Eng. Chem., 51, 1349, (1959)
65. Satterfield, C. N., Modell, M., Mayer, J. F., Am. Inst. Chem. Eng. J., 21, 1100, (1975)
66. Furimsky, E., Am. Inst. Chem. Eng. J., 25, 306, (1979)
67. De Beer, V. H. J., van der Aalst, M. J. M., Machiels, C. J., Schuit, G. C. A., J. Catal., 43, 78, (1976)
68. Laine, J., Pratt, U. C., Trimm, D. L., J. Chem. Tech. Biotechnol., 29, 397, (1979)
69. Paraskos, J. A., Frayer, J., A., Shah, Y. T., Ind. Eng. Chem. Process Des. Dev., 14, 315, (1975)
70. Satterfield, C. N., Am. Inst. Chem. Eng. J., 21, 209, (1975)
71. De Beer, V. H. J., Bevelander, C., Van Sint Fiet, T. H. M., Werter, P. G. A. J., Amberg, C. H., J. Catal., 43, 68, (1976)
72. Aitken, A. R., Merrill, W. H., Pleet, M. P., Can. J. Chem. Eng., 42, 234, (1964)
73. Broderick, D. H., Schuit, G. C. A., Gates, B. C., J. Catal., 54, 94, (1978)
74. Gissy, H., Bartsch, R., Tanielan, C., J. Catal., 65, 158, (1980)



75. Weast, R. C., ed., "Handbook of Chemistry and Physics, 53 ed.", CRC Press, Cleveland, 1972, p. C-201
76. Ralston, M., "PAR: Derivative-free Non-linear Regression", in "BMDP-79", W. J. Dixon and M. B. Brown, eds. , Univ. of California Press, Berkeley, 1979
77. Owens, P. J., Amberg, C. H., Can. J. Chem., 40, 947, (1962)
78. Desikan, P., Amberg, C. H., Can. J. Chem., 41, 1966, (1963)
79. Frye, C. G., Mosby, J. F., Chem. Eng. Progr., 63, 66, (1967)
80. McLeish, D., personal communication
81. Dietz, W. A., J. Gas Chromatog., 5, 68, (1967)
82. Weast, R. C., ed., op. cit., p. C-327
83. Perry, R. H., Chilton, C. H., "Chemical Engineers Handbook, 5ed", McGraw-Hill, Toronto, 1973, p. 3-120
84. Weast, R. C., ed., op. cit., p. D-130
85. Weast, R. C., ed., op. cit., p. D-134
86. Weast, R. C., ed., op. cit., p. F-183 to F-189





## APPENDIX A - ROTAMETER CALIBRATION DATA

The hydrogen and nitrogen rotameters were calibrated using a stopwatch (accurate to 0.1 s) and a soap-bubble flowmeter manufactured from a 50 ml burette. The procedure consisted of setting a flow rate on the rotameter, adjusting the pressure to 101 kPa using a globe valve located downstream of the rotameter, and measuring the length of time it took for a given volume of gas to pass through the flowmeter. This volume was usually chosen so that the time measured would be on the order of 30 s, although when the flow rate was very high and the full volume of the flowmeter was used, the measured times were as low as 5 s.

The calibration data are presented in Table A-1. The volumetric flow rates shown were measured at 24°C and 92.6 kPa. The following polynomials were fitted to these data using a least squares algorithm<sup>10</sup>:

$$Q_{hg} = 1.6258 \times 10^{-1} + 1.3138 \times 10^{-3} R + 1.1197 \times 10^{-4} R^2 - 2.1589 \times 10^{-7} R^3 \quad (A-1a)$$

$$Q_{hs} = 7.2424 + 3.7017 \times 10^{-2} R + 1.8662 \times 10^{-4} R^2 + 4.118 \times 10^{-7} R^3 \quad (A-1b)$$

$$Q_{ng} = 8.5157 \times 10^{-2} + 6.4351 \times 10^{-4} R + 8.2782 \times 10^{-5} R^2 - 5.7607 \times 10^{-7} R^3 + 1.8400 \times 10^{-9} R^4 \quad (A-1c)$$

$$Q_{ns} = -3.0917 + 1.4885 \times 10^{-1} R - 2.1137 \times 10^{-3} R^2 + 1.4609 \times 10^{-5} R^3 - 3.5941 \times 10^{-8} R^4 \quad (A-1d)$$

where

$Q$  = Volumetric flow rate, cm<sup>3</sup>/s



R = Rotameter reading

h = Hydrogen Rotameter

n = Nitrogen Rotameter

g = Glass Float

s = Steel Float

The order of the polynomial was the minimum such that the addition of another term would not give a statistically better fit to the data. Both the data and the fitted polynomials are shown graphically in Figure A-1.



Table A-1a - Calibration Data for Hydrogen Rotameter  
(glass ball)

Rotameter Reading	Flow Rate cm <sup>3</sup> /s	Rotameter Reading	Flow Rate cm <sup>3</sup> /s
25.0	0.2503	91.8	1.0000
25.5	0.2519	91.3	1.0067
26.0	0.2407	90.8	1.0135
25.5	0.2519	90.5	1.0239
29.0	0.3035	90.6	1.0239
29.0	0.2869	90.0	0.9967
28.5	0.2813	90.5	0.9772
28.5	0.2703	101.0	1.1364
33.3	0.3231	100.8	1.1173
32.0	0.3211	101.2	1.1236
32.0	0.3247	100.5	1.1205
30.0	0.3284	100.7	1.1364
40.5	0.3752	107.0	1.2270
40.0	0.3953	106.0	1.2346
40.0	0.4024	105.8	1.2461
40.0	0.3839	105.5	1.2422
51.3	0.4890	111.8	1.3333
51.3	0.5195	110.5	1.3513
51.7	0.5168	111.0	1.3468
52.5	0.4975	110.6	1.3559
52.5	0.5102	110.0	1.3559
59.5	0.5634	110.0	1.3559
59.7	0.5848	120.8	1.4970
59.8	0.5747	120.0	1.5198
59.6	0.5682	119.5	1.5106
67.1	0.6515	119.5	1.5060
66.4	0.6601	119.5	1.5106
66.0	0.6515	118.2	1.4620
66.2	0.6410	118.4	1.4620
65.8	0.6515	118.4	1.4663
74.2	0.7605	118.6	1.4620
73.4	0.7519	124.3	1.6026
73.4	0.7463	124.3	1.5873
72.8	0.7605	124.2	1.5974
73.2	0.7547	124.2	1.5974
72.0	0.7463	124.2	1.5823
71.5	0.7519	124.2	1.5924
80.0	0.8389	133.0	1.6949
79.2	0.8451	133.0	1.7065
78.2	0.8446	133.0	1.7007
77.2	0.8361	132.7	1.7065
84.5	0.9146	132.7	1.7065
83.6	0.9202	132.7	1.7123
82.4	0.9615	140.8	1.9011
82.5	0.9375	140.8	1.9011
91.3	1.0169	140.8	1.8797



Table A-1a (cont.)

Rotameter Reading	Flow Rate cm <sup>3</sup> /s	Rotameter Reading	Flow Rate cm <sup>3</sup> /s
140.8	1.9011	135.5	1.7483
140.8	1.9084	135.5	1.7422
150.0	2.0492	114.8	1.4205
150.0	2.0243	114.8	1.4045
150.0	2.0243	114.8	1.4045
150.0	2.0492	114.8	1.4006
150.0	2.0325	95.1	1.1390
145.6	1.9084	94.9	1.1359
145.6	1.9084	95.0	1.1013
145.6	1.8727	95.0	1.1312
135.5	1.7606		





Table A-1b - Calibration Data for Hydrogen Rotameter  
(steel ball)

Rotameter Reading	Flow Rate cm <sup>3</sup> /s	Rotameter Reading	Flow Rate cm <sup>3</sup> /s
28.0	1.9305	93.0	6.1728
22.5	1.6340	93.5	6.1728
23.0	1.6287	93.0	6.1728
23.0	1.6234	107.5	7.3529
24.0	1.5924	107.3	7.3529
22.0	1.6129	107.3	7.2464
30.0	2.0243	107.2	7.2464
30.0	2.0243	106.5	7.3529
29.5	2.0000	106.0	7.2464
29.2	1.9608	120.5	8.6207
28.5	2.0000	120.0	8.6207
52.5	3.2051	120.0	8.7719
52.5	3.1250	120.0	8.4746
53.0	3.1646	119.0	8.4746
52.5	3.1646	119.0	8.6207
53.0	3.1250	118.5	8.4746
37.5	2.3474	130.8	9.8039
36.0	2.3697	130.8	9.8039
36.0	2.3364	130.8	9.8039
34.5	2.3364	129.5	9.6154
33.5	2.2624	129.6	9.8039
34.0	2.3148	130.0	9.8039
71.5	4.3860	150.0	11.6279
71.3	4.3860	150.0	11.9048
71.3	4.3860	150.0	11.9048
71.6	4.3478	150.0	11.9048
71.4	4.3103	145.0	11.6279
71.2	4.3478	145.0	11.6279
71.0	4.3860	145.0	11.6279
79.8	5.1546	139.5	10.8696
79.5	5.0505	139.5	10.2041
79.3	4.8544	139.5	10.2041
78.0	5.0505	139.5	10.6383
77.5	5.1020	139.0	10.4167
76.0	5.0505	135.0	10.2041
76.0	5.0505	134.8	9.8039
86.2	5.6180	134.8	10.0000
86.3	5.5556	134.7	9.8039
86.0	5.5556	134.2	9.8039
85.5	5.4945	126.5	9.2593
84.5	5.5556	126.3	8.9286
81.0	5.6180	125.5	9.6154
83.0	5.5556	125.5	9.4340
94.0	6.0976	125.0	9.0909
93.0	6.0976	125.0	9.0909
92.5	6.0976	114.5	7.9365



Table A-1b (cont.)

Rotameter Reading	Flow Rate cm <sup>3</sup> /s	Rotameter Reading	Flow Rate cm <sup>3</sup> /s
114.5	7.6923	57.5	3.4722
114.5	7.8125	57.5	3.4722
114.0	7.8125	57.0	3.4965
113.8	7.8125	58.0	3.4965
111.2	7.8125	58.0	3.4965
111.2	7.6923	47.3	2.8249
111.2	7.6923	47.8	2.8249
111.2	7.6923	47.5	2.8409
111.2	7.8125	47.3	2.8249
102.2	6.7568	47.5	2.8409
101.8	6.7568	39.8	2.5381
101.8	6.7568	40.5	2.5510
101.5	6.6667	38.8	2.5381
101.5	6.7568	44.0	2.8090
89.0	5.8139	43.0	2.7933
88.5	5.6818	44.0	2.8090
88.8	5.8823	34.0	2.2831
88.2	5.6818	35.0	2.4390
63.5	4.0323	36.0	2.4390
63.0	4.0000	26.0	1.8050
64.5	4.0650	26.5	1.8248
65.0	4.0650	26.0	1.8315
64.5	4.0650	26.0	1.8382
57.5	3.4722		



Table A-1c - Calibration Data for Nitrogen Rotameter  
(glass ball)

Rotameter Reading	Flow Rate cm <sup>3</sup> /s	Rotameter Reading	Flow Rate cm <sup>3</sup> /s
19.6	0.1247	68.2	0.3717
19.6	0.1289	94.0	0.5348
19.6	0.1012	93.3	0.5333
19.6	0.1572	92.9	0.5333
19.6	0.1359	92.6	0.5333
24.2	0.1433	92.2	0.5333
24.2	0.1401	100.0	0.5848
24.2	0.1335	100.0	0.5848
24.2	0.1292	99.8	0.5848
24.2	0.1276	99.8	0.5848
36.8	0.1776	99.5	0.5865
37.0	0.1799	104.8	0.6192
36.2	0.1789	104.4	0.6173
40.8	0.2347	104.2	0.6173
40.7	0.2257	104.2	0.6173
40.0	0.2262	104.0	0.6173
40.2	0.2262	111.0	0.6667
40.2	0.2247	110.6	0.6667
40.0	0.2222	110.2	0.6667
39.5	0.2217	110.1	0.6667
43.0	0.2242	110.0	0.6667
43.4	0.2247	115.4	0.7067
42.5	0.2247	115.3	0.7067
50.0	0.2632	115.0	0.7042
50.0	0.2611	115.0	0.7017
49.5	0.2611	114.8	0.7042
49.3	0.2691	119.4	0.7407
49.0	0.2558	119.8	0.7353
48.7	0.2545	123.1	0.7576
48.2	0.2545	122.9	0.7576
58.5	0.3077	122.6	0.7605
58.2	0.3058	122.5	0.7634
58.2	0.3040	122.2	0.7634
57.9	0.3049	130.0	0.8163
57.5	0.3049	129.9	0.8231
57.2	0.3040	129.6	0.8197
63.8	0.3448	129.5	0.8231
63.3	0.3460	129.6	0.8197
62.8	0.3413	134.6	0.8645
62.5	0.3378	134.0	0.8571
62.2	0.3367	134.0	0.8596
70.0	0.3759	133.8	0.8571
69.4	0.3745	133.6	0.8596
69.3	0.3731	140.3	0.9231
69.0	0.3717	139.2	0.9174
68.5	0.3717	138.9	0.9174





Table A-1c (cont.)

Rotameter Reading	Flow Rate cm <sup>3</sup> /s	Rotameter Reading	Flow Rate cm <sup>3</sup> /s
138.8	0.9293	141.7	0.9464
138.8	0.9464	149.2	1.0274
142.2	0.9464	149.0	1.0135
142.0	0.9434	148.6	1.0204
141.9	0.9434	148.7	1.0169
141.8	0.9464	148.8	1.0135
141.7	0.9464		



Table A-1d - Calibration Data for Nitrogen Rotameter  
(steel ball)

Rotameter Reading	Flow Rate cm <sup>3</sup> /s	Rotameter Reading	Flow Rate cm <sup>3</sup> /s
59.8	0.8850	105.7	1.8116
59.5	0.8876	105.8	1.8182
59.0	0.8902	105.8	1.8182
59.7	0.8902	105.9	1.7986
58.2	0.8902	109.8	1.8868
64.0	0.9901	109.9	1.8797
63.3	0.9868	109.9	1.8657
63.1	0.9836	109.9	1.8797
62.7	0.9868	109.9	1.8727
61.8	0.9836	114.6	1.9920
68.5	1.0714	114.5	1.9685
67.8	1.0753	114.3	1.9685
67.0	1.0791	114.3	1.9608
66.3	1.0753	114.1	1.9608
65.5	1.0753	120.5	2.1368
74.2	1.1494	120.3	2.1097
73.7	1.1494	120.1	2.1097
72.9	1.1538	120.1	2.1186
72.3	1.1493	120.0	2.0920
71.8	1.1538	124.0	2.2624
80.4	1.3072	124.1	2.2422
79.5	1.3029	124.0	2.2522
78.8	1.2987	124.2	2.2624
78.6	1.3029	124.3	2.2422
78.3	1.3029	129.4	2.3697
84.7	1.3605	129.1	2.3809
84.2	1.3559	129.6	2.3585
83.3	1.3605	129.5	2.3148
82.6	1.3605	129.5	2.4510
82.0	1.3605	129.7	2.3697
91.8	1.4981	134.5	2.5641
91.7	1.4981	145.9	2.6455
91.4	1.4981	145.8	2.6738
91.3	1.4925	145.8	2.6455
91.1	1.4925	145.7	2.6455
96.9	1.6026	145.7	2.6455
96.7	1.5924	149.9	2.8249
96.6	1.5974	149.9	2.8409
96.3	1.5974	149.9	2.8409
96.2	1.6026	149.9	2.8249
99.5	1.6502	149.9	2.8409
99.5	1.6447	140.6	2.5510
99.4	1.6556	140.5	2.5126
99.5	1.6556	137.5	2.5510
99.3	1.6556	137.5	2.5641
105.6	1.8182	137.4	2.5510



Table A-1d (cont.)

Rotameter Reading	Flow Rate $\text{cm}^3/\text{s}$	Rotameter Reading	Flow Rate $\text{cm}^3/\text{s}$
137.5	2.5907	137.7	2.5641
137.7	2.5641		



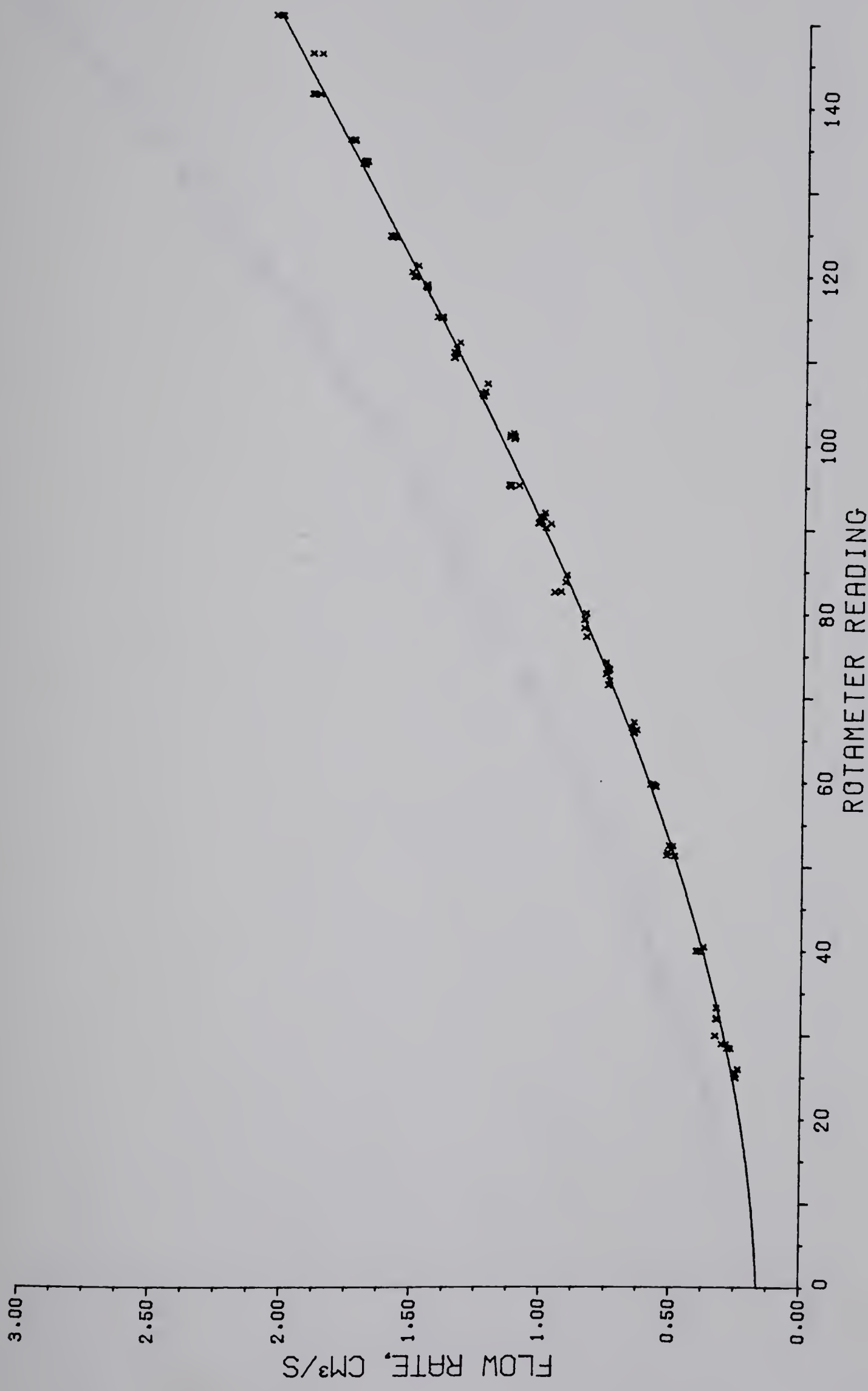


Figure A-1a - Calibration Curve for Hydrogen Rotameter (glass ball)





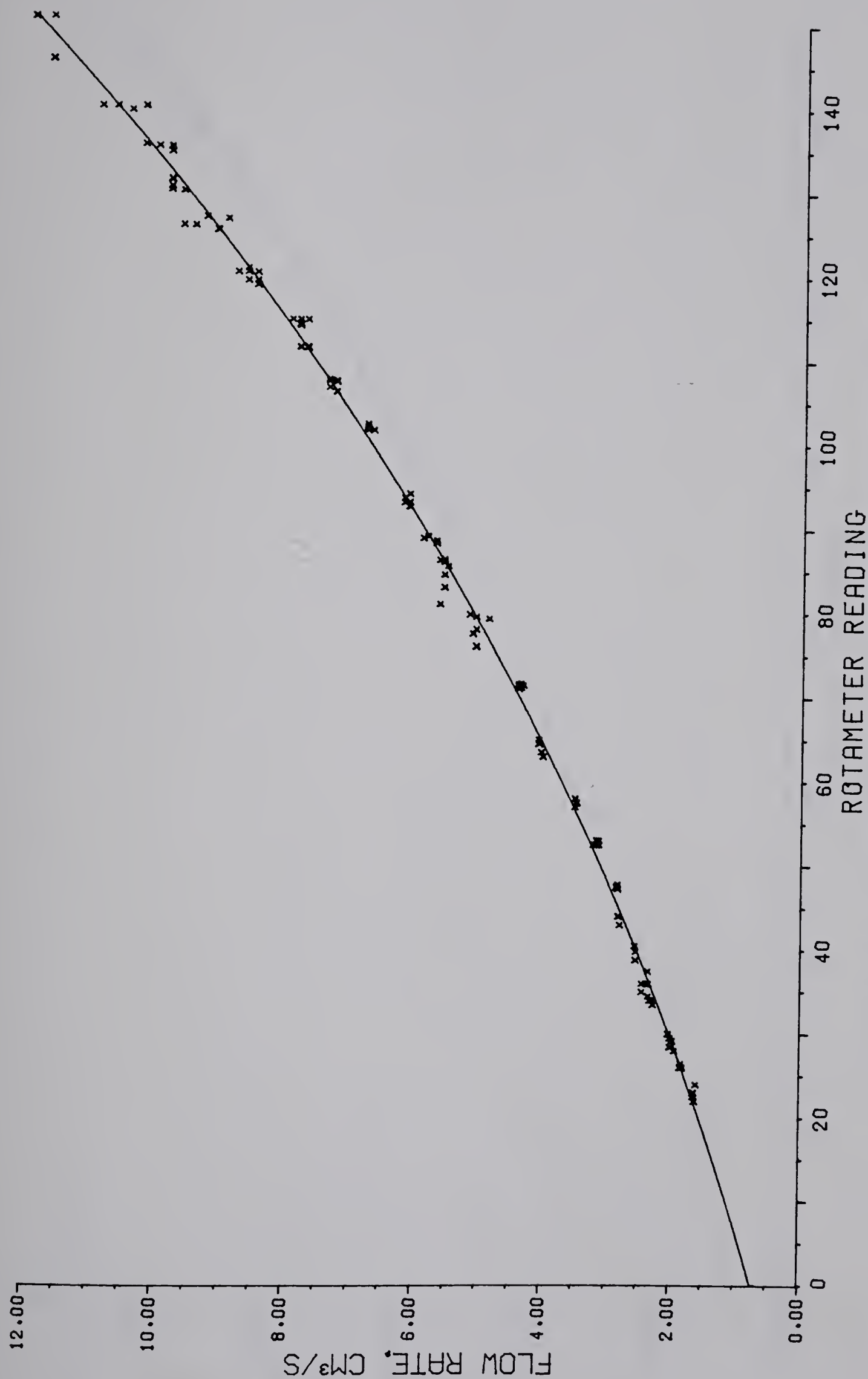


Figure A-1b - Calibration Curve for Hydrogen Rotameter (steel ball)



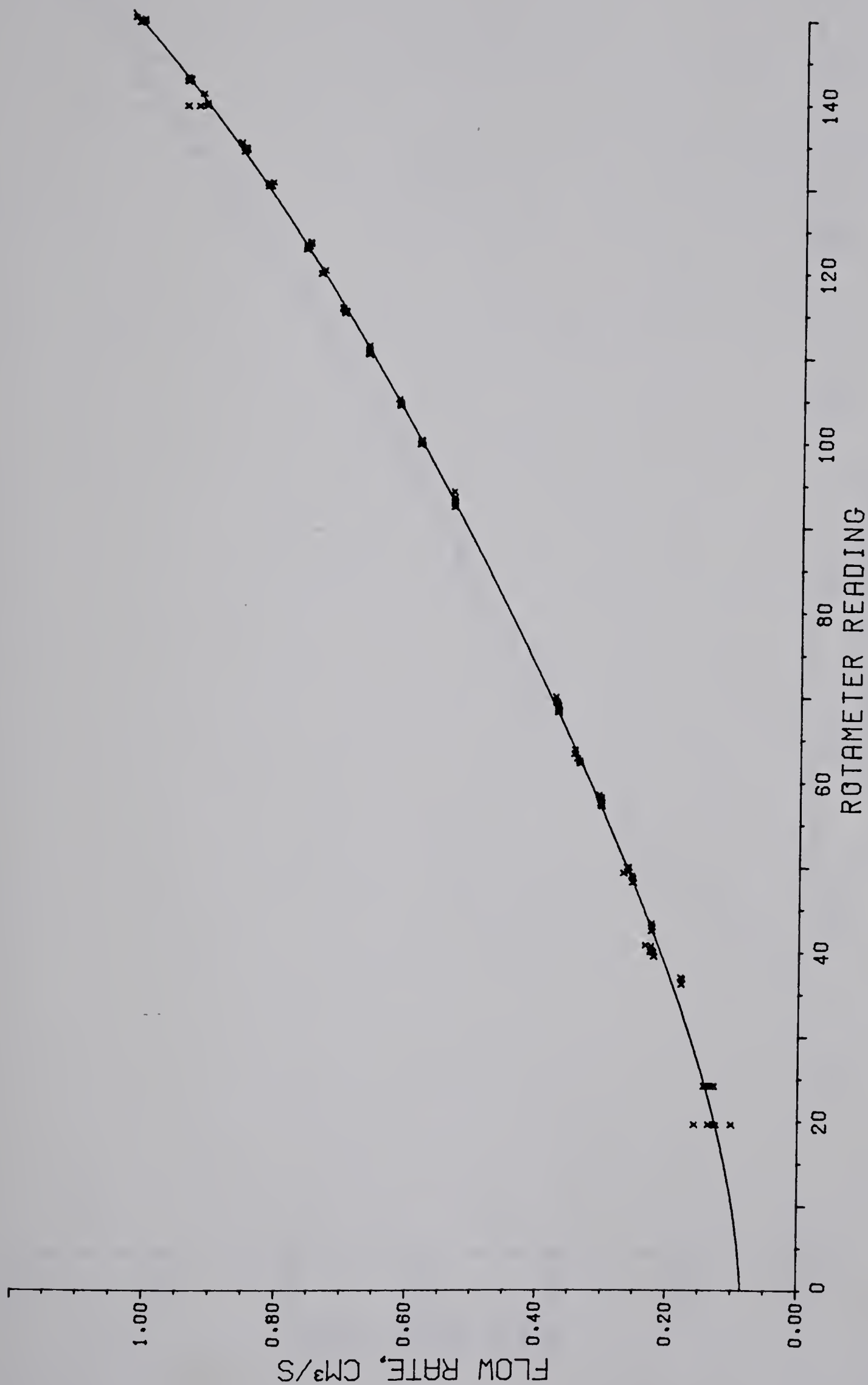


Figure A-1c - Calibration Curve for Nitrogen Rotameter (glass ball)



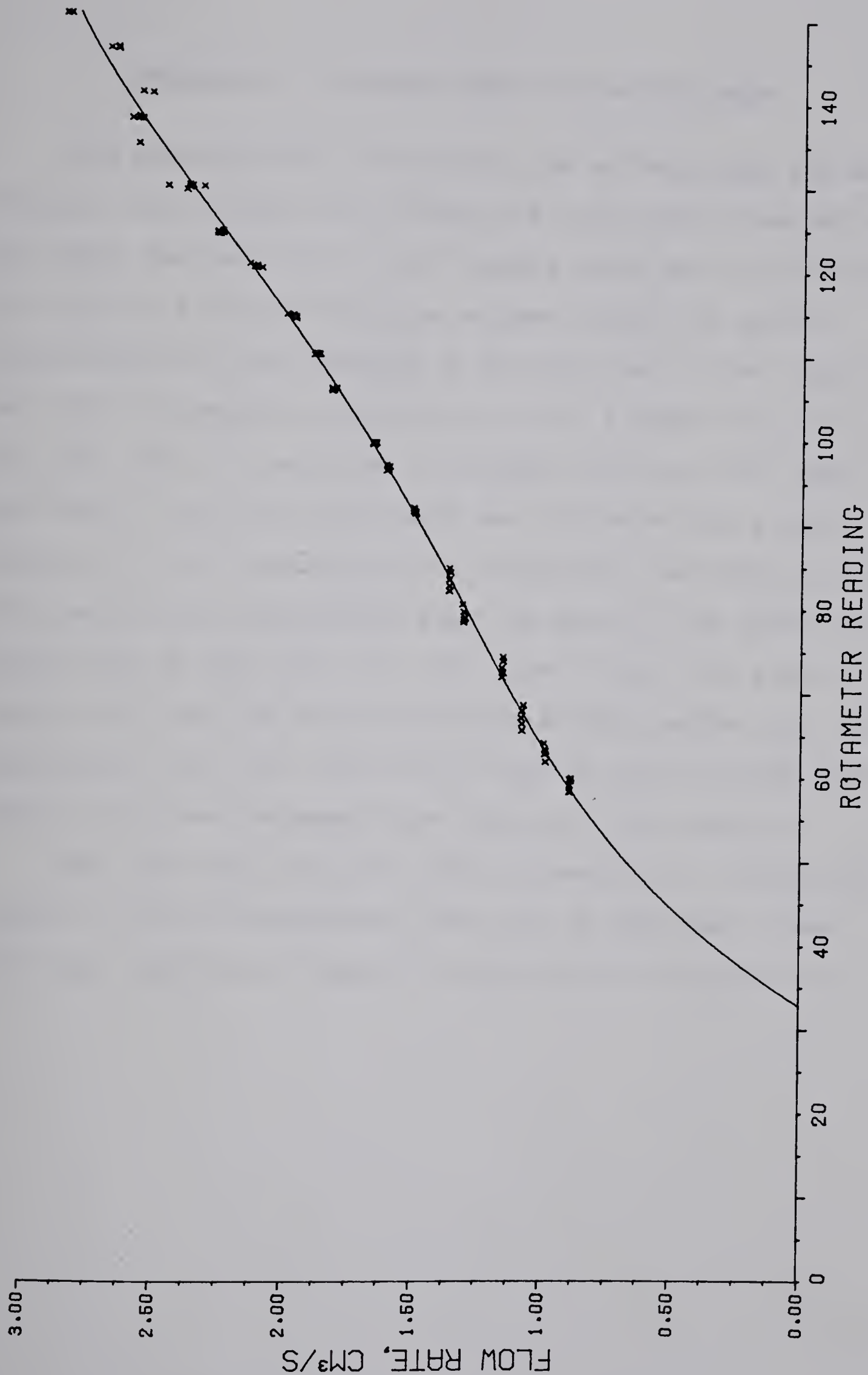


Figure A-1d - Calibration Curve for Nitrogen Rotameter (steel ball)





## APPENDIX B - SYRINGE PUMP CALIBRATION DATA

The procedure for calibrating the syringe pump was as follows: The syringe was filled with water and connected to the pump. The section of 1/16" tubing which was to lead from the syringe to the flowing gas stream during the actual experimentation was attached to the syringe. A flow rate was set and the pump was allowed to run for a short while for the flow rate to stabilize. A weighed flask was set under the end of the tubing and water was collected for a given period of time, measured with a stopwatch. The length of the time period was adjusted so that the mass of the liquid collected was on the order of a few grams. Since the flow of water fell into the flask as discrete drops rather than as a continuous flow, the time period started and finished just after a drop was released from the end of the tubing.

The flow rates measured fell between  $10\% \times 1/1000$  and  $100\% \times 1/100$  of the maximum flow rate of the pump; these data are reported in Table B-1 and plotted in Figure B-1.



Table B-1 - Syringe Pump Calibration Data

Flow Setting % Max. Rate	Flow Rate ml/min.
10% x 1/1000	0.0088
20% x 1/1000	0.0172
30% x 1/1000	0.0262
40% x 1/1000	0.0335
50% x 1/1000	0.0443
60% x 1/1000	0.0520
70% x 1/1000	0.0596
80% x 1/1000	0.0690
90% x 1/1000	0.0768
100% x 1/1000	0.0881
10% x 1/100	0.0894
20% x 1/100	0.1798
30% x 1/100	0.2639
40% x 1/100	0.3513
50% x 1/100	0.4390
60% x 1/100	0.5182
70% x 1/100	0.6103
80% x 1/100	0.6998
90% x 1/100	0.8026
15% x 1/100	0.1337
25% x 1/100	0.2201
35% x 1/100	0.3057
45% x 1/100	0.3954
55% x 1/100	0.4851
65% x 1/100	0.5833
75% x 1/100	0.6574
85% x 1/100	0.7622
95% x 1/100	0.8291
100% x 1/100	0.8758



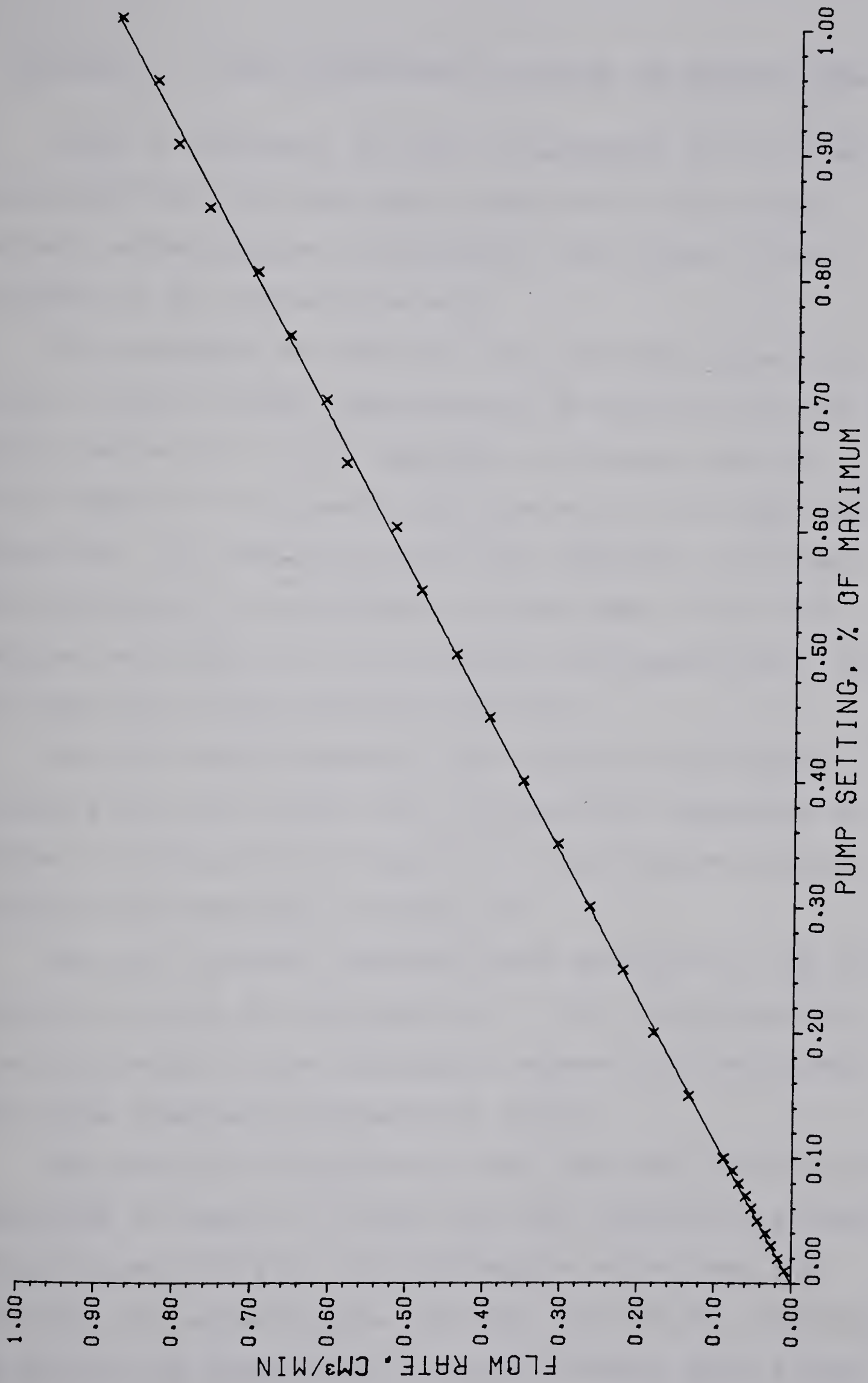


Figure B-1 - Syringe Pump Calibration data



## APPENDIX C - GAS CHROMATOGRAPH DETECTOR CALIBRATION DATA

Prior to analysis, the gas chromatograph detector was calibrated for the three major components in the product stream, benzothiophene, ethylbenzene, and styrene, using n-hexane as an internal standard.

The procedure was identical for all three components. First, a small volume (approximately 50 ml) of a solution of known composition of the component in n-hexane was made. Five samples of 10  $\mu$ l each were injected into the gas chromatograph, the response ratio of the component to n-hexane was calculated for each sample, and the mean of the five samples was computed. This procedure was repeated until six or seven data points had been collected.

For all three components, the response ratio varied linearly with the weight ratio. The data are summarized in Table C-1 and plotted in Figure C-1. The relative response factors are summarized in Table C-2.

The only relative response factor available in the literature was that for ethylbenzene<sup>11</sup>, 1.17. No explanation can be offered for the discrepancy between this value and the value obtained experimentally (0.99).

The analysis was performed under the same conditions as described in Chapter 3, except that the temperature programming rate was 15°/min. for ethylbenzene and styrene and 20°/min. for benzothiophene, and that the run was terminated as soon as the component of interest had been fully eluted.







Table C-1 - Detector Calibration Data

Component	Weight Ratio Component/HEX	Response Ratio Component/HEX
Styrene	0.0543	0.0562
	0.0188	0.0194
	0.0067	0.0067
	0.0857	0.0888
	0.0261	0.0254
	0.1092	0.1098
Ethylbenzene	0.1814	0.1823
	0.0208	0.0222
	0.0134	0.0139
	0.0088	0.0089
	0.1396	0.1401
	0.0704	0.0706
	0.0511	0.0521
Styrene	0.0374	0.0364
	0.0181	0.0174
	0.0050	0.0045
	0.0728	0.0711
	0.1063	0.1040
	0.1637	0.1648



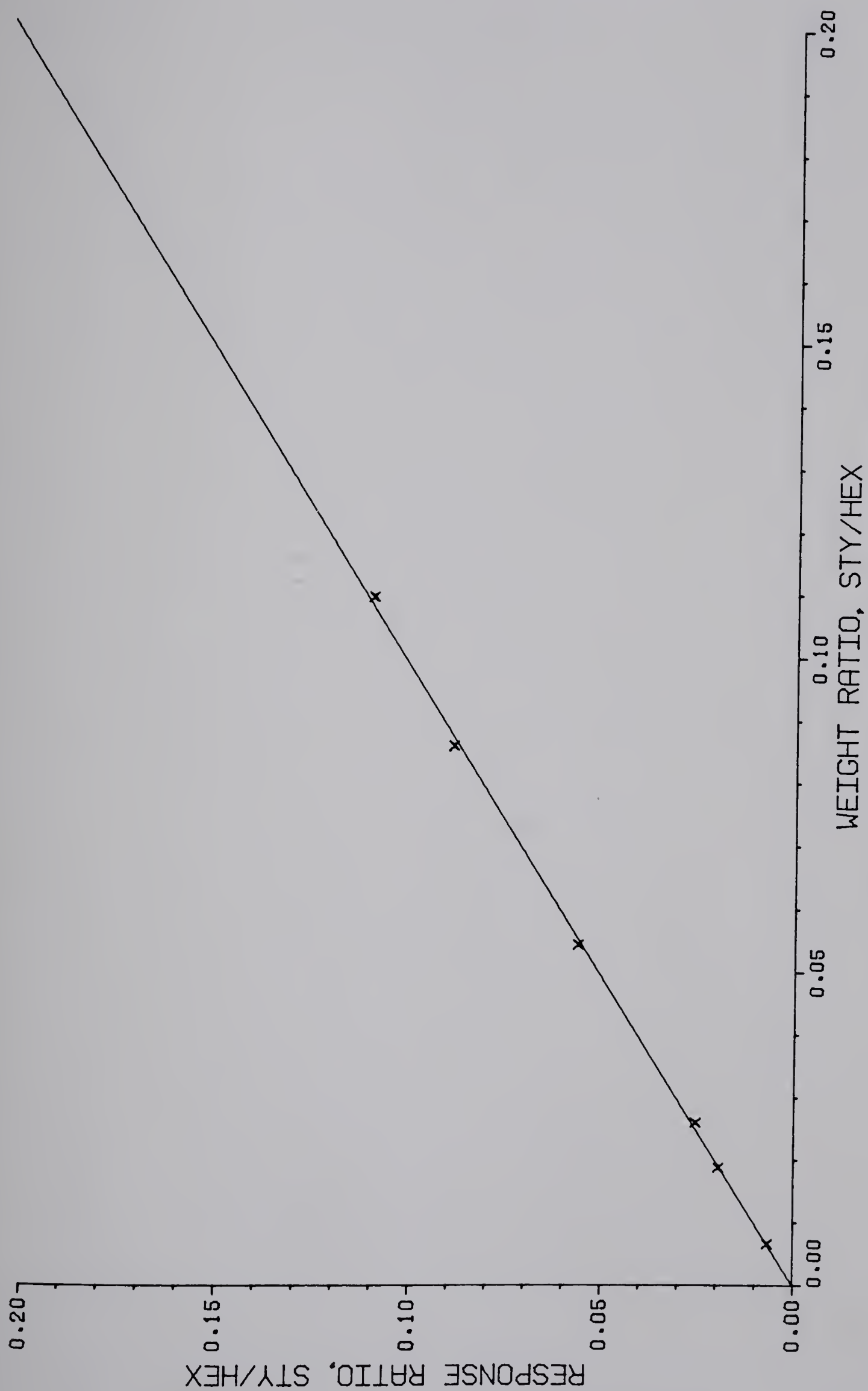


Figure C-1a - Calibration Data for Styrene



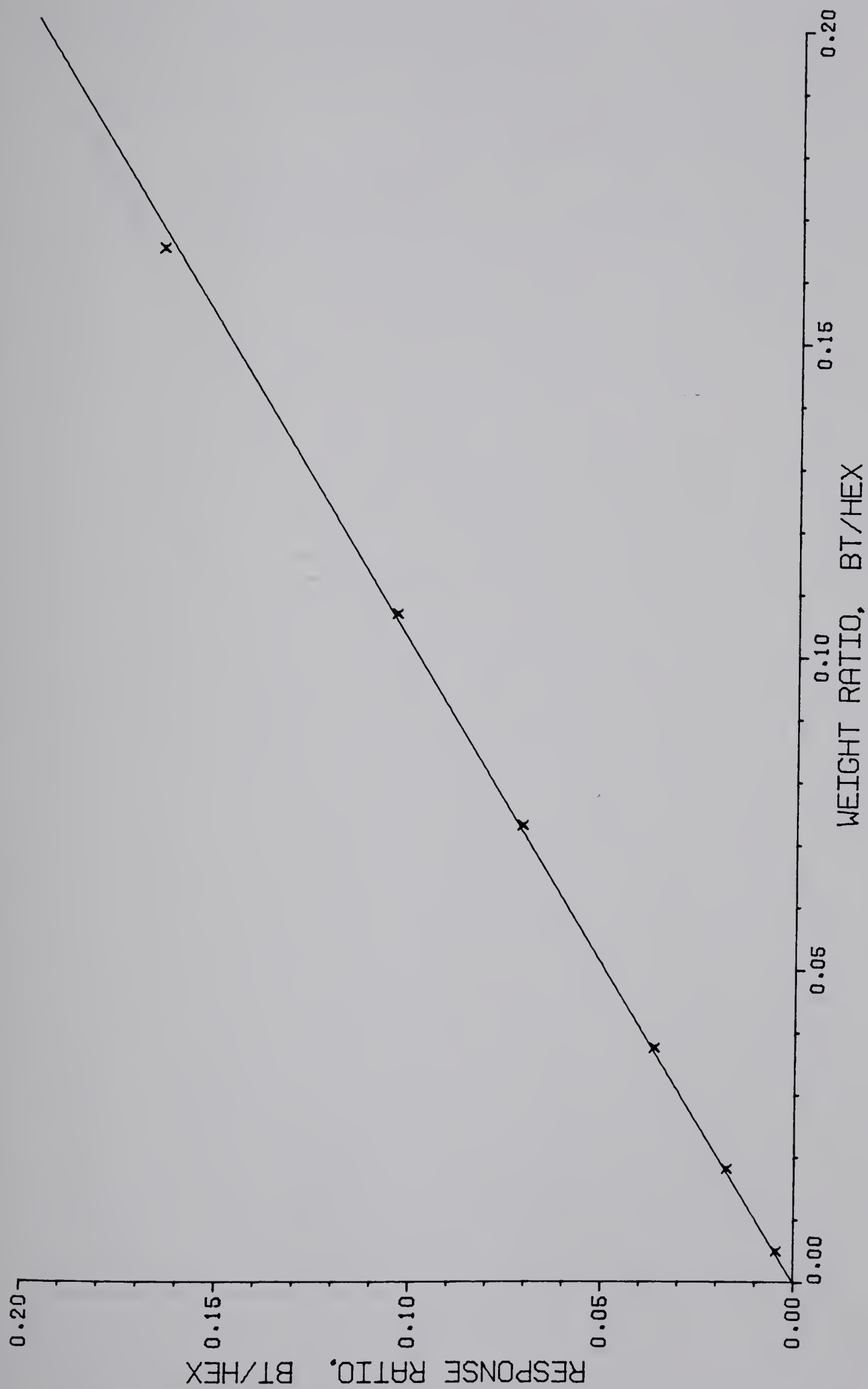


Figure C-1b - Calibration Data for Benzothlophene



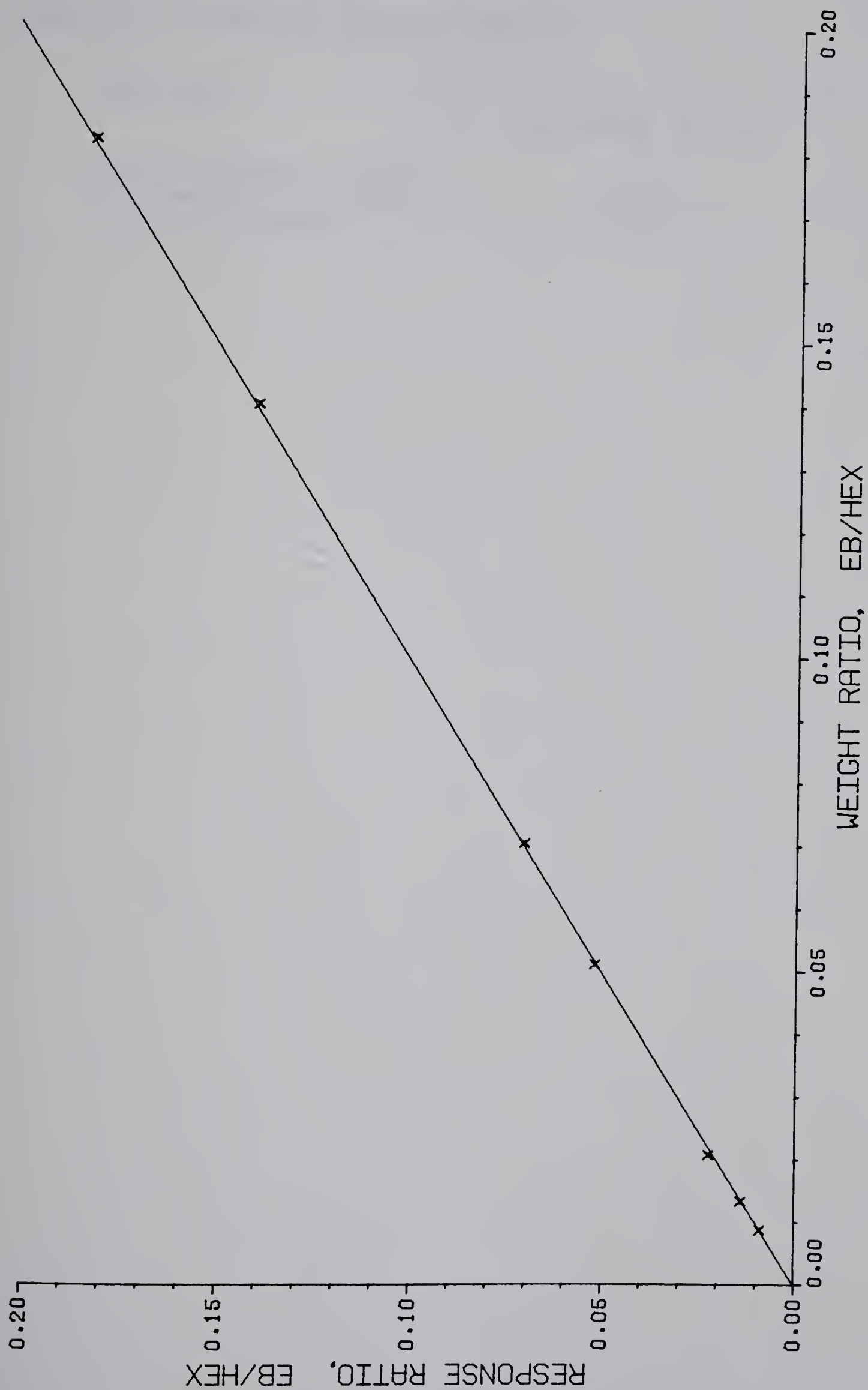


Figure C-1c - Calibration Data for Ethylbenzene





Table C-2 - Relative Response Factors

Component	Relative Response Factor
Benzothiophene/n-Hexane	1.0272
Ethylbenzene/n-Hexane	0.9942
Styrene/n-Hexane	0.9697



## APPENDIX D - DENSITY-COMPOSITION DATA FOR LIQUID FEED SOLUTIONS

This appendix describes work done to verify that the specific gravity of solutions of benzothiophene in n-hexane could be predicted by simply adding the products of the weight fractions and specific gravities of each pure component.

A total of four data points were collected. In each case a small volume (about 50 ml) of solution was mixed on a balance and immediately used to fill a 25 ml specific gravity bottle. The bottle was weighed, and the specific gravity calculated. The weight ratios of benzothiophene to n-hexane in the test solutions and the experimental and theoretical specific gravities are shown in Table D-1. The experimental points and the theoretical curve are shown in Figure D-1.

The specific gravity of pure n-hexane is 0.6603<sup>82</sup>; the specific gravity of pure solid benzothiophene is 1.149<sup>75</sup>. The experimental conditions were 20 °C and 93.3 kPa.



Table D-1 - Density-Composition Data for  
Benzothiophene/n-Hexane Solutions

Wt. Ratio BT/HEX	Experimental S.G.	Theoretical S.G.
0.7334	0.8648	0.8671
0.6206	0.8524	0.8474
0.5521	0.8302	0.8341
0.3974	0.8007	0.7993



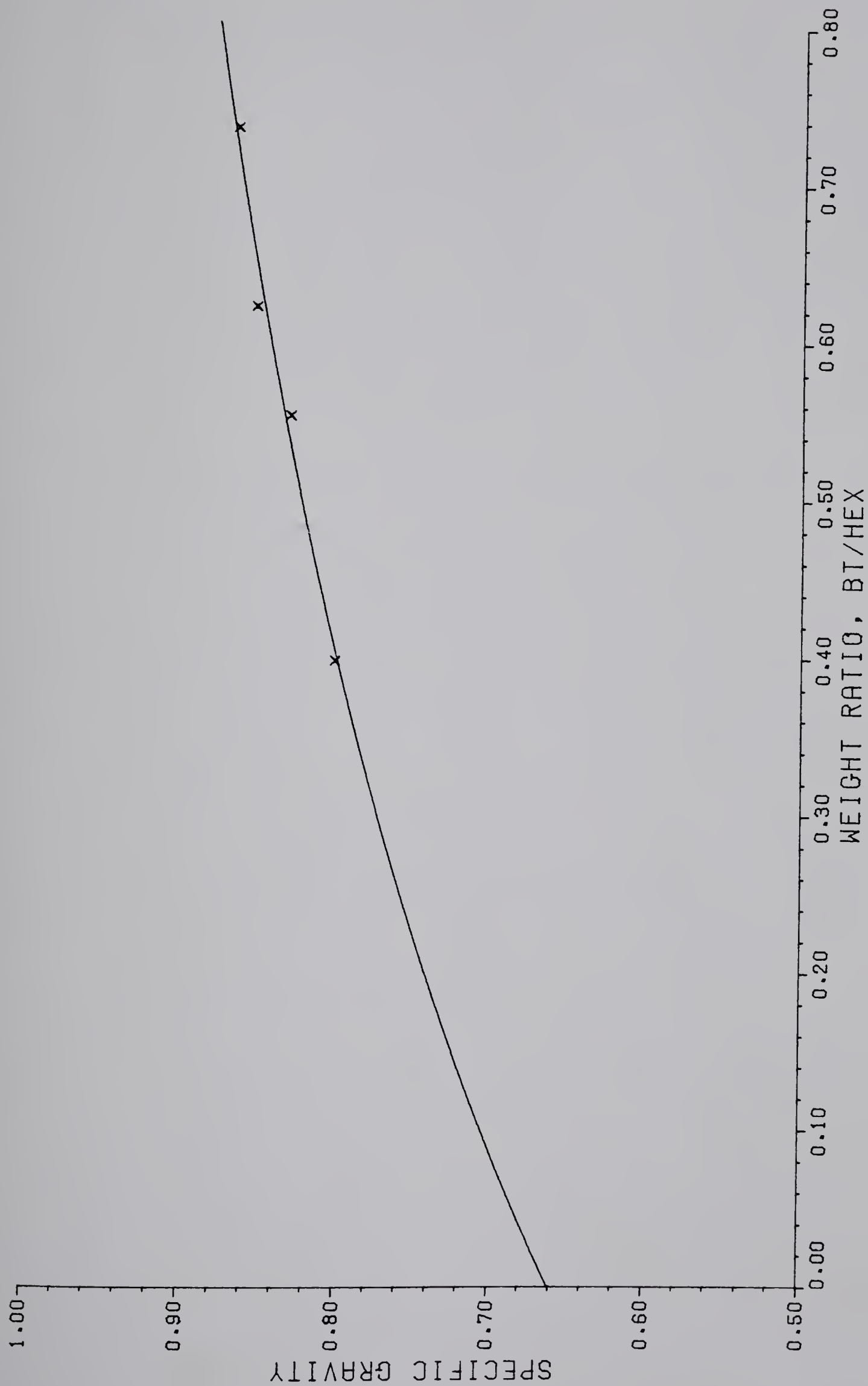


Figure D-1 - Density-composition data for Benzothioophene-Hexane Solutions





## APPENDIX E - LISTING OF COMPUTER PROGRAMS

The main data analysis program used in the preparation of this thesis was entitled THEUNIVERSE, listed beginning on the next page. It was used to calculate the fractional conversions of benzothiophene to each of the major products and to compute an estimate of the composition of the liquid feed. A typical output from this program is given in Table 3.

The program used to fit a least squares exponential to the fractional conversion data making up each individual data point was called REGPT, and is listed after THEUNIVERSE. The constants returned by this program are given in Table 4, and the curves themselves are plotted in Figures 5a through 5p. The actual output from this program can be obtained from the author on request.

The library subroutine ("AR") called by this program has been documented elsewhere<sup>76</sup>. The function to which the data are fitted (Equation 2) is passed to the program as a single line of FORTRAN in a separate file.



# THEUNIVERSE

This is the main data analysis program used in the present thesis. It takes all the data recorded during the actual experimentation as input, and outputs the following for each series of gas samples:

- Series identification number
- Date
- Reactor pressure
- Reactor temperature
- Catalyst bed mass
- Catalyst pellet mesh size
- Catalyst bed identification number
- Liquid feed batch identification number
- Molar flow rates of all feed components
- Partial pressures of all feed components
- Reciprocal space velocity

For each individual gas sample, the following are printed out:

- Percent of total peak area for each component in the product stream
- A hypothetical feed concentration based on a mass balance for that gas sample
- Fractional conversion of bt to each of the reaction products

Finally, the program prints the means and 95% confidence intervals of the fractional conversions over the series of gas samples, and gives an estimate of the original liquid feed composition based on a composite mass balance over the entire liquid feed batch.

The input to the program for each series of gas samples is as follows:

- NSER: Identification number for the series
- NBED: Identification number for the catalyst bed
- NFEED: Identification number for the liquid feed batch
- NDATE: Date on which the data were obtained
- NPTS: Number of gas samples in the series
- BTCONC: Wt. ratio bt/hex in the liquid feed  
(Although this program will calculate a value based on a composite mass balance of all gas samples in the data file, this input value will be the one used to calculate bt and hex flow rates. In other words, this program must be run twice for any given set of data - once to find out the value of BTCONC, and a second time to use it in the calculations.)
- ATM: Average atmospheric pressure for the series, mm. Hg
- P: Average reactor pressure for the series, inches Meriam fluid (s.g. 1.75)
- TC: Average reactor temperature, deg. C



```

C      CATWT: Catalyst bed weight, g.
C      MESH1,MESH2: Catalyst pellet size, standard mesh
C              (e.g. -40+60)
C      H2: Hydrogen rotameter reading
C      NHROT: Hydrogen rotameter float (1=glass, 2=steel)
C      SP: Syringe pump setting, % x 1/1000 of full rate
C      EN2: Nitrogen rotameter reading
C      NNROT: Nitrogen rotameter float (as above)
C      In addition, the following data are inputted for
C      each gas sample:
C          THR,TMIN: Time elapsed between reactor going
C                  on stream and sampling time, in hours and
C                  minutes
C          GAS: Sum of peaks for hydrogen, nitrogen, and
C              hydrogen sulfide, % of total area of all
C              peaks (not used in any calculations)
C          HEX: N-hexane peak size, % of total area
C          EB: Ethylbenzene peak size, % of total area
C          STY: Styrene peak size, % of total area
C          BT: benzothiophene peak size, % of total area
C          DH: Dihydrobenzothiophene peak size, % of total
C              area
C

```

```

      DIMENSION MESH(2),GAS(80),HEX(80),EB(80),STY(80),
@      CONV(80),BTTOEB(80),BTTOST(80),T(70),BALNCE(80),
@      BTTODH(80),THR(80),TMIN(80),BT(80),DH(80)

```

```

C      Initialize variables
C

```

```

      DATA T/12.71,4.30,3.18,2.78,2.57,2.45,2.36,2.31,
@      2.26,2.23,2.2,2.18,2.16,2.14,2.13,2.12,2.11,
@      2.1,2*2.09,2.08,2*2.07,3*2.06,2*2.05,2*2.04,
@      5*2.03,8*2.02,12*2.01,16*2./
      TOTCOM=0.
      TOTSQ=0.
      NCOMP=0
      NNROT=1

```

```

C      Input data for a new series of runs and re-initialize
C      variables
C

```

```

100 READ(5,101)NSER,NBED,NFEED,NDATE,NPTS,BTCONC,ATM,P,
@      TC,CATWT,MESH(1),MESH(2),H2,NHROT,SP,EN2,NNROT
      IF(NSER.EQ.0) GO TO 200
      CONVST=0.0
      CONVDH=0.0
      BTDHT=0.
      BTDHT2=0.
      BTEBT=0.
      BTEBT2=0.
      BTSTT=0.
      BTSTT2=0.
      BTCT=0.
      BTCT2=0.

```





```

DO 110 I=1,NPTS
  READ(5,111)THR(I),TMIN(I),GAS(I),HEX(I),EB(I),
@    STY(I),BT(I),DH(I)
  THR(I)=THR(I)+TMIN(I)/60.
110 CONTINUE
C
C  Calculate reactor pressure (kPa) and temperature
C  (deg. K)
C
  PR=P*0.4358935+ATM*.1333224
  TK=TC+273.16
C
C  Calculate volumetric (Q) and molar (F) flow rates for
C  gas (cm3/s,mol/s) and liquid (ml/min, mol/s) feeds;
C  Calculate reciprocal space velocity
C
  IF(NHROT.EQ.1) QH2=1.625815615E-1+1.313837578E-3*H2
@    +1.119669541E-4*H2**2-2.518931661E-7*H2**3
  IF(NHROT.EQ.2) QH2=7.242407802E-1+3.701697921E-2*H2
@    +1.866222346E-4*H2**2+4.118887046E-7*H2**3
  IF(NNROT.EQ.1) QN2=8.515653607E-2+6.435097751E-4*EN2
@    +8.278195381E-5*EN2**2-5.76040392E-7*EN2**3
@    +1.83998824E-9*EN2**4
  IF(NNROT.EQ.2) QN2=-3.091740296+1.488523368E-1*EN2
@    -2.113716022E-3*EN2**2+1.46093048E-5*EN2**3
@    -3.594074268E-8*EN2**4
  FH2=3.7476E-5*QH2
  FN2=3.7476E-5*QN2
  IF(EN2.EQ.0) FN2=0.
  BTFRAC=BTCONC/(1.+BTCONC)
  QLIQ=9.678E-4*SP
  FBT=BTFRAC*QLIQ*1.42697E-4
  FHEX=(1.-BTFRAC)*QLIQ*1.2769E-4
  WF=CATWT/FBT
C
C  Calculate total molar flow rate and partial pressures
C  of each feed component (kPa)
C
  F=FH2+FBT+FHEX+FN2
  PH2=PR*FH2/F
  PBT=PR*FBT/F
  PHEX=PR*FHEX/F
  PN2=PR*FN2/F
C
C  Calculate fractional conversion of bt to eb, sty,
C  dhbt for each run
C
C  First, a weight ratio and then a mole ratio of each
C  component to n-hexane is calculated
C
  DO 120 I=1,NPTS
    WRBTHX=BT(I)*1.027193/HEX(I)
    WREBHX=EB(I)*0.994211/HEX(I)
    WRSTHX=STY(I)*0.969739/HEX(I)

```





```

WRDHHX=DH(I)*1.0272/HEX(I)
BTMOL=WRBTHX*86.18/134.2
EBMOL=WREBHX*86.18/106.07
STYMOL=WRSTHX*86.18/104.15
DHMOL=WRDHHX*86.18/136.2
TOTMOL=BTMOL+EBMOL+STYMOL+DHMOL
BALNCE(I)=TOTMOL*134.2/86.18

```

Next, a benzene ring balance on the product stream is computed. TOTMOL is the mole ratio of total aromatics to n-hexane in the product stream, which should be the same as the mole ratio of bt/hex in the feed. (the weight ratio of bt/hex in the original feed is given by BALNCE.) Based on this estimate of bt/hex mole ratio, the fractional conversions of benzothiophene to ethylbenzene, styrene, and dihydrobenzothiophene are calculated.

```

BTTOEB(I)=EBMOL/TOTMOL
BTSTOST(I)=STYMOL/TOTMOL
BTTODH(I)=DHMOL/TOTMOL
CONV(I)=BTTOEB(I)+BTSTOST(I)

```

The rest of the loop is used to store intermediate values of variables used to compute means and confidence intervals in the next section.

```

BTEBT=BTEBT+BTTOEB(I)
BTSTT=BTSTT+BTSTOST(I)
BTCT=BTCT+CONV(I)
BTDHT=BTDHT+BTTODH(I)
BTEBT2=BTEBT2+BTTOEB(I)**2.
BTSTT2=BTSTT2+BTSTOST(I)**2.
BTCT2=BTCT2+CONV(I)**2.
BTDHT2=BTDHT2+BTTODH(I)**2
NCOMP=NCOMP+1
TOTCOM=TOTCOM+BALNCE(I)
TOTSQ=TOTSQ+BALNCE(I)**2

```

120 CONTINUE

Compute mean and confidence interval at .95 level of significance

```

CONVEB=BTEBT/NPTS
CONVBT=BTCT/NPTS
CONVST=BTSTT/NPTS
CONVDH=BTDHT/NPTS
SIGEBC=(BTEBT2/NPTS-CONVEB*CONVEB)**0.5
SIGCON=(BTCT2/NPTS-CONVBT*CONVBT)**0.5
SIGSTC=(BTSTT2/NPTS-CONVST*CONVST)**0.5
SIGDHC=(BTDHT2/NPTS-CONVDH*CONVDH)**0.5
NU=NPTS-1
CIEB=T(NU)*SIGEBC/NU**0.5
CISTY=T(NU)*SIGSTC/NU**0.5

```



```
CITOT=T(NU)*SIGCON/NU**0.5
```

```
CIDH=T(NU)*SIGDHC/NU**0.5
```

```
Output everything
```

```
WRITE(6,131) NSER,NDATE
```

```
WRITE(6,132) PR,TK
```

```
WRITE(6,133) CATWT,MESH(1),MESH(2)
```

```
WRITE(6,139) NBED,NFEED
```

```
WRITE(6,134) FH2,FBT,FHEX,FN2
```

```
WRITE(6,135) PH2,PBT,PHEX,PN2
```

```
WRITE(6,138) WF
```

```
WRITE(6,136)
```

```
DO 130 I=1,NPTS
```

```
WRITE(6,137) I,GAS(I),HEX(I),EB(I),STY(I),BT(I),
```

```
@ DH(I)
```

```
130 CONTINUE
```

```
WRITE(6,151)
```

```
DO 150 I=1,NPTS
```

```
WRITE(6,152) I,BALNCE(I)
```

```
150 CONTINUE
```

```
WRITE(6,141)
```

```
DO 140 I=1,NPTS
```

```
WRITE(6,142) I,THR(I),BTTOEB(I),BTTOST(I),
```

```
@ BTTOBH(I),CONV(I)
```

```
WRITE(7,142) I,THR(I),BTTOEB(I),BTTOST(I),
```

```
@ BTTOBH(I),CONV(I)
```

```
140 CONTINUE
```

```
WRITE(6,143) CONVEB,CONVST,CONVDH,CONVBT,CIEB,
```

```
@ CISTY,CIDH,CITOT
```

```
NFEEDX=NFEED
```

```
GO TO 100
```

```
Calculate avg. feed composition based on all runs
```

```
200 AVCOMP=TOTCOM/NCOMP
```

```
SIGCOM=(TOTSQ/NCOMP-AVCOMP**2)**.5
```

```
NUNU=NCOMP-1
```

```
CICOMP=T(NUNU)*SIGCOM/NUNU**0.5
```

```
WRITE(6,201) NFEEDX,NCOMP,AVCOMP,CICOMP
```

```
STOP
```

```
101 FORMAT(3I3,I7,I3,F7.4,F6.1,F5.1,F6.1,F8.5,2I3,F6.1,
```

```
@ I2,2F6.1,I2)
```

```
111 FORMAT(2F2.0,6F8.4)
```

```
131 FORMAT('1','SERIES ',I3,/,I7,//)
```

```
132 FORMAT(' ','TOTAL PRESSURE IN REACTOR: ',F7.2,' KPA'
```

```
@ ,/, 'TEMPERATURE IN REACTOR: ',F6.1,' DEG. K')
```

```
133 FORMAT(' ','CATALYST: NALCO NM 502, ',F7.4,' G., ',
```

```
@ I3,'+',I2,' MESH')
```

```
139 FORMAT(' ','CATALYST BED NUMBER: ',I2,/,
```

```
@ 'LIQUID FEED BATCH NUMBER: ',I2)
```

```
134 FORMAT(' ','FEED RATES TO REACTOR: ',/,5X,'H2: ',
```

```
@ E11.6,' GMOL/SEC',/,5X,'BT: ',E11.4,' GMOL/SEC'
```



```

@      ,/,5X,'HEX: ',E11.4,' GMOL/SEC',/,5X,'N2: ',
@      E11.4,' GMOL/SEC')
135 FORMAT(' ','PARTIAL PRESSURES OF FEED TO REACTOR:',
@      /,5X,'H2: ',F6.2,' KPA',/,5X,'BT: ',F6.2,
@      ' KPA',/,5X,'HEX: ',F6.2,' KPA',/,5X,'N2: ',
@      F6.2,' KPA')
138 FORMAT(' ','W/F= ',E11.4,' G-SEC/GMOL(BT)',/)
136 FORMAT(' ','RAW DATA (AREA %):',/,5X,'RUN',3X,
@      'N2+H2',2X,'N-HEXANE',4X,'ETHYL-',3X,'STYRENE',
@      4X,'BENZO- DIHYDROBENZO',/,12X,'+H2S',13X,
@      'BENZENE',11X,'THIOPHENE',4X,'THIOPHENE')
137 FORMAT(' ',4X,12,2X,6(F7.4,3X))
151 FORMAT(' ',/,,'LIQUID FEED COMPOSITION BASED ON MASS',
@      ' BALANCE (WT. RATIO):',/,5X,'RUN',3X,'BT/HEX')
152 FORMAT(' ',4X,12,3X,F8.6)
141 FORMAT(' ',/,,'FRACTIONAL CONVERSION OF BENZOTHIO',
@      ' PHENE:',/,5X,'RUN',3X,'TIME',6X,'TO EB:',4X,
@      'TO STY:',3X,'TO DHBT:',4X,'EB+STY:')
142 FORMAT(' ',4X,12,3X,F6.3,4(3X,F8.6))
143 FORMAT(' ',3X,'MEAN: ',9X,4(F8.6,3X),/,5X,'+/-',11X,
@      4(F8.6,3X))
201 FORMAT('1','LIQUID FEED BATCH: ',12,/,,'COMPOSITE ',
@      'MASS BALANCE BASED ON ',12,' DATA POINTS',/,
@      'AVG. FEED RATIO BT/HEX: ',F7.4,' +/- ',F7.4)
END

```





```
/PROB      TITLE IS 'REGPT'.  
/INPUT     VARIABLES ARE 2.  
           FORMAT IS '(9X,F6.3,3X,F8.6)'.  
           CASES ARE 54.  
           MTSFILE IS 'POINT12'.  
/VAR       NAMES ARE THR,CT.  
/REGR      DEPEND IS CT.  
           INDEP IS THR.  
           PARAM ARE 4.  
           ITER ARE 200.  
           HALV ARE 200.  
           TITLE IS 'POINT 12'.  
/PARAM     INITIAL ARE 0.15,-0.002,0.1,-0.5.  
           MAX ARE 1.0,0.0,1.0,-0.3.  
           MIN ARE 0.0,-0.1,0.0,-1.0.  
/END
```





## APPENDIX F - CALCULATION OF HEAT LOAD IN REACTOR

Literature values of the heat capacities of the reactants and products are shown in Table F-1. The relevant bond strengths at 25°C are summarized in Table F-2.

The heat of reaction for the hydrodesulfurization of dihydrobenzothiophene was estimated as 62.4 kcal per mole of dihydrobenzothiophene reacted, based on the net change in bond energy between the reactants and products, assuming that the C-S bond strengths do not differ greatly from the value shown in this table for an aliphatic chain. If the heat of reaction for the hydrogenation of benzothiophene is assumed to be 30 kcal/mol, then the net heat of reaction for the overall desulfurization of benzothiophene can be calculated as about 92.4 kcal/mol.

Assuming that benzothiophene is converted into only ethylbenzene and hydrogen sulfide, the heat capacities of the reactants and products at 25 and 400°C were used to calculate an estimate of the heat of reaction at the higher temperature of 98.4 kcal/mol.

The feed to the reactor under normal operating conditions consisted of hydrogen, n-hexane, and benzothiophene in the approximate molar proportions of 57:4:1. Assuming only 40% of the benzothiophene is desulfurized, the average heat capacity of the product stream was calculated as about 11.5 cal/mol-K at 400°C and the net temperature rise as 53°.



Table F-1 - Heat Capacities of Reactants and Products

Compound	Heat Capacity (cal/mol-K)		
	298°K	800°K	673°K
Hydrogen	6.64 <sup>8 3</sup>		7.16 <sup>8 3</sup>
Nitrogen	6.80 <sup>8 3</sup>		7.17 <sup>8 3</sup>
Hydrogen Sulfide	8.28 <sup>8 3</sup>		9.62 <sup>8 3</sup>
n-Hexane	34.20 <sup>8 4</sup>	70.36 <sup>8 4</sup>	61.18*
Benzothiophene	31.6**	64.0**	52.8*
Ethylbenzene	30.70 <sup>8 4</sup>	67.15 <sup>8 4</sup>	57.89*

\* estimated by linear interpolation

\*\* estimated assuming the same mass heat capacity as methylthiophene<sup>8 5</sup>



Table F-2 - Bond Strengths of Reactants and Products

Bond	Strength (kcal/mol)
H-H	104.2
C-H (aromatic)	112.0
C-H (aliphatic)	98.0
S-H (in H <sub>2</sub> S)	90.0
C-S (aliphatic)	60.0

All bond strengths<sup>a</sup> are at 25°C



A change in the liquid feed concentration from a mole ratio of n-hexane to benzothiophene of 4:1 to 4.6:1 results in an average heat capacity of 12.1 cal/mol-K, and a change to 3.2:1 results in an average heat capacity of 10.6 cal/mol-K.





## APPENDIX G - CALCULATION OF KINETIC CONSTANTS

The minimum apparent activation energy for the reaction path through dihydrobenzothiophene was calculated from the reaction rates (cf. Table 6) at 350° and 400°C. It was assumed in this calculation that the rate could be described by a zero-order Arrhenius-type equation of the form:

$$\text{Rate} = A \exp(-E/RT)$$

where

A = preexponential factor, mol/g cat-s

E = apparent activation energy, cal/mol

R = gas constant, 1.987 cal/mol-°K

T = temperature, °K

Thus,

$$E = \frac{-1.987 \ln(0.06243/0.036107)}{673^{-1} - 623^{-1}} = 9123$$

From this value of E and the measured rate at 400°C, the preexponential factor was calculated:

$$A = 0.06243 \exp(+9123/673 \times 1.987) = 57.33$$





B30354